Bacterial social interactions influencing *Pseudomonas aeruginosa* biofilm formation

Catherine Rebecca Armbruster

A dissertation
submitted in partial fulfillment of the
requirements for the degree of
Doctor of Philosophy

University of Washington
2017

Reading Committee:
Matthew R. Parsek, Chair
Lucas R. Hoffman
Caroline S. Harwood

Program Authorized to Offer Degree:
Microbiology

University of Washington

Abstract

Bacterial social interactions influencing *Pseudomonas aeruginosa* biofilm formation

Catherine Rebecca Armbruster

Chair of the Supervisory Committee:
Professor Matthew R. Parsek
Department of Microbiology

Pseudomonas aeruginosa is an opportunistically pathogenic bacterium that frequently co-infects with other bacterial species in a variety of diseases and has a propensity to form biofilms. Biofilms are dense aggregates of bacteria encased in a protective extracellular matrix that promote interactions between *P. aeruginosa* cells, as well as with other microbial community members. The goal of my doctoral thesis work in the Parsek and Hoffman labs has been to identify inter- and intra-species interactions that influence *P. aeruginosa* biofilm formation. In my dissertation, I describe novel inter-species interactions between *P. aeruginosa* and *Staphylococcus aureus*, as well as a division of the labor of biofilm formation among a population of *P. aeruginosa* cells. This work provides a glimpse into *P. aeruginosa* sociality and contributes to the growing body of literature detailing how bacterial social interactions drive the composition and function of biofilms.

Table of Contents

Tables

Figures

Chapter I

Chapter II

Chapter III

Conclusions and Future Directions

There is a pleasure in the pathless woods,
There is a rapture on the lonely shore,
There is society, where none intrudes,
By the deep Sea, and music in its roar:
I love not Man the less, but Nature more.

— Lord Byron, excerpt from "Childe Harold's Pilgrimage"

Nature is a language, can't you read?

— The Smiths, "Ask"

In memoriam

Liam Elgin Douglas Rattray
October 10, 1987 – May 30, 2011

Forever young, forever on my mind.

ACKNOWLEDGEMENTS

I am grateful for the many mentors who have supported me over the years, allowing me to follow my own path as I pursued my academic interests.

My parents, Violet and Mike Armbruster, supported my decision to leave our home in south Florida to begin my undergraduate education at age 14 at a small, liberal arts women's college in rural Virginia. Thank you both for the opportunity to stray from a traditional path. Thanks also to my older brother Dr. Michael Armbruster for being a particularly unique and inspiring role model throughout childhood and into adulthood.

My professors at Mary Baldwin College ignited a full-on feminist awakening in me at age 14, and through them I developed a lifelong love of the liberal arts alongside my interest in the natural sciences. I am thankful for the enrichment of my daily life that my liberal arts education has afforded me, from spotting Gustav Klimt paintings as my eyes wandered up to the ceiling during a research talk in Vienna to catching snippets of traditional Appalachian folk songs sung by street performers while biking in Seattle. Thank you to Dr. Paul Deeble for giving me my first science job, as a 14 year old with absolutely no work experience and a middle school education, and for taking the time to train me during my very first days working in a lab. I benefitted from mentorship by Dr. Peter McCarthy and Dr. Wolfram Brück at Harbor Branch Oceanographic Institution, where I got my feet wet working in a microbiology lab, and Dr. ShiLi Miao at South Florida Water Management District. I am also grateful for the guidance I received from Dr. Eric Jones, Dr. Peggy Ankney, and Dean Jeffrey Buller when I needed help and inspiration as a teenager who was sometimes overwhelmed by college life.

I am thankful for the opportunity to have lived and worked in India while pursuing my master's degree in Public Health at the Rollins School of Public Health in Atlanta, GA. My adviser Dr. Venkat Narayan and the researchers at Dr. Mohan's Diabetes Specialties Centre in Chennai, especially Dr. V. Mohan and Dr. Ranjani Harish, went above and beyond both to support my research and to enthusiastically participate in a documentary on diabetes that I filmed throughout my time in India.

At the U.S. Centers for Disease Control and Prevention in Atlanta, I was fortunate to encounter a few great mentors who were generous with their time and patience. Thank you to Dr. Judith Noble-Wang for taking a chance and hiring me, an 18-year-old public

health student studying diabetes epidemiology, to work on bacterial environmental outbreaks and cementing my interest in microbiology. After completing my MPH at Emory, I joined the Biofilm Lab at CDC where Dr. Margaret Williams spent countless hours with me at the bench, training me to think as a scientist and serving as the principal investigator of my first first author research publication. I am also thankful for Dr. Rodney Donlan who served as a great role model as I developed my interest in the field of biofilm research. And, thank you to Drs. Judith Noble-Wang, Margaret Williams, Matthew Arduino, Rod Donlan, Heather Moulton-Meissner, and Laura Rose for their support and encouragement when I decided to pursue my Ph.D. in Microbiology.

At the University of Washington, I would like to thank my doctoral advisers Dr. Matt Parsek and Dr. Luke Hoffman for giving me the freedom to pursue my interest in the sociality of bacterial biofilms in both of their labs. I would also like to thank Dr. Carrie Harwood for serving on my reading committee, along with my advisers, and Dr. Joseph Mougous, Dr. Josh Woodward, and Dr. Jim Bryers for serving on my thesis committee. Finally, I would like to thank the many post docs and research scientists who took the time to train me over the years, particularly Dr. Boo Shan Tseng, Dr. Dan Wolter, Dr. Chris Pope, Dr. Joe Harrison, Dr. Katie Hisert, Dr. Hemantha Kulasekara, and Dr. Maureen Thomason. My doctoral work has been incredibly intellectually satisfying and I hope to pay forward even a fraction of the kindness and patient mentorship I have experienced.

Finally, thank you to Jeffrey Davis for injecting adventure into my life. Thank you for sharing your love of the Pacific Northwest and your wonderful family with me.

INTRODUCTION

A historical perspective on biofilms

The vast majority of bacteria in nature live in communities called biofilms, which are surface- or interface-associated aggregates of bacteria encased in a protective, extracellular matrix (1). Biofilms facilitate a diversity of cell-cell interactions by bringing microbes into close proximity and they allow bacteria to resist predation by protozoa, infection by bacteriophages, and a variety of physical and chemical stresses, including nutrient limitation, desiccation, and shear forces (2). The biofilm mode of growth is integral to prokaryotic life, and bacteria form biofilms in virtually all nutrient-sufficient ecosystems, from the viscous biofilms termed "snotties" hanging from sulfidic caves (pH of 0) in Italy (3), to the biofilms lining ikaite columns in the permanently cold (< 4^{o}C), alkaline (pH >10), and low nutrient Ikka Fjord in Southern Greenland (4), to the vibrantly colored microbial communities associated with the constantly erupting geysers and hot springs (70 to 90°C) of Yellowstone National Park (5). Biofilm-like structures have been detected among the earliest records of life on Earth, such as the "consortium of rod-vibroid cells" embedded in "copious quantities of extracellular polymeric substances" (biofilm matrix) associated with microbial mats in 3.3-3.5 billion-year-old cherts in the Barberton and Pilbara greenstone belts in South Africa and Australia, respectively (6). A propensity toward a biofilm mode of growth has been observed among the most ancient lineages of the phylogenetic tree, including the 'living fossils' Korarchaeota in the Kingdom Archaea and Aquificales in Bacteria (7). The remarkable ability of bacteria to survive and thrive within protective biofilms since the Archean eon is likely the key reason that bacteria are the most successful form of life on earth today (8), in terms of their total biomass, as well as the sheer diversity and extent of the habitats they colonize.

The Dutch businessman and scientist Antonie van Leeuwenhoek (1632-1723) first identified biofilms over 300 years ago in a series of reports to the Royal Society of London, in which he described using a tiny single-lens microscope he constructed to examine scrapings from his own mouth. In his letters, van Leeuwenhoek described aggregates of "animalcules" in the "scurf of the teeth", which contemporary scientists know to be the normal microbial community of dental plaque, and he alluded to the

scurf's polymicrobial nature when he commented on "an inconceivable number of exceeding small animalcules and these of divers sorts.(9)" One hundred years later, the French scientist Louis Pasteur (1822-1895) described the formation of 'la matière visqueuse', a viscous 'membrane' containing a rod-shaped microbe (which he named *Mycoderma aceti*) forming at the air-liquid interface in vats of beet root alcohol that spoiled the otherwise pleasant drink by fermenting the alcohol into vinegar (10, 11). In the early to mid 20th century, microbiologists began to appreciate that the majority of bacteria in free-flowing freshwater grow attached to submerged surfaces, as opposed to planktonically (12), that these surface-attached bacteria contribute to the biofouling of ship hulls and other industrial marine surfaces (13), and that bacteria transition from a stage of reversible to irreversible attachment when they encounter a surface (14). By the mid-to-late 1970s, two microbiologists made the first descriptions of a self-produced extracellular matrix: Niels Hoiby in Copenhagen, Denmark described mucoid *Pseudomonas aeruginosa* isolated from the lungs of cystic fibrosis patients (15), and John W. (Bill) Costerton in Calgary, Alberta, Canada described the requirement of a 'glycocalyx' for bacterial cells to attach to each other and to surfaces (16). The term "biofilm" was first introduced into the literature by Bill Costeron in 1981 to describe the matrix-encased bacteria firmly adhered to an abiotic surface that his group was characterizing *in vitro* (17); now, 35 years later, a PubMed search of "biofilm" returns almost 36,000 articles.

Pseudomonas aeruginosa **biofilm composition**

In addition to the ubiquity of biofilms in the environment, all higher organisms, including humans, are colonized by commensal bacterial biofilms (18), and biofilm infections are known to persist despite aggressive antibiotic treatment and a robust host immune response in a variety of chronic diseases (19). *Pseudomonas aeruginosa* is an opportunistically pathogenic bacterium that has a propensity to form biofilms in diverse habitats, including soil, water, plants, and in numerous animal hosts. The *P. aeruginosa* biofilm matrix is composed of a combination of polysaccharides (including Pel, Psl, and alginate), proteins (including the adhesin CdrA), and extracellular DNA that provide structural, protective, and social functions for biofilm bacteria (20–25). Biofilm matrix

production is an energetically costly process that is regulated at the transcriptional, post-transcriptional, and post-translational levels (26) such that these adhesive molecules are rapidly but appropriately deployed, primarily during growth on a surface.

P. aeruginosa biofilm lifecycle and regulation

The process of biofilm formation in pseudomonads is a regulated developmental sequence that includes an attachment phase as planktonic bacteria first encounter a surface, a growth phase during which attached bacteria form microcolonies that develop into structured communities of hundreds of cells encased in a self-derived extracellular matrix, and a detachment phase when cells disperse from the mature biofilm to go on to colonize new niches (27). This transition from a planktonic to a sessile lifestyle involves the coordinated change in expression of hundreds of genes, leading to striking physiological changes between planktonic and biofilm cells (28, 29). Many factors have been shown to contribute to each step in biofilm formation, including extracellular appendages that mediate both initial attachment to a surface (such as flagella and pili (30, 31)) and surface motility (32–34), as well as the production of polysaccharides (including Pel, Psl, and alginate) and other matrix components that contribute to the biofilm structure (35–37). The production of these extracellular factors is regulated largely by two-component signal transduction systems (TCSs) that sense and respond to environmental cues, such as divalent cations (38, 39), iron (40, 41), nitrate (42), and metabolic products from surrounding microbes (22, 43).

P. aeruginosa has a tremendous capacity to sense and respond to its environment; nearly 10% of the lab strain PAO1's genes are predicted to encode either transcriptional regulators or two-component regulatory system proteins (44). Classical TCSs consist of a dimeric, membrane-bound sensor histidine kinase and a cognate response regulator with an aspartate-containing receiver domain (REC domain). Upon detection of an environmental stimulus or ligand in the periplasm, the sensor kinase autophosphorylates at a conserved histidine residue, then this phosphoryl group is transferred to the conserved aspartate residue of the response regulator's REC domain, which modifies the output regulatory domain's activity. The output domains of response regulators can have many functions, including DNA-binding transcriptional regulators, a variety of enzymatic

activities (including domains with GGDEF, EAL, or HD-GYP motifs), RNA-, protein-, or ligand-binding, as well as domains of unknown function; other response regulators have apparently standalone receiver domains without an obvious output domain. One canonical example of two-component systems is provided by bacterial chemotaxis signal transduction systems, in which CheA is a histidine kinase that autophosphorylates in response to the methylation state of the chemoreceptor to which it is bound and then transfers the phosphoryl group to CheY, a response regulator that regulates activity of the flagellar rotor (45). Further variations on the classical TCSs exist, including phosphorelays and hybrid two-component systems in which a single protein harbors a sensory domain at the amino terminus and a sensor kinase domain, a receiver domain, and a response regulator domain at the carboxy terminus.

Many TCSs have been identified to play roles in modifying the *P. aeruginosa* cell surface in response to the environment. During biofilm development, TCS signaling leads to modifications to appendages on the cell surface that are involved in motility and adhesion, including FleS/FleR, which regulates production of the flagellum (46), the Roc, Rcs/Pvr systems that control cup fimbriae expression (47, 48), the PprA/B system that regulates both Flp and Cup fimbriae, and PilRS, Pil-Chp, and AlgR/FimS, which regulate Type IV pili (49). Additional TCSs regulate production of the biofilm matrix, including the RetS/LadS/GacS, FimS/AlgR, Pil-Chp, and Wsp systems that regulate production of polysaccharides, and BfrmR/S and MfiR, which regulate microcolony formation and biofilm maturation (47). Thus, two-component systems act through coordinated signaling cascades to drive the transition from planktonic to sessile growth, through each stage of biofilm formation, in response to environmental cues, many of which remain unknown. Of particular importance for biofilm formation are the response regulators containing output domains containing GGDEF, hybrid GGDEF/EAL, or EAL domains, of which *P. aeruginosa* encodes six (48), because these proteins can play a role in regulating cellular levels of cyclic diguanylate monophosphate (cyclic di-GMP), an important regulator of biofilm-associated behaviors.

Cyclic diguanylate monophosphate

A major factor that drives biofilm formation in *P. aeruginosa* and other bacteria is cyclic diguanylate monophosphate (c-di-GMP). C-di-GMP is an intracellular second messenger signaling molecule that is used ubiquitously by bacteria to rapidly modify their cell surfaces in response to their environments (50). *P. aeruginosa* biofilm cells have been shown to contain on average 3.5-4 times more c-di-GMP compared to their planktonic counterparts, when normalized to total protein level (51, 52), and these c-di-GMP levels can be up to 7 times higher in hyper-biofilm forming rugose small colony variants that emerge during chronic cystic fibrosis lung infections (53). Diguanylate cyclases (DGC) are proteins containing a GGDEF amino-acid sequence and that synthesize c-di-GMP from two molecules of GTP, and phosphodiesterases (PDE) are proteins with EAL or HD-GYP motifs that hydrolyze c-di-GMP into linear pGpG or GMP. The genomes of *P. aeruginosa* lab strains PAO1 and PA14 each encode almost 40 of these putative c-di-GMP-metabolizing enzymes, the majority of which contain additional predicted domains involved in environmental sensing (including PAS, GAF, and HAMP domains) and signal transduction (e.g., REC domains) (54). Thus, *P. aeruginosa* integrates diverse environmental signals through the activity of its DGCs and PDEs to modulate intracellular levels of c-di-GMP, leading to regulation of a variety of bacterial behaviors, including the transition to a biofilm mode of growth.

Elevated c-di-GMP levels promote cell surface adhesiveness by interacting with specific receptors and effectors that activate production of biofilm extracellular matrix components and suppress expression of motility genes. The affinities for c-di-GMP of these various proteins and molecules range from low nanomolar to micromolar levels (55). This large range of binding constants has been suggested to be a mechanism by which a single signaling molecule can be used to specifically and sequentially regulate a variety of behaviors occurring during the transition from the planktonic to biofilm mode of growth (54, 55). Alternatively, some researchers hypothesize that specificity of diguanylate cyclase and phosphodiesterase activity to regulate only their target cellular function is due to subcellular pools of c-di-GMP (56–58), although it is not currently understood how high and low localized concentrations of c-di-GMP could be maintained due to the ability of small molecules like c-di-GMP to rapidly diffuse throughout the cell.

The sociality of biofilms

Early microbiological research was rooted in what is referred to as the 'pure-culture paradigm' (2), the reductionist study of bacteria as single cells suspended in liquid culture. This approach proved to be instrumental in driving early advances in microbial physiology and pathogenesis; however, it fails to capture the full diversity and complexity of differentiated behaviors exhibited by bacteria growing as biofilms. Bacterial communities were first viewed through the lens of multicellularity by James A. Shapiro at the University of Chicago when, in the late 1980's, he wrote an article in Scientific American describing coordinated behavior among populations of bacteria that differentiate into various cell types (the multicellular fruiting bodies of Myxobacteria) and organize reproducibly into highly elaborate colonies in which production of enzymes, such as beta-galactosidase in *E. coli*, was regulated spatio-temporally (59). As the field of biofilm research progressed, a large variety of bacterial behaviors have been observed, even within single-species biofilms. For example, by promoting cell-cell contact, biofilms are thought to function as environmental reservoirs where efficient exchange of genetic material occurs, including antibiotic resistance genes (60).

This promotion of social interactions through the maintenance of close cellular contact, resulting in high cellular densities, is a defining characteristic of biofilms; environmental biofilm cell densities frequently range from 10^8 to 10^{11} cells per gram of wet weight (61). A common feature of organized, interacting communities of cells like biofilms is cooperation, which is a social behavior that emerges among genetically homogenous populations of bacterial cells. Cooperation usually involves the development of phenotypic heterogeneity among member cells, which is thought to benefit populations by allowing a single genotype of an organism to survive sudden environmental changes and by promoting the distribution among population members of costly behaviors that support the growth and survival of the population. Many of these cooperative interactions occur through the production of "public goods" such as siderophores, digestive enzymes, adhesins, and exopolysaccharides (62). The biofilm matrix promotes these social interactions by retaining cells and their extracellular products in close proximity. An advantage of the division of labor among cooperative bacteria is that it relieves individual cells from the regulatory and metabolic burdens of either switching between tasks or

performing each task simultaneously (63). For example, *P. aeruginosa* has been suggested to undergo a division of labor as biofilms mature during *in vitro* growth on glucose, a condition that results in "mushroom" shaped biofilms. The population diversifies, including a subpopulation of non-motile cells that becomes the stalk of the biofilm, and a subpopulation that later forms the mushroom cap (requiring type IV-mediated surface motility) (32, 64).

One major factor driving phenotypic heterogeneity within a biofilm in particular is chemical variation within the biofilm itself, including gradients of oxygen (65), nutrients (66), and pH (67). Bacteria sense these environmental conditions directly or indirectly, leading to differential gene expression and metabolic activities within a genetically homogenous population (68). Variability in metabolic activity may affect clinically important behaviors; for example, persister cells are bacteria that are phenotypically tolerant to antibiotics, and one source of their tolerance is proposed to be metabolic inactivity (69). This and other types of antibiotic tolerance are thought to play a role in the persistence of many chronic infections, such as those suffered by people with the genetic disorder cystic fibrosis (CF). CF is characterized by chronic lung infection by bacteria in a biofilm mode of growth (65, 70, 71). One hypothesis as to the recalcitrance of these infections despite decades of aggressive antibiotic treatment is that a subpopulation of bacteria encased in self- or host-derived extracellular matrix resides in a state of metabolic quiescence, leading to antibiotic tolerance (72). Additional sources of phenotypic heterogeneity unrelated to the physiochemical environment bacteria experience within a biofilm include bistability (73) and stochasticity (74) of gene expression, unequal partitioning of proteins during cell division due to low abundance (74), epigenetic modifications resulting in phase variation (75), or through asymmetrical cell division (76). Together, these sources of phenotypic heterogeneity lead to cooperation between cells and promote the fitness of a clonal population of bacterial cells in the face of an ever-changing environment (77).

However, not all social interactions are cooperative in biofilms. The vast majority of naturally-occurring bacterial biofilms consist of a consortium of bacteria, fungi, and viruses. In these polymicrobial communities, antagonistic interactions are common and serve to shape the biofilm's community composition, as well as its interaction with its

environment. A growing body of literature suggests that most bacteria posses contact-dependent and/or -independent mechanisms of competing with their neighbors for space and resources (78). Contact independent competition occurs through the production of diffusible small molecule antibiotics, antimicrobial peptides, and proteinaceous toxins that target neighboring cells (79). *P. aeruginosa* can sense non-Pseudomonads in its environment and respond by upregulating antagonistic behaviors, many of which lead to enhanced *P. aeruginosa* virulence during polymicrobial infection. For example, in response to sensing peptidoglycan from gram positive bacteria, *P. aeruginosa* upregulates production of the phenazine antimicrobial pyocyanin (80), which is toxic both to other microbes and to eukaryotic cells (81). In addition to sensing other bacteria, *P. aeruginosa* is able to sense kin cell lysis through the orphan sensor kinase RetS, which activates the Gac/Rsm pathway to express its regulon of competitive (type VI secretion system and hydrogen cyanide) as well as defensive (polysaccharide production) mechanisms (82, 83). The contact-dependent type VI secretion system directly injects toxic effectors into neighboring bacterial cells (84). This broad repertoire of contact-dependent and independent mechanisms of interbacterial competition contribute *P. aeruginosa*'s role as a prominent pathogen in a variety of acute and chronic polymicrobial infections.

Summary and Objective

In order to understand the recalcitrance of *P. aeruginosa* to eradication or suppression during infection, it is necessary to examine the diversity of social interactions bacterial cells have with each other and their environment. The goal of my doctoral thesis work in the Parsek and Hoffman labs has been to identify inter- and intra-species interactions that influence *P. aeruginosa* biofilm formation. In chapter one, I describe a novel inter-species function for the adhesin Staphylococcal protein A in influencing *P. aeruginosa* biofilm formation and killing by immune cells. In chapter two, I describe a *P. aeruginosa* protein that binds a small molecule from *S. aureus* and many other non-Proteobacteria, leading to enhanced *P. aeruginosa* biofilm formation. In chapter three, I describe how a genetically homogenous population of *P. aeruginosa* cells diversifies upon initial surface attachment into subpopulations of cells with high- and low-c-di-GMP, leading to a division of labor during early biofilm formation. This work provides a

glimpse into the sociality of bacteria and has contributed to the growing body of literature detailing how bacterial interactions drive the composition and function of biofilms.

CHAPTER I

Staphylococcus aureus Protein A Mediates Interspecies Interactions at the Cell Surface of *Pseudomonas aeruginosa*

Published as: Armbruster, C.R., Wolter, D.J., Mishra, M., Hayden, H.S., Radey, M.C., Merrihew, G., MacCoss, M.J., Burns, J., Wozniak, D.J., Parsek, M.R., Hoffman, L.R. *mBio*. 7(3):e00538-16.

Abstract

While considerable research has focused on the properties of individual bacteria, relatively little is known about how microbial interspecies interactions alter bacterial behaviors and pathogenesis. *Staphylococcus aureus* frequently co-infects with other pathogens in a range of different infectious diseases. For example, co-infection by *S. aureus* with *Pseudomonas aeruginosa* occurs commonly in people with cystic fibrosis and is associated with higher lung disease morbidity and mortality. *S. aureus* secretes numerous exoproducts that are known to interact with host tissues, influencing inflammatory responses. The abundantly secreted *S. aureus* protein A (SpA) binds a range of human glycoproteins, immunoglobulins, and other molecules, with diverse effects on the host, including inhibiting phagocytosis of *S. aureus* cells. However, the potential effects of SpA and other *S. aureus* exoproducts on co-infecting bacteria have not been explored. Here we show that *S. aureus* secreted products, including SpA, significantly alter two behaviors associated with persistent infection. We found that SpA inhibited biofilm formation by specific *P. aeruginosa* clinical isolates, and it also inhibited phagocytosis by neutrophils of all isolates tested. Our results indicate that these effects were mediated by binding to at least two *P. aeruginosa* cell surface structures—type IV pili and the exopolysaccharide Psl— that confer attachment to surfaces and to other bacterial cells. Thus, we found that the role of a well-studied *S. aureus* exoproduct, SpA, extends well beyond interactions with the host immune system. Secreted SpA alters multiple persistence-associated behaviors of another common microbial community member, likely influencing co-colonization and co-infection with *S. aureus*.

Significance

Bacteria rarely exist in isolation, whether on human tissues or in the environment, and they frequently co-infect with other microbes. However, relatively little is known about how microbial interspecies interactions alter bacterial behaviors and pathogenesis. We identified a novel interaction between two bacterial species that frequently infect together—*Staphylococcus aureus* and *Pseudomonas aeruginosa*. We show that the *S. aureus* secreted protein Staphylococcal protein A (SpA), which is well-known for interacting with host targets, also binds to specific *P. aeruginosa* cell-surface molecules

and alters two persistence-associated *P. aeruginosa* behaviors: biofilm formation and uptake by host immune cells. Because *S. aureus* frequently precedes *P. aeruginosa* in chronic infections, these findings reveal how microbial community interactions can impact persistence and host interactions during co-infections.

Introduction

The majority of research on bacterial infections has focused on individual species. However, many diseases are caused by consortia of co-infecting microbes. For example, *Staphylococcus aureus* is an opportunistic pathogen that frequently infects along with other bacteria in a range of diseases (19, 85). Many of the most common and devastating of these infections afflict the heart, blood vessels, and lungs (86, 87) (particularly those of transplant and cystic fibrosis (CF) patients (88)), as well as skin wounds, medical devices, and the urinary tract (89, 90). These infections frequently result in chronic persistence (27) and dissemination (91), two disease characteristics that are often attributed to the formation of biofilms: dense aggregates of bacteria encased in a protective extracellular matrix (1). Biofilm matrix composition differs among species, but generally includes exopolysaccharides (EPS), proteins, and extracellular DNA (eDNA) (92). While biofilm matrices have traditionally been thought to play a primarily passive, structural role, recent studies have identified additional matrix functions, such as selectively retaining bioactive proteins (93) and even acting as a signaling molecule (22).

The airways of CF patients' lungs are host to chronic infections that are typically polymicrobial. While *S. aureus* is the bacterium cultured most frequently from CF patient sputum samples, *P. aeruginosa* is increasingly prevalent as patients age (94). Co-infection with *P. aeruginosa* and *S. aureus* occurs in approximately 40% of US children with CF (95) and has been associated with increased airway inflammation(96), reduced lung function, and increased mortality (97). These infections are notoriously persistent despite aggressive antibiotic treatment and robust host inflammation, and evidence indicates that biofilm formation contributes to this recalcitrance (71, 98, 99).

Studies have found that *P. aeruginosa* and *S. aureus* can alter each other's behavior *in vitro,* suggesting that co-infection could impact each species' pathogenesis and persistence (23, 80, 100–102). Most of the research on these interactions has focused

on how *P. aeruginosa* influences *S. aureus* (23, 80, 100, 103). For example, *P. aeruginosa* secreted products can inhibit the growth of *S. aureus*, influencing its response to antibiotics (100). *P. aeruginosa* exoproducts can lyse *S. aureus* and extract its iron stores for growth (101), as well as induce airway epithelial cells to kill *S. aureus* and other gram-positive bacteria (104). Therefore, many of the known interactions between these two species are mediated by *P. aeruginosa* exoproducts. By comparison, the impact of *S. aureus* on *P. aeruginosa* behavior is less understood. As *S. aureus* usually infects at high densities when *P. aeruginosa* is acquired during CF and other infections (94), studying the impact of *S. aureus* on *P. aeruginosa* behaviors has the potential to reveal whether *S. aureus* influences downstream infection by *P. aeruginosa*.

S. aureus secretes a large repertoire of exoproducts that could affect other bacteria and the host. This list includes 21 different extracellular adhesins (which bind a variety of host targets), a large variety of enzymes (including proteases, autolysins, and nucleases) and small molecules (such as pore-forming exotoxins and surfactant peptides), extracellular DNA, and a polysaccharide (105). Together, these *S. aureus* molecules can mediate attachment to and invasion of eukaryotic cell surfaces, as well as evasion of the host immune response, leading to persistent and recurring infections. However, how these factors impact the microbes that frequently co-infect with *S. aureus* has not been explored.

The goal of this study was to evaluate the potential of *S. aureus* extracellular products to influence *P. aeruginosa* behaviors relevant for persistent infection, including biofilm formation and survival against the host immune response. To identify *S. aureus* products that interact with *P. aeruginosa,* we first used a high-throughput biofilm assay to screen a collection of *P. aeruginosa* CF clinical isolates for alteration of biofilm formation when exposed to *S. aureus* cell-free culture supernatant. Here we report the first evidence of a role for a well-studied *S. aureus* adhesin, SpA, in mediating bacterial interspecies interactions and for altering the interaction of another bacterial species with host immune cells. We found that SpA exerts these effects by binding to *P. aeruginosa* cell-surface targets. These findings highlight the importance of considering the role of bacterial exoproducts, which have been traditionally studied in pure culture, in multispecies infections.

Results

S. aureus alters *P. aeruginosa* biofilm formation.

In order to identify interspecies interactions relevant to establishing a chronic infection, we initially screened a small collection of *P. aeruginosa* respiratory isolates from children with CF for altered biofilm formation during co-culture with the lab strain *S. aureus* SA113 (106), and also in SA113 cell-free culture supernatant (SA113 Sup). We observed that co-culture with *S. aureus* resulted in a significant decrease in biofilm biomass formed by many of the *P. aeruginosa* clinical isolates (9 of 24 isolates tested, Table 2) compared to that formed by these isolates when grown in pure culture (Figure 1a). Plating experiments showed the resulting biofilms to be comprised almost entirely of *P. aeruginosa* (data not shown). Furthermore, culture supernatant derived from SA113 inhibited *P. aeruginosa* biofilm formation on plastic surfaces as well as did co-culture, indicating that biofilm inhibition activity was attributable to a molecule released by *S. aureus* into the media (Figures 1b-c). Notably, inhibited isolates still formed air-liquid interface aggregates (pellicles) in SA113 supernatant, suggesting that the observed biofilm inhibition was due to decreased attachment to abiotic surfaces, but not decreased cell-cell adhesion.

To determine whether other *S. aureus* strains were able to inhibit *P. aeruginosa* biofilm formation, we measured biofilm formation by *P. aeruginosa* clinical isolate 102-21 in cell-free supernatants from two additional *S. aureus* laboratory strains and from 7 CF *S. aureus* isolates from the same children from whom the *P. aeruginosa* were collected (including two isolates from Patient 102, the source of the test *P. aeruginosa* isolate). All supernatants tested had the same inhibitory activity as SA113 (Supplemental Table 3).

S. aureus secretes protein(s) responsible for biofilm inhibition.

To identify the molecule(s) in *S. aureus* supernatant responsible for *P. aeruginosa* biofilm inhibition, we first subjected SA113 Sup to various physical and chemical treatments in an attempt to abrogate the inhibition of biofilm formation by *P. aeruginosa* 102-21. We found that boiling and proteinase K treatment eliminated biofilm inhibition by SA113 Sup (Figure 5). Centrifugation with molecular weight cutoff filters indicated that the molecule(s) conferring biofilm inhibition activity was larger than 30kDa (Figure

5). Biofilm inhibition activity was not impacted by treatment of the supernatant with either Dnase I or Rnase (Figure 5). These data suggest that biofilm inhibition is attributable to at least one protein larger than 30kDa.

The secreted protein SpA is responsible for *P. aeruginosa* biofilm inhibition.

In order to identify the protein(s) responsible for inhibiting biofilm formation, *S. aureus* SA113 supernatant was fractionated by size exclusion chromatography and the fractions were tested for biofilm inhibitory activity. LC-MS/MS was performed on the four fractions that inhibited *P. aeruginosa* biofilm formation (Figure 6), as well as on total supernatant and 3 inactive fractions. The normalized spectral abundance factor (NSAF(107)) was used to characterize the relative abundances of specific proteins in active fractions compared to inactive fractions. The NSAF for a *S. aureus* adhesin, Staphylococcal protein A (SpA), was increased tenfold in active versus inactive fractions (NSAF of 0.2 in active, 0.02 in control), identifying it as a candidate biofilm inhibitor. SpA is one of a variety of broadly-adhesive extracellular proteins produced by *S. aureus* known as "microbial surface components recognizing adhesive matrix molecules", or MSCRAMMs. While most studies of SpA have focused on the fraction that is covalently anchored to the cell wall, a significant amount of SpA is known to be released into the extracellular milieu during growth (108, 109).

To determine if SpA directly inhibits *P. aeruginosa* biofilms, we constructed a clean deletion of the *spa* gene in two *S. aureus* genetic backgrounds that produced inhibitory activity, SA113 and HG003. Biofilm inhibition of *P. aeruginosa* 102-21 by supernatants from these mutants was greatly reduced compared to inhibition by wild-type supernatants (Figure 2a). Additionally, purified SpA directly added to unconditioned medium resulted in biofilm inhibition (Figure 2b). It is possible that other MSCRAMMs produced by *S. aureus*, a few of which were identified in total SA113 Sup by LC-MS/MS but not enriched in active fractions (data not shown), could also inhibit *P. aeruginosa* biofilm formation. Thus, we tested five MSCRAMM transposon insertion mutants and their parent strain, *S. aureus* JE2. Of these, only mutants defective for SpA production significantly lost biofilm inhibition activity (Figure 7). Therefore, SpA was primarily responsible for biofilm inhibition by *S. aureus* supernatant.

SpA binds to Psl and Type IV pili on the *P. aeruginosa* cell surface.

We hypothesized that SpA inhibited *P. aeruginosa* biofilm formation by binding to specific targets on the cell surface required for surface adhesion. To test this hypothesis, we compared the abilities of representative *P. aeruginosa* isolates that did and did not exhibit biofilm inhibition (102-21 and 102-2, respectively) to bind fluorescently-labeled SpA (FITC-SpA). We found that 102-2 bound an amount of FITC-SpA comparable to that bound by wild type laboratory strain PAO1 (which also does not exhibit biofilm inhibition), and that each bound more SpA than 102-21 (Figure 8a). Therefore, the isolate that exhibited biofilm inhibition (102-21) bound the least SpA of the three tested, suggesting that this isolate lacks one or more SpA binding targets present in uninhibited isolates.

To identify the binding targets of FITC-SpA on *P. aeruginosa*, we screened a collection of PAO1 mutants and over-expression strains for relative SpA binding. *P. aeruginosa* produces at least three exopolysaccharides, two of which play a role in biofilm formation by non-mucoid strains (Pel and Psl (37). We found that overexpression of the Psl, but not Pel, exhibited increased FITC-SpA binding (Figure 3a), suggesting that SpA bound to Psl. Similarly, a mutant known to overproduce Psl (MPAO1 Δ*wspF*) exhibited enhanced FITC-SpA binding relative to wild type, but a deletion of the *pslD* gene in the Δ*wspF* genetic background abrogated this effect (MPAO1 Δ*wspF* Δ*pslD;* Figure 8b). To further test whether SpA binds Psl, we performed co-immunoprecipitations with SpA-coated beads followed by immunoblots with anti-Psl antibody, and demonstrated SpA-Psl binding (Figure 9a).

Additionally, we found that SpA bound a component of the type IV pilus, PilA (Figure 3b), but not to FliC, an external protein component of flagella (Figure 8c). We confirmed that SpA binds PilA by co-immunoprecipitation followed by a western blot for the PilA protein (Figure 9b). The PilA protein was present in our co-immunoprecipitation from two strains producing type IV pili (wild type PAO1 and PAO1 Δ*pilT*), but absent in negative controls (PAO1 ΔpilA and supernatant from PAO1 Δ*pilT* to which SpA was not added). Additionally, binding of SpA to PilA was confirmed by LC-MS/MS analysis of the SpA immunoprecipitate (NSAF 0.3 in co-IP, 0.2 in PAO1 supernatant loading control). In contrast, the LC-MS/MS analysis did not identify FliC as a SpA binding

partner (NSAF of 0.03 in co-IP, 0.2 in PAO1 supernatant loading control), in support of the FITC-SpA experimental results.

***P. aeruginosa* Psl production impacts biofilm inhibition by *S. aureus* supernatant.**

To investigate the genetic relationships between inhibited and uninhibited *P. aeruginosa* isolates, we performed pulsed-field gel electrophoresis (PFGE) on the *P. aeruginosa* isolates collected from Patient 102 over the course of 2 years (n=16). While all of the PFGE patterns among these isolates were highly similar, indicating they arose from a single lineage, the isolates could be placed into 3 PFGE groups based on a single band shift (Figure 10a). Isolates that did not display biofilm inhibition had one of two patterns (Pattern 1: 22 isolates, Pattern 2: 2 isolates), and these patterns differed by a downward shift in the largest band. Strains that displayed biofilm inhibition in SA113 Sup exhibited an additional downward shift of this PFGE band compared to Pattern 2 isolates (Pattern 3: 9 isolates), suggestive of an additional, larger genomic deletion in the *P. aeruginosa* isolates that displayed the biofilm inhibition phenotype.

We hypothesized that inhibited strains were missing genetic material that protects against biofilm inhibition by *S. aureus*. To better define the genetic differences between these isolates, and to characterize the genomic deletion suggested by PFGE, we sequenced the genomes of isolates representing each PFGE pattern from Patient 102: 102-2 (Pattern 1; not inhibited), 102-26 (Pattern 2; not inhibited), 102-21 (Pattern 3; inhibited), 102-30 (Pattern 3; inhibited). In the Pattern 3 isolates, we identified a large genomic deletion, encompassing 202 genes, corresponding to the subsequent PFGE shift relative to Pattern 2 described above (Figure 10b). Based upon our knowledge of genetic determinants that influence *P. aeruginosa* biofilm formation, one set of genes of interest that were absent in the Pattern 3 isolates was the entire Psl biosynthetic operon. As expected, these isolates did not produce Psl (Figure 10c). Nevertheless, the inhibited isolates still formed pure culture biofilms at levels equivalent to their clonally-related, non-inhibited, Psl-producing counterparts (Table 2). These data suggest an important role for Psl in the biofilm-inhibitory effect of *S. aureus* supernatant. In support of this hypothesis, the 9 *P. aeruginosa* isolates (collected from 3 different patients) that displayed biofilm inhibition did not produce appreciable amounts of Psl, as measured by Psl immunoblot (Table 2).

Psl protects *P. aeruginosa* from biofilm inhibition by *S. aureus* supernatant.

Non-mucoid *P. aeruginosa* isolates were previously divided into four classes based on their dependencies on EPS for biofilm formation(35). To further investigate the role of Psl production in biofilm inhibition by *S. aureus*, we assayed a subset of *P. aeruginosa* isolates from both clinical and environmental sources that represented each of these four classes. We found that mutants defective for Psl production (Δ*pslD*) were inhibited for biofilm formation regardless of matrix usage class, whereas isogenic wild type strains that produced Psl were not inhibited (Table 2). Additionally, we found that whereas a PAO1 mutant lacking Psl is inhibited for biofilm formation by S. aureus supernatant (PAO1 Δ*pslD*), a mutant in SpA's other *P. aeruginosa* cell surface (type IV pili; PAO1 Δ*pilA*) is not inhibited in *S. aureus* supernatant (Figure 10d). Together with the clinical isolate observations, these results indicate that Psl protects *P. aeruginosa* from biofilm inhibition by *S. aureus*.

SpA reduces phagocytosis of *P. aeruginosa* by neutrophils. While the *in vitro* biofilm assay provided a convenient platform for identifying *P. aeruginosa* cell-surface targets of SpA binding, and biofilm formation on abiotic surfaces is likely important for some chronic infections, the relevance of this model for CF and other chronic infections without abiotic surfaces is less clear. In contrast, each of these chronic infections is characterized by a marked host response. SpA is known to influence host immune responses to *S. aureus*. For example, *S. aureus* surface-associated SpA is known to protect *S. aureus* cells from opsonization by host immunoglobulin G (IgG), and thus from neutrophil phagocytosis (110). SpA binds many mammalian IgG molecules at the nonvariable Fc region (111). Since SpA can bind to at least two abundant *P. aeruginosa* surface structures, Psl and PilA, we hypothesized that extracellular SpA would also protect *P. aeruginosa* from neutrophil phagocytosis by inhibiting opsonization by IgG. To test this hypothesis, we measured neutrophil phagocytosis of *P. aeruginosa* when opsonized with anti-*Pseudomonas* antibody in the presence and absence of SpA (Figure 4a). We found that the addition of SpA significantly altered IgG-mediated neutrophil phagocytosis; however, further mechanistic insight came from altering the order of addition of antibody and SpA. Opsonizing *P. aeruginosa* with IgG prior to incubating with SpA (followed by washing) led to decreased phagocytosis of wild-type MPAO1 by

neutrophils, presumably because exposed Fc receptors on *Pseudomonas*-bound antibody were then "capped" by SpA, preventing uptake. Furthermore, incubation with SpA prior to opsonization (analogous to the effect of membrane-associated SpA on *S. aureus* cells) decreased uptake by neutrophils by approximately 60% in wild-type MPAO1 (the strain that binds the most SpA).

To determine whether SpA protection against neutrophil uptake was mediated by its association with Psl and PilA when pre-incubated with *P. aeruginosa* prior to antibody challenge, we repeated the phagocytosis experiments in MPAO1 Δ*pslD* Δ*pilA*. Opsonization prior to adding SpA protected this mutant from phagocytosis similar to that for wild-type MPAO1. In contrast with wild-type MPAO1, however, pre-incubating this mutant with SpA prior to opsonization did not significantly decrease uptake by neutrophils (Figure 4a and 4b IV), suggesting that this mechanism of protection requires the presence of cell surface binding targets for SpA.

Together, these results suggested that SpA inhibited neutrophil phagocytosis of *P. aeruginosa* by at least two mechanisms: (1) by blocking antibody pre-bound to *P. aeruginosa* from being recognized by neutrophils (Figure 4b I, III), and (2) analogous to its function on the *S. aureus* cell surface, by binding antibody such that the Fc region was obscured from recognition by the neutrophils' Fc receptor (Figure 4b, II). Therefore, SpA protects at least one bacterial species other than *S. aureus* against IgG-mediated neutrophil phagocytosis when attached to the bacterial cell surface.

Discussion

We found that the *S. aureus* extracellular adhesin SpA binds to specific cell-surface targets of *P. aeruginosa,* impacting its persistence-related behaviors. Co-infection with these two organisms is common in CF; in a recent study among our local pediatric CF population, 40% of patients were co-infected with *P. aeruginosa* and *S. aureus* over a two-year period (95). It has been suggested that early infection by *S. aureus* may prime the airway for future infection by *P. aeruginosa* (112, 113). In two separate studies, detection of *S. aureus* was a risk factor for earlier infection with *P. aeruginosa* (114, 115). Our results indicate that *S. aureus* may impact the adhesion and phagocytosis of *P. aeruginosa in vivo* through secreted products, particularly SpA, which is known to be highly expressed during growth of CF *S. aureus* clinical isolates in a medium that mimics

CF sputum (116). SpA is an important *S. aureus* virulence factor that is known to play multiple roles in mediating the interaction of *S. aureus* with eukaryotic cell targets within the host environment. This study provides the first evidence of an additional role for extracellular SpA in mediating bacterial interspecies interactions, and for influencing the interaction of another bacterial species with the host.

Our results also indicate that SpA interacts with two specific structures on the *P. aeruginosa* cell surface: the Psl polysaccharide and the PilA protein component of type IV pili, both of which are known to be important determinants for *P. aeruginosa* biofilm formation (30, 37). Furthermore, our results demonstrate that SpA inhibits biofilm formation by *P. aeruginosa* strains that do not produce Psl, and that SpA binding to type IV pili, but not to Psl, inhibits biofilm formation. Psl and type IV pili are known to affect biofilm formation in complex, connected ways. For example, type IV pili are known to contribute only to the earliest stage of biofilm formation (surface attachment) in strains not producing Psl (e.g. PA14) (30), but in Psl-producing strains, type IV pili also contribute to later stages of biofilm formation (32). Therefore, Psl protection against SpA-mediated biofilm inhibition could occur via two different, but not mutually exclusive mechanisms. First, Psl may "mask" or otherwise out-compete or prevent SpA binding to PilA, thereby leaving type IV pili free to contribute to biofilm development. Alternatively, the Psl polysaccharide itself may be sufficient to mediate cell attachment to surfaces, independent of SpA binding to type IV pili. *P. aeruginosa* forms different types of biofilms, including surface-associated communities and unattached aggregates. We found that SpA inhibited the former, but not the latter type of biofilm. While the relevance of abiotic surface-attached biofilms for CF infections is not known, this observation provided a convenient and sensitive assay for identifying cell-surface structures important for the effect of SpA on phagocytosis and, perhaps, other behaviors relevant to chronic infection.

Clinical isolates of *P. aeruginosa* defective for Psl production have not been previously described. However, *P. aeruginosa* populations are known to diversify phenotypically and genotypically during chronic infections, such as in CF, often impacting EPS production (117–119). We found that *P. aeruginosa* strains that produce high levels of Psl (rugose small colony variants (RSCVs) PAO1 Δ*fliC* and PAO1 Δ*wspF;*

Figure 9c) hyper-bind extracellular SpA *in vitro*. As clinical isolates with this EPS hyperproduction phenotype are isolated frequently from CF patients (120), it is possible that this interaction with SpA may serve to protect a diverse population of *P. aeruginosa* isolates from opsonophagocytosis in polymicrobial infections. Future work will be required to identify whether *P. aeruginosa* biofilm matrix production phenotypes impact the persistence of one or both species during co-infection, and the extent to which an interaction of the Psl polysaccharide with extracellular SpA is involved.

SpA is often described as a multifunctional virulence factor, and among its best-known binding targets is the Fcγ domain of mammalian IgGs. For SpA associated with the *S. aureus* cell surface, Fcγ binding results in coating of the *S. aureus* cell surface with IgG molecules oriented "outward", such that they cannot bind to the neutrophil Fc receptor (105), preventing Fc receptor-mediated opsonophagocytosis and bacterial killing (121). Here, we found that SpA can perform a similar function for other bacteria: SpA protected *P. aeruginosa* from IgG-mediated neutrophil opsonophagocytosis *in vitro,* and full protection required the presence of both Psl and PilA. SpA's ability to bind to the Psl polysaccharide suggests that the *P. aeruginosa* EPS matrix could selectively retain SpA. However, the contribution of extracellular SpA to multifactorial behaviors like bacterial persistence, particularly in a polymicrobial community, remains largely understudied.

We found that exogenous addition of SpA subsequent to opsonization of *P. aeruginosa* by IgG impeded phagocytosis by neutrophils regardless of whether the *P. aeruginosa* strain expressed either Psl or type IV pili. Under these conditions, we predict that SpA binds to and blocks the exposed Fc region on IgG, thus rendering it unavailable for binding by a neutrophil Fc receptor, an early step in initiation of IgG-mediated phagocytosis (Figure 4b I, III). It is likely that this protective effect of extracellular SpA is broadly applicable to other bacterial species when co-infecting with *S. aureus* in a polymicrobial infection independent of the bacterium's ability to bind SpA on its cell surface. Second, and more specific to *P. aeruginosa*, we found that SpA bound to the cell surface of *P. aeruginosa* prior to exposure to IgG significantly reduced phagocytosis by neutrophils. We showed that this effect was dependent on the ability of SpA to bind to the cell surface of *P. aeruginosa*: phagocytosis of a strain of *P. aeruginosa* incapable of producing either Psl or type IV pili was unaffected by pre-incubation with SpA.

Therefore, our results suggest that *P. aeruginosa* is able to share the protective benefit of extracellular SpA produced by *S. aureus*, resulting in a reduction in IgG-mediated phagocytosis of *P. aeruginosa* by neutrophils, through at least two mechanisms. While protective *in vitro* interactions between these two species have been previously observed (23, 100, 122), none have involved a manipulation of the host immune response.

In addition to identifying a new interspecies role for SpA, our findings also suggest a novel social role for Psl, in which this EPS interacts with nearby bacterial species through their exoproducts. Specifically, production of Psl determines the ability of a *P. aeruginosa* strain to attach to surfaces and influences neutrophil uptake of opsonized *P. aeruginosa* cells when SpA is present. While SpA bound to the cell surface of *P. aeruginosa* retains at least one important known function, protection from IgG-mediated phagocytosis, further work to define whether SpA retains any of its additional known functions when bound to *P. aeruginosa* (such as binding to von Willebrand factor (123) or tumor necrosis factor-a receptor 1 (124)) will allow us to better understand the full scope of this interspecies interaction and its relevance for a variety of diseases. Given that bacteria rarely exist in isolation, whether on human tissues or in the environment, these results underscore the need for more work to define the collective function of extracellular microbial virulence factors in polymicrobial systems.

Methods

Bacterial Strains and Media. Bacterial isolates and plasmids used in this study are listed in Table 1. Unless otherwise noted, strains were grown at 37°C in Luria-Bertani (LB, Becton Dickinson) broth buffered with 50mM MOPS, pH 7.0 (LB MOPS). Clinical bacterial isolates identified in Table 1 were collected as part of a single-center clinical study of children with CF (95) approved by the Seattle Children's Hospital IRB (#12496). For plasmid selection, 10μg/ml erythromycin (Sigma-Aldrich, St. Louis, MO) or 10 or 12.5μg/ml chloramphenicol (Sigma-Aldrich, St. Louis, MO) was used with *S. aureus* and12.5μg/ml chloramphenicol was used with *Escherichia coli*.

Screen for Altered Biofilm Phenotypes in *S. aureus* Supernatant. We screened 24 *P. aeruginosa* clinical isolates from 9 pediatric cystic fibrosis patients for altered biofilm formation in *S. aureus* cell-free culture supernatant, as measured by the crystal violet

(CV) attachment assay in microtiter plates (Nunc, Thermo Scientific, Waltham, MA). Biofilm "inhibition" was defined as a statistically significant decrease ($p < 0.05$) in biofilm biomass as measured by the CV assay in *S. aureus* SA113 supernatant over the same strain grown in LB MOPS.

DNA Macrorestriction Analysis of Patient 102 *P. aeruginosa* Isolates

Genetic relatedness of the clinical isolates was determined by Pulsed-field Gel Electrophoresis (PFGE) according to the Centers for Disease Control and Prevention PulseNet protocol (125). Chromosomal DNA was digested with 30 U of *Spe*I (Roche) at 37°C for 16 hr. The DNA restriction fragments were separated in a 1% SeaKem Gold agarose gel using a CHEF DR-III (Bio-Rad) with the following conditions: field strength 6 V/cm, angle 120°, initial switch time 1 s, final switch time 35 s, total run time 23 hr. at 14°C. DNA restriction patterns were analyzed using BioNumerics software (v. 6.5; Applied Maths, Sint-Martens-Latem, Belgium). The dendrogram was constructed by the UPGMA (Unweighted Pair Group Method with Arithmetic mean) clustering method and Dice similarity coefficients with an optimization setting of 0.5% and position tolerance of 1.0%.

Whole Genome Sequencing of Patient 102 *P. aeruginosa* isolates

For each genome either a random-fragment library was constructed using a custom paired-end protocol (126) or standard Illumina Nextera libraries were constructed according to manufacturer's guidelines (Illumina Inc., San Diego, CA). Paired-end libraries for each genome were used to generate 76 bp or 100 bp reads with the Illumina GAIIx or HiSeq 2000, respectively (coverage > 100 reads/genomic position). Sequencing of libraries was performed according to manufacturer's standards (Illumina Inc., San Diego, CA). Draft genome assemblies were generated with ABySS 1.3.4 (127) using the complete PAO1 genome (NC_002516) as a reference. Genomes were annotated using the Prokaryotic Genome Analysis Tool (PGAT)(128), which grouped all genes into orthologous gene families (genes within a family share at least 96% homology and 80% coverage of the total gene sequence). Gene family annotation was based on previously annotated genomes, including PAO1, PA14 and LESB58, when available. Open reading frames (ORFs) in regions lacking known genes were predicted using Prodigal (129), and new gene families were annotated based on searches in the National Center for

Biotechnology Information (NCBI) Conserved Domain Database (CDD) (130). Annotated genomes can be viewed at http://tools.nwrce.org/pgat/.

S. aureus Supernatant Treatment and Bioassay-guided fractionation. *S. aureus* cell-free supernatant was subjected to the following treatments in order to characterize the biofilm inhibition signal: boiling, Proteinase K (Sigma-Aldrich, St. Louis, MO), Dnase I (NEB, Ipswitch, MA), Rnase I (Thermo Scientific, Waltham, MA), and molecular weight cutoff filters (Amicon, Sigma-Aldrich, St. Louis, MO). Crystal violet assays were performed with PA102-2 and PA102-21 as previously described, to test for retention of biofilm-inhibitory activity in the supernatant after each treatment. *S. aureus* SA113 was inoculated to an OD_{600} of 0.05 from mid-log cells and grown shaking at 37°C for 6 hours in LB broth buffered with 50mM MOPS (LB MOPS). Supernatant was harvested by pelleting cells in a centrifuge at 4°C and filter-sterilizing the supernatant with a 0.22 µm low protein binding filter. CV attachment assays were performed in 96 well plates using mid-log *P. aeruginosa* diluted to an OD_{600} of 0.05 in either LB MOPS or in SA113 cell-free supernatant. Plates were incubated at 37°C for 2, 4, or 6 hours without shaking. To assay for biofilm formation, the liquid culture was removed without disturbing the pellicle and wells were rinsed gently with ddH_2O to remove planktonic cells. After staining for 10 minutes with 0.1% crystal violet, wells were rinsed gently with ddH_2O. Crystal violet was eluted from the biofilm biomass with 95% ethanol for 10 minutes, then transferred into a new 96 well plate and absorbance read at 595nm. Six replicate wells were used for each condition. For supplemental figure S.6e, purified SpA and purified Psl were pre-incubated in sterile water for 30 minutes at room temperature on a rotator, then added at a final concentration of 10µg/mL SpA and 100µg/mL Psl into LB MOPS for the crystal violet assay.

Size exclusion fast protein liquid chromatography (FPLC) was performed using a HiPrep 16/60 Sephacryl S200 (GE Healthcare) column and each fraction was screened for biofilm-inhibitory activity against PA102-21 in the CV assay. *S. aureus* cell-free supernatant was fractionated with a 3kDa MWCO filter and the fraction containing molecules >3kDa was resuspended in LB MOPS to one half of the initial volume. Five milliliters of this concentrated sample was applied onto the gel filtration column and eluted in LB MOPS at a flow-rate of 0.5 ml/min at 4°C, with 4mL per fraction. Each

fraction was screened for biofilm-inhibitory activity against PA102-21 in the CV assay. Inhibitory fractions were defined as having an average biofilm biomass (OD_{595}) of less than 1 standard deviation below the mean biofilm biomass of all supernatant fractions. Six inhibitory fractions and three non-inhibitory control fractions were chosen for LC-MS/MS.

Identification of Candidate Biofilm-Inhibitory Proteins by Mass Spectrometry (LC-MS/MS).

Total protein in each of the 9 fractions from size exclusion FPLC were denatured in RapiGest (Waters), reduced, alkylated, and digested with trypsin. One microgram of each sample was loaded onto a 75µm inner diameter fused silica capillary (Polymicro) loaded with 30cm of Jupiter Proteo 5 µm reverse-phase material (Phenomenex). Nanoflow liquid chromatography was performed using the Waters nanoACQUITY UPLC system, eluting the peptides over a 180 minute gradient of increasing acetonitrile at a flow rate of 250nL/min. Peptides were ionized via electrospray ionization with a home-built ESI source and analyzed with a Thermo LTQ-FT mass spectrometer. Accurate mass and charge predictions were determined for MS/MS fragmentation spectra using Hardklör and Bullseye (131) algorithms. SEQUEST 2.7 software (132) was used to identify peptides against the *S. aureus* NCTC 8325 FASTA database (SA113 parental strain) and false discovery rates were determined via a decoy database using Percolator (133). Peptides were assembled into protein identifications using ID Picker (134). Candidate biofilm-inhibitor proteins were identified based on their frequency of detection in active fractions compared to inactive control fractions, as determined by normalized spectral abundance factor (NSAF), with a focus on predicted extracellular proteins.

Construction of SA113 Δ*spa*

Chromosomal DNA upstream and downstream of *S. aureus* SA113 or HG003 *spa* was amplified via PCR using primers spaUpF01, spaUpR01, spaDownF01, and spaDownR01, then used as a template for SOE-PCR using primers spaUpF01 and spaDownR01. The *spa* deletion construct was cloned into the KpnI and NotI sites of the temperature sensitive vector pIMAY, creating plasmid pIMAY::Δ*spa* (spa deletion construct), then transformed into *E. coli* DH10B cells. The *spa* deletion construct was purified from DH10B cells, transformed into *S. aureus* RN4220, and maintained in RN4220 grown on

BHI with 10ug/mL chloramphenicol at 30°C. Cell lysates were prepared for transduction of the *spa* deletion construct into strain SA113 using bacteriophage phi-11 (135). Following passage at the permissive temperature of 30°C, colonies were screened for chromosomal integration of pIMAY::Δ*spa* by growing at 37°C with 10ug/mL chloramphenicol and PCR with MCS primers IM151 and IM152 to verify that colonies did not contain replicating pIMAY plasmid. To select for double recombination and excision of the pIMAY plasmid backbone from the chromosome, cells were grown overnight in BHI at 30°C, then screened for growth on BHI + 1ug/mL Anhydrotetracycline (Atc), but sensitivity to killing on BHI + 10ug/mL chloramphenicol. Deletion of *spa* was confirmed by PCR and sequencing with primers spaUPF-SEQ and spaDOWNR-SEQ.

Identification of SpA as biofilm inhibitor protein. Cell-free culture supernatant was prepared from SA113 Δ*spa* and the CV assay was repeated with PA102-2 and PA102-21. "Loss of biofilm inhibition" activity was defined as a statistically significant increase in PA102-21 biofilm biomass in SA113 Δ*spa* supernatant compared to wild type SA113 supernatant. Purified Staphylococcal Protein A (SpA; Sigma) was added into LB MOPS at 10 and 100 μg/mL and the CV assay was repeated with PA102-2 and PA102-21. "Biofilm inhibition" activity was defined as a statistically significant decrease in PA102-21 biofilm biomass in wells with purified SpA compared to LB MOPS alone and compared to wells with 10 and 100 μg/mL BSA (negative control).

Sequencing of 102 Series. Whole genome sequencing was performed on four clonally-related, clinical *P. aerigunosa* isolates: two biofilm-inhibited (102-21 and 102-30), and two non-inhibited (102-2 and 102-26) essentially as previously described(136). Annotated genomes can be viewed at http://tools.nwrce.org/pgat/.

Psl immunoblot assay. *P. aeruginosa* isolates were grown n LB MOPS overnight at 37°C with shaking (225rpm). The Psl immunoblot assay was performed as previously described(35).

FITC-SpA Binding Assay. *P. aeruginosa* isolates were grown to mid-log in LB MOPS. FITC-labeled SpA (Sigma-Aldrich, St. Louis, MO) was added to each culture at a final concentration of 100ug/mL. Cultures were incubated for 10 minutes at room temperature, then pelleted and washed three times with Phosphate Buffered Saline (PBS). The cell

suspension was transferred to a Costar flat bottom, black with clear bottom 96 well plate (Sigma-Aldrich, St. Louis, MO). Relative FITC-SpA binding of each strain was determined by calculating the relative fluorescence: the FITC fluorescence (excitation: 495, emission: 519) normalized to cell density (OD at 600nm).

Co-immunoprecipitations of SpA with PilA and Psl. Protein G dynabeads (Life Technologies, Carlsbad, CA) were incubated with 100ug/mL anti-SpA monoclonal antibody (Sigma-Aldrich, St. Louis, MO) following manufacturer's instructions, then incubated with 100ug/mL purified protein A (Sigma-Aldrich, St. Louis, MO) for 20 minutes at 4^{o}C. Beads were washed three times with Tris-buffered saline (TBS) plus 0.1% Tween and resuspended in TBS. To assay for SpA binding to Psl, wild type MPAO1, MPAO1 PBAD-psl with 1% arabinose, or MPAO1 Δ*pslD* were grown overnight in LB MOPS. Cultures were normalized for cell density, cells were pelleted, and the supernatant was saved for co-immunoprecipitation with SpA. Triton X-100 was added to each supernatant sample to a final concentration of 0.1% in supernatant. Co-immunoprecipitation reactions were incubated at 4^{o}C for 1 hour on a low-speed rotator. Beads were washed four times with washing buffer (TBS with 200mM NaCl and 0.1% Triton X-100), then resuspended in 0.5M EDTA, pH 8.0. Psl dot blots were performed as described above. For the PilA co-immunoprecipitation, the following strains were used: wild type MPAO1, MPAO1 Δ*pilT*, and MPAO1 Δ*pilA*. Supernatants from overnight cultures of each strain were spiked with 100ug/mL SpA and incubated on a rotator at 4^{o}C for 1 hour. Protein G dynabeads that had been pre-loaded with anti-SpA monoclonal antibody were added to each reaction, incubated at 4^{o}C on a rotator for 1 hour, then washed and resuspended in Laemmli buffer (Bio-Rad Laboratories, Hercules, CA). Proteins were run on an SDS-PAGE gel (Bio-rad), then transferred to a nitrocellulose membrane for Western blotting with anti-PilA polyclonal and an anti-SpA polyclonal antibody (Sigma-Aldrich, St. Louis, MO). For experiments with boiled *P. aeruginosa* supernatants, supernatant was taken from overnight cultures of wild type MPAO1, MPAO1 Δ*pslD*, and MPAO1 Δ*cdrA* grown in LB with 50mM MOPS. Supernatant samples were aliquoted into duplicate samples, then one set of samples was boiled for 25 minutes at 100^{o}C. Co-immunoprecipitations with purified SpA and Psl immunoblots were then performed as described above.

Identification of SpA binding target on the *P. aeruginosa* cell surface by Mass Spectrometry (LC-MS/MS).

Co-immunoprecipitations of SpA with *P. aeruginosa* supernatants were performed as described above and samples were run on an SDS-PAGE gel. Bands were cut from the gel, and LC-MS/MS was performed as described above, but using in-gel protein digests. Peptides were identified using a *P. aeruginosa* PAO1 FASTA database. An NSAF score greater than 0.05 was considered a SpA binding target.

Neutrophil isolation and phagocytosis assays

Human neutrophils were obtained from healthy adult donors using an approved IRB protocol (2009H0314) at The Ohio State University, isolated, and phagocytosis assays performed as previously described (137) using an anti-Pseudomonal antibody and 100μg/mL SpA.

Bacteria were taken from overnight plates, washed with PBS, and opsonized with anti-Pseudomonal antibody that was generated against whole surface antigens of PAO1 (1:100), either before or after 10 minute incubation with 100μg/mL purified SpA. Bacteria–neutrophil association was examined by confocal microscopy (Olympus FV 1000) using a 60× oil objective to directly visualize interactions between *P. aeruginosa* and neutrophils as previously described (137). Attached *P. aeruginosa* was distinguished from internalized bacteria, as *P. aeruginosa* cells attached to neutrophils and stained by fluorescently-labeled anti-Pseudomonal antibodies before permeabilization of neutrophils stained green, whereas internalized bacteria are counterstained red after neutrophil permeabilization. Image analysis software was used to count cell-associated versus internalized *P. aeruginosa* bacteria on 100 randomly selected neutrophils, and compared within each strain of *P. aeruginosa* (with versus without SpA pre-treatment), in three biological replicates.

Table 1. Strains, plasmids and primers used in this study.

***P. aeruginosa* Strains**		**Reference**
MPAO1	wild-type	Jacobs, 2003
MPAO1Δ*pslD*	*pslD* nonpolar mutant of MPAO1	Provided by J Harrison[a]
MPAO1Δ*pelC*Δ*pslD*	*pelC pslD* nonpolar mutant of MPAO1	Provided by J Harrison[a]
MPAO1Δ*pilA*Δ*pslD*	*pilA pslD* nonpolar mutant of MPAO1	Provided by J Harrison[a]
MPAO1 Δ*pilT*	*pilT* nonpolar mutant of MPAO1	Provided by J Harrison[a]
PAO1 P_{BAD}-pel	chromosomal replacement of the native promoter with *araC*-P_{BAD} promoter	Provided by J Harrison[a]
PAO1 P_{BAD}-psl	chromosomal replacement of the native promoter with *araC*-P_{BAD} promoter	Provided by J Harrison[a]
PA14	wild type	Rahme, 1995
E2	wild type	Wolfgang, 2003
E2 Δ*pslD*	*pslD* nonpolar mutant of E2	Colvin, 2012
MSH3	wild type	Wolfgang, 2003
MSH3 Δ*pslD*	*pslD* nonpolar mutant of MSH3	Colvin, 2012
CF127	wild type	Wolfgang, 2003
CF127 Δ*pslD*	*pslD* nonpolar mutant of CF127	Colvin, 2012
102-2	CF patient 102 sputum isolate	This Study[b]
102-5a	CF patient 102 sputum isolate	This Study[b]
102-5b	CF patient 102 sputum isolate	This Study[b]
102-6	CF patient 102 sputum isolate	This Study[b]
102-7	CF patient 102 sputum isolate	This Study[b]
102-8	CF patient 102 sputum isolate	This Study[b]
102-20	CF patient 102 sputum isolate	This Study[b]
102-21	CF patient 102 sputum isolate	This Study[b]
102-25	CF patient 102 sputum isolate	This Study[b]
102-26	CF patient 102 sputum isolate	This Study[b]
102-30	CF patient 102 sputum isolate	This Study[b]
102-34	CF patient 102 sputum isolate	This Study[b]
102-35	CF patient 102 sputum isolate	This Study[b]
102-36	CF patient 102 sputum isolate	This Study[b]
102-39	CF patient 102 sputum isolate	This Study[b]
102-40	CF patient 102 sputum isolate	This Study[b]
115-7	CF patient 115 sputum isolate	This Study[b]
151-10	CF patient 151 sputum isolate	This Study[b]
159-1	CF patient 159 sputum isolate	This Study[b]
71-22	CF patient 71 sputum isolate	This Study[b]
200-4	CF patient 200 sputum isolate	This Study[b]
134-2	CF patient 134 sputum isolate	This Study[b]

141-2	CF patient 141 sputum isolate	This Study[b]
166-1	CF patient 166 sputum isolate	This Study[b]
***S. aureus* Strains**		
SA113	wild type	Iordanescu, 1976
SA113 Δ*spa*	*spa* nonpolar mutant of SA113	This Study
HG003	wild type	Herbert, 2010
HG003 Δ*spa*	*spa* nonpolar mutant of HG003	This Study
S. aureus ATCC29213	wild type	Kim, 1997
S. aureus Newman	wild type	Duthie, 1952
SA47-34	CF patient 47 sputum isolate	This Study[b]
SA102-10	CF patient 102 sputum isolate	This Study[b]
SA37-12	CF patient 37 sputum isolate	This Study[b]
SA134-5	CF patient 134 sputum isolate	This Study[b]
SA102-12	CF patient 102 sputum isolate	This Study[b]
SA23-71	CF patient 123 sputum isolate	This Study[b]
SA200-3	CF patient 200 sputum isolate	This Study[b]
JE2	Wild type	Fey, 2013
JE2 Tn::*sbi*	Transposon inserted into *sbi*	Fey, 2013
JE2 Tn::*clfA*	Transposon inserted into *clfA*	Fey, 2013
JE2 Tn::*clfB*	Transposon inserted into *clfB*	Fey, 2013
JE2 Tn::*sdrD*	Transposon inserted into *sdrA*	Fey, 2013
JE2 Tn::*spa*	Transposon inserted into *spa*	Fey, 2013
RN4220 pIMAY:: Δ*spa*	restriction defective strain carrying plasmid with *spa* deletion allele	This Study
***E. coli* Strains**		
DH10B pIMAY:: Δ*spa*	cloning strain carrying plasmid with *spa* deletion allele	This Study
Primers		
spaUpF01	ATATGGTACCGTTTTGTAGAATTCACA ATTCTAGC	
spaUpR01	GTATTGTTTGTTTTTACAAATTAATACCCCCTGTATGTAT	
spaDownF01	GGGGTATTAATTTGTAAAAACAAACAATACACAACGATAG	
spaDownR01	ATATGCGGCCGCGAAGCAATTAAAGAATTATGG	
spaUPF-SEQ	GAGCGTAATACTTACATTTC	
spaDOWNR-SEQ	GCCAATTCCAAATACTGTG	
IM151	TACATGTCAAGAATAAACTGCCAAAGC	
IM152	AATACCTGTGACGGAAGATCAC	

	TTCG	
Plasmids		
pIMAY	Suicide cloning vector, chloramphenicol resistance	Monk, 2012
pIMAY::Δ*spa*	*spa* deletion vector	This study

[a]Kindly provided by Dr. J. Harrison, University of Calgary

[b]Collected from subjects enrolled in an ongoing, IRB-approved study (methods)

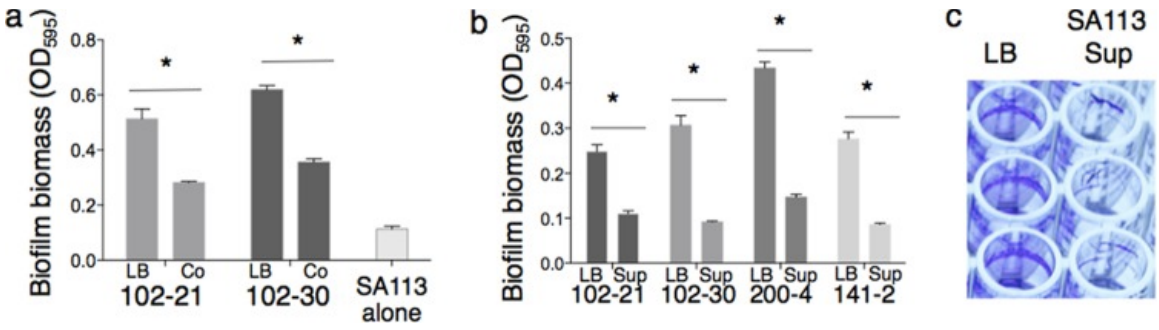

Figure 1. 1a) Clonally related *P. aeruginosa* isolates from Patient 102 exhibit inhibition of biofilm formation when grown in co-culture with *S. aureus* SA113, compared to monoculture in LB. All experiments shown are from crystal violet-stained biofilms after 4 hours of growth. Left bar = grown in LB. Right bar = grown in co-culture with SA113. 1b) *P. aeruginosa* respiratory isolates from multiple CF patients, including Patient 102, display biofilm inhibition when grown in *S. aureus* SA113 supernatant compared growth in LB. Experiments are from crystal violet-stained biofilms after 4 hours of growth. Left bar = grown in LB. Right bar = grown in SA113 supernatant. Asterisk indicates biofilm biomass of Patient 102 *Pa* isolates grown in SA113 supernatant differed significantly from that of each strain in LB ($p < 0.05$). 1c) A representative image of the biofilm inhibition phenotype in the crystal violet assay. The isolate shown is *P. aeruginosa* 102-21, after 4 hours of growth in buffered medium (LB-MOPS) or cell-free SA113 supernatant after growth in the same medium.

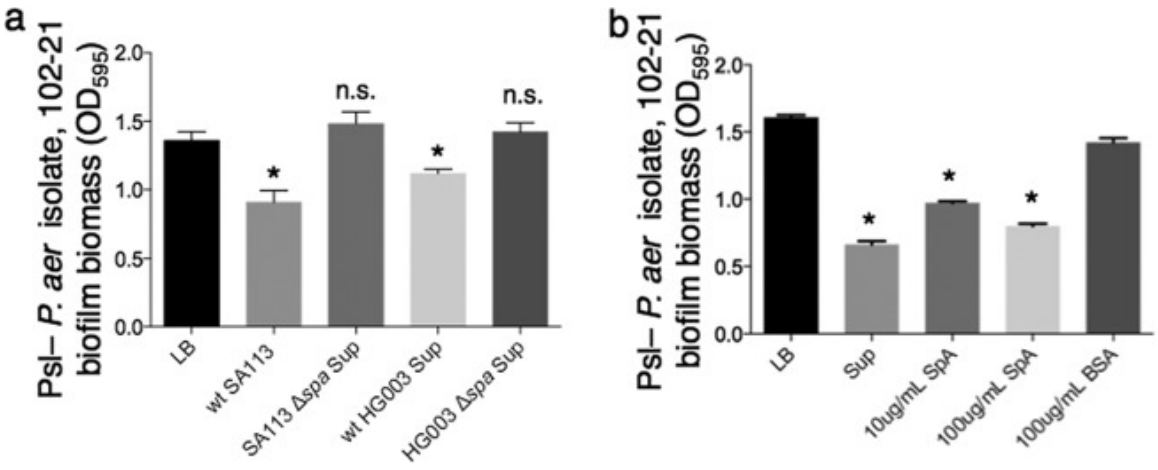

Figure 2. (a) Inhibition of biofilm formation by *P. aeruginosa* isolate 102-21 is lost in the absence of SpA. Culture supernatant from*S. aureus* lab strain HG003 exhibited biofilm inhibitory activity against isolate 102-21, but HG003 Δ*spa* supernatant did not. An asterisk indicates a significant difference in biofilm biomass compared to the LB control ($P < 0.05$); n.s., not statistically significant compared to the LB control ($P > 0.05$). (b) Purified SpA inhibited biofilm formation by Psl^{-} *P. aeruginosa* in a 4-h crystal violet assay. An asterisk indicates a significant difference in biofilm biomass compared to that of the LB control ($P < 0.001$).

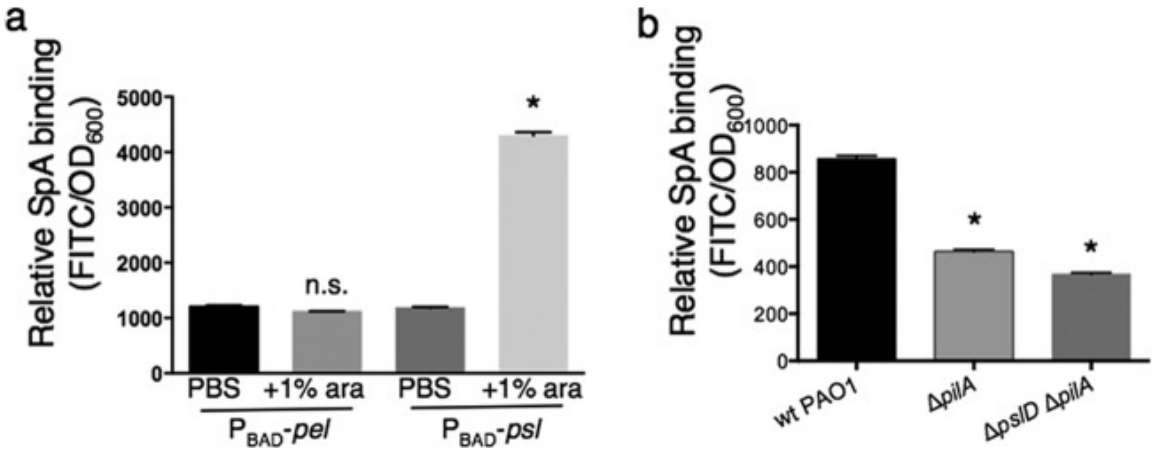

Figure 3. (a) SpA binds to *P. aeruginosa* Psl. Shown are fluorescence levels of FITC-SpA after incubation with the indicated strains, followed by washing. The asterisk indicates a significant difference in relative FITC fluorescence compared to the PBS control ($P < 0.05$); n.s., not statistically significant compared to the PBS control ($P > 0.05$). (b) FITC-SpA binding assay with the indicated strains, suggesting that SpA binds to *P. aeruginosa* surface type IV pili. Asterisks indicate a significant difference in relative FITC fluorescence compared to that of wild-type PAO1 ($P < 0.05$).

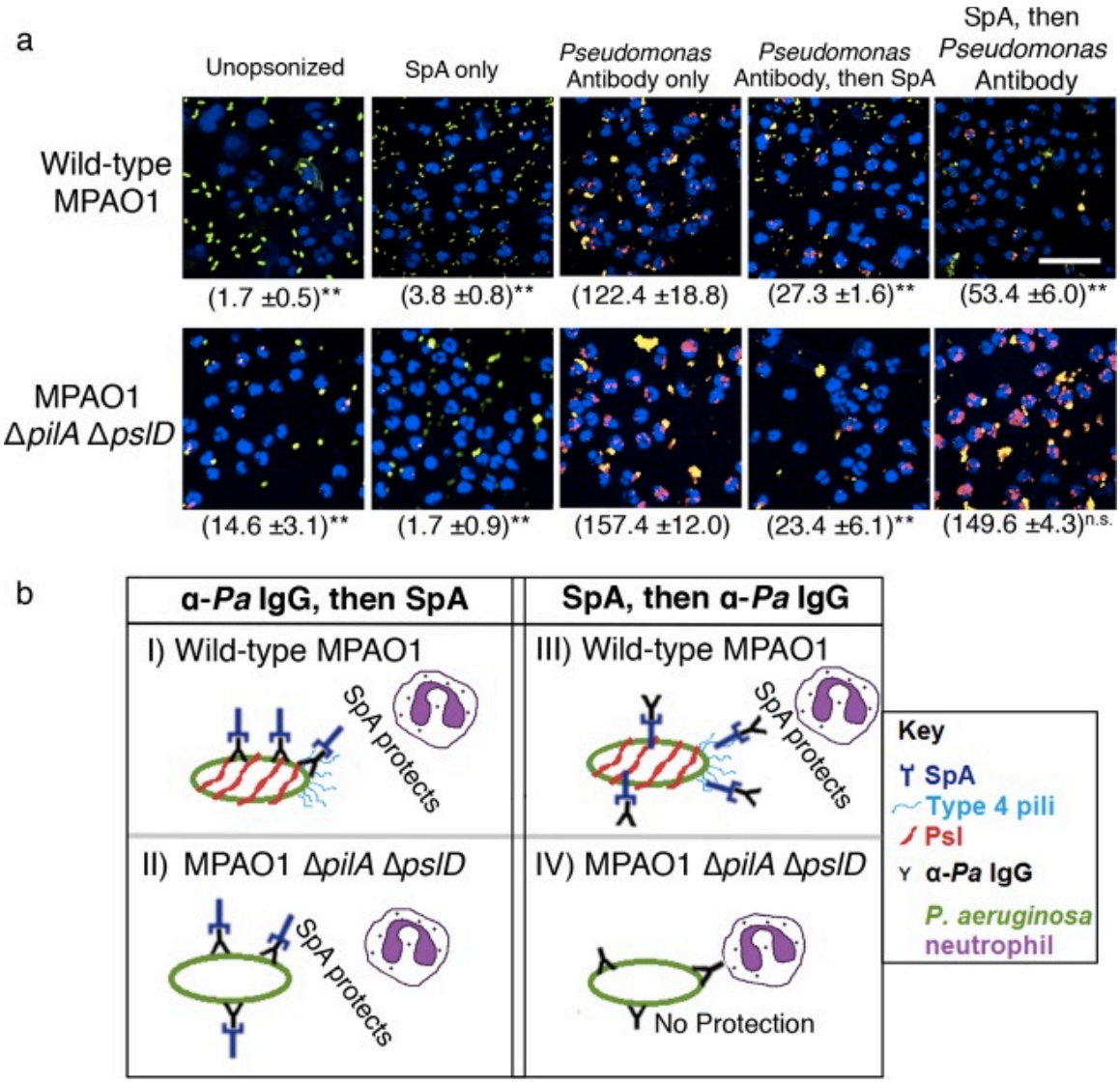

Figure 4. (a) SpA protects *P. aeruginosa* from neutrophil phagocytosis, as shown in these representative images from neutrophil phagocytosis experiments of the indicated *P. aeruginosa* strains, with and without the addition of SpA and/or antipseudomonal antibody. Blue, nuclei; green/yellow, extracellular *P. aeruginosa*; red, internalized *P. aeruginosa*. Asterisks indicate a significant difference in phagocytosis compared to the addition of *Pseudomonas* antibody only (*, $P < 0.05$; **, $P < 0.001$; n.s., no significant difference relative to *Pseudomonas* antibody only). Bar, 20 μm. Magnification (oil objective), ×60. The numbers (means ± standard deviations) of internalized bacteria are indicated in parentheses and are representative of 100 infected cells (neutrophils), examined from triplicate coverslips. (b) Model of two mechanisms of

SpA protection of *P. aeruginosa* from IgG-mediated opsonophagocytosis. (I and II) Broad protection for both wild-type MPAO1 and MPAO1 Δ*pilA* Δ*pslD* due to SpA binding to the exposed Fc region of the antipseudomonal (α-*Pa*) IgG. (III) Specific protection of wild-type MPAO1 via binding of SpA to two receptors on the *P. aeruginosa* cell surface (Psl and type 4 pili) prior to opsonization with IgG. (IV) When preincubated with SpA prior to opsonization by IgG, MPAO1 Δ*pilA* Δ*pslD* is not protected from neutrophil phagocytosis, because it is unable to bind SpA on its cell surface.

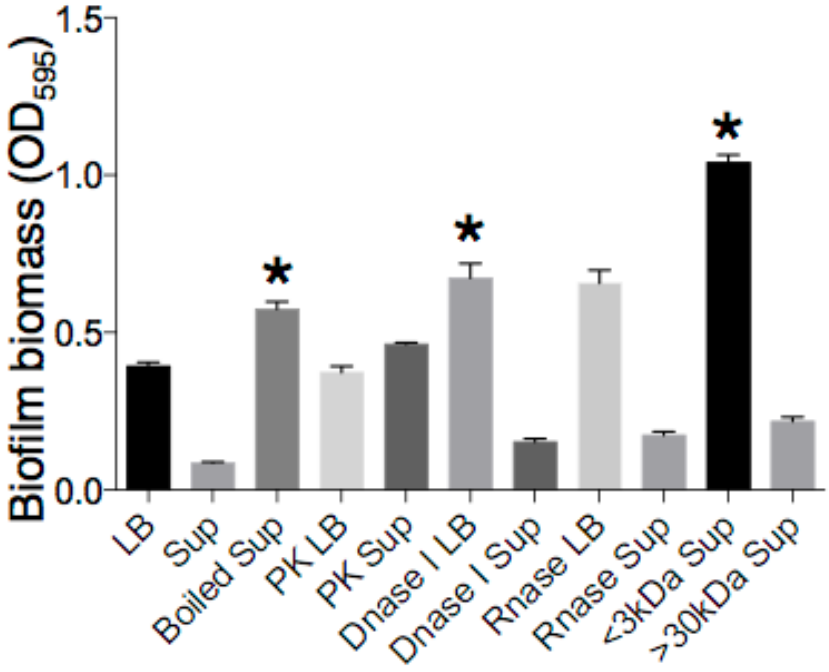

Figure 5. Analysis of SA113 supernatant by chemical and physical treatments indicate that biofilm inhibition activity is due to a protein larger than 30 kDa. In each case, treated supernatants were added to a Psl– CF clinical isolate (102-21) and biofilm formation assayed as above. Asterisks indicate statistically significant increases in biofilm biomass compared to growth in untreated SA113 supernatant ($p < 0.05$) and loss of biofilm inhibition.

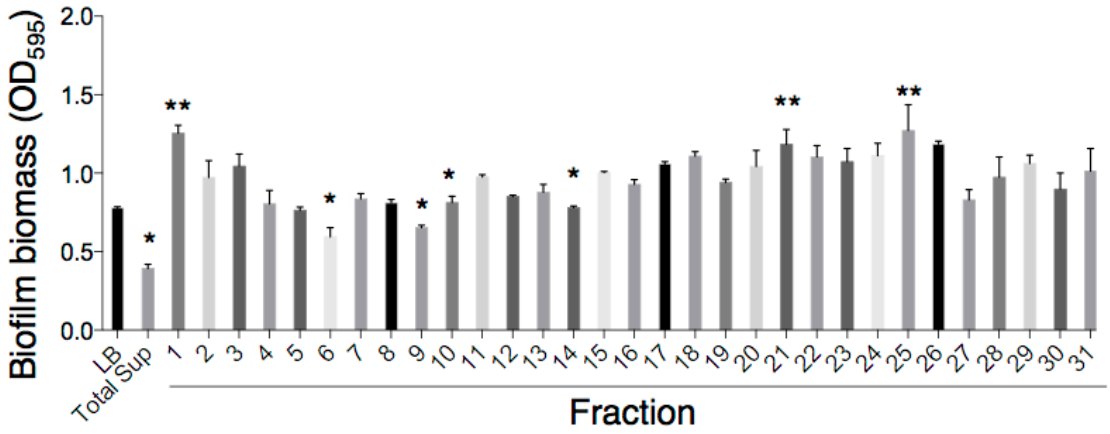

Figure 6. Screen for FPLC fraction activity in a Psl– clinical isolate (102-21) using the CV assay (4hr). * indicates active biofilm inhibitor fractions chosen for LC-MS/MS. ** indicates inactive fractions to compare relative abundance of candidate inhibitor proteins.

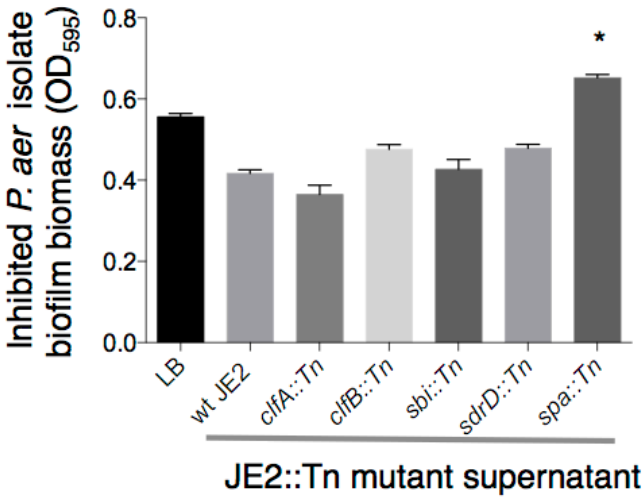

Figure 7. Crystal violet assay (4hr) screen of supernatant from NARSA collection transposon mutants of all available MSCRAMMs in JE2 background, performed on a Psl– *P. aeruginosa* clinical isolate (102-21). A transposon insertion in the *spa* gene resulted in a loss of the biofilm-inhibition phenotype. Asterisk indicates a significant increase in biofilm biomass compared to LB control and wild type JE2 supernatant ($p < 0.05$), suggesting a loss of the biofilm inhibition phenotype due to transposon insertion.

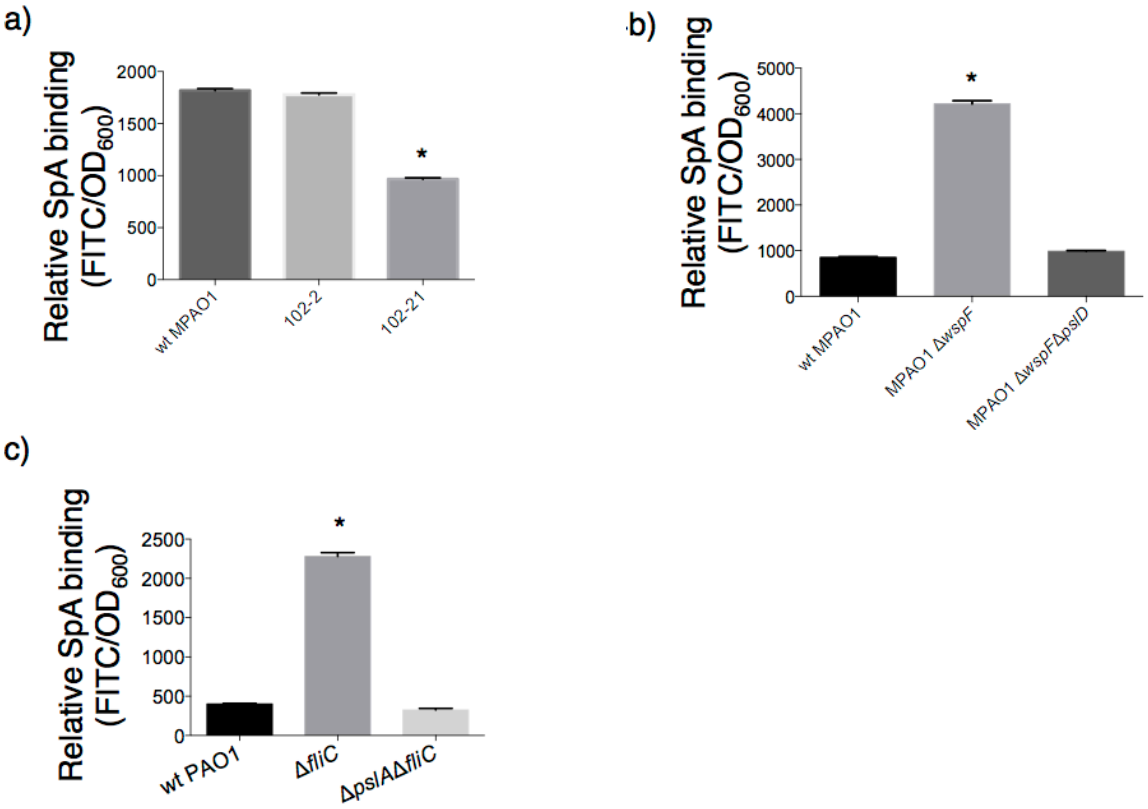

Figure 8. a) The Psl-producing clinical isolate 102-2 binds more FITC-SpA than the clonally-related Psl non-producer, 102-21. * $p < 0.001$ compared to wild type PAO1 or MPAO1. b) PAO1 Δ*fliC* is an RSCV that is commonly isolated from CF patient sputum and hyper-binds FITC-SpA in a Psl-dependent manner. c) PAO1 Δ*wspF*, another common CF RSCV that is known to overproduce Psl, also hyper-binds SpA in a Psl-dependent manner.

a)

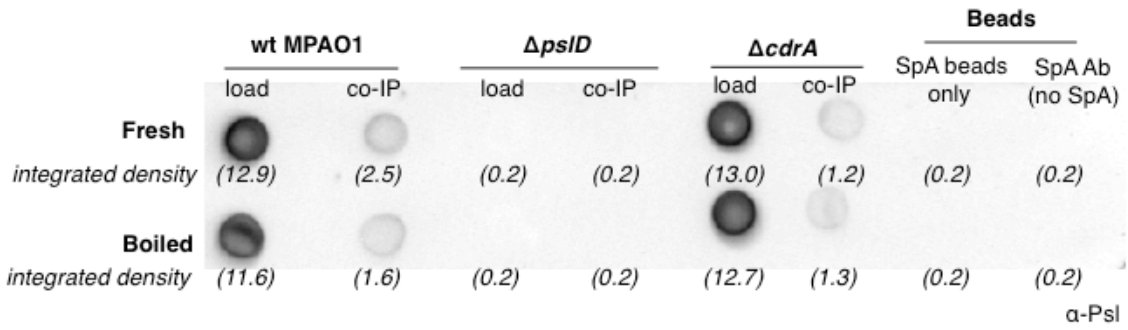

b)

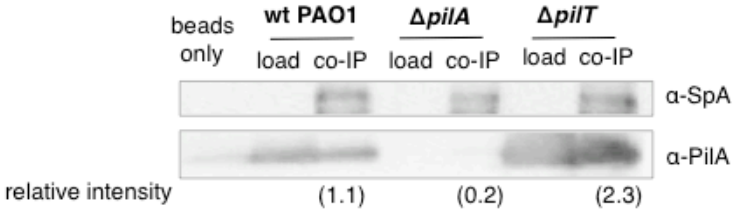

Figure 9. a) Co-immunoprecipitation experiments with *P. aeruginosa* culture supernatants followed by Psl dot blot. Magnetic beads bearing covalently-linked SpA were incubated with culture supernatants from the indicated *P. aeruginosa* strains, followed by centrifugation, washing, and dot blot with α-Psl antibody. SpA beads only control indicates beads with both α-SpA antibody and bound SpA to control for cross-reactivity of the α-Psl antibody with SpA-coated beads. SpA Ab control is beads with α-SpA antibody, incubated in PBAD-*psl* culture supernatant, in the absence of SpA to control for non-specific binding of Psl by the α-SpA antibody. Densitometry values (in parentheses) were measured with ImageJ. Load is a loading control, i.e. the supernatant sample input into the co-Immunoprecipitation.

b) Co-immunoprecipitation experiments of the indicated *P. aeruginosa* culture supernatants as in Figure 5b, except with Western blot using α-PilA antibody. Beads only control represents beads bound to α-SpA antibody, but without SpA, incubated in wild type PAO1 supernatant to control for non-specific binding of PilA to beads. PilT deletion

overproduces PilA. Densitometry (in parentheses), performed to quantify the amount of protein in the PilA lane, normalized to the amount of SpA. Load, a loading control, i.e., the supernatant sample input into the coimmunoprecipitation.

a)

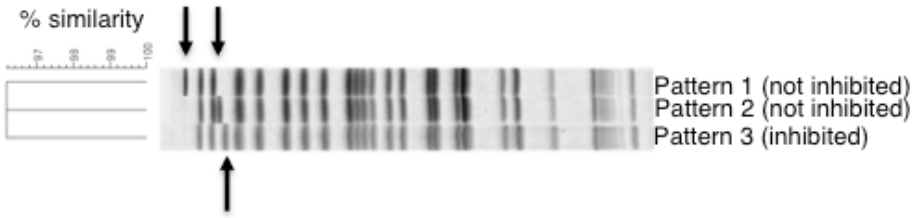

b)

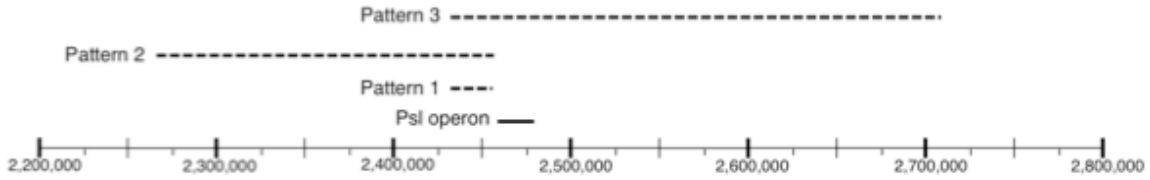

c)

d)

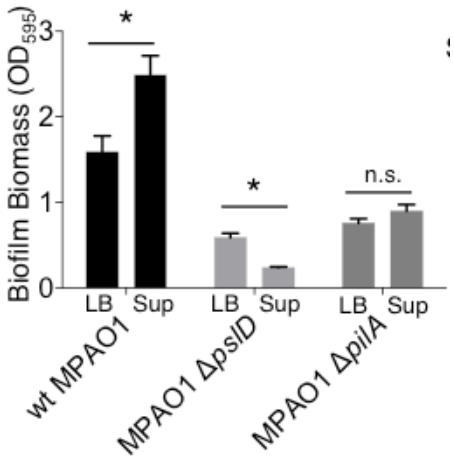

e)

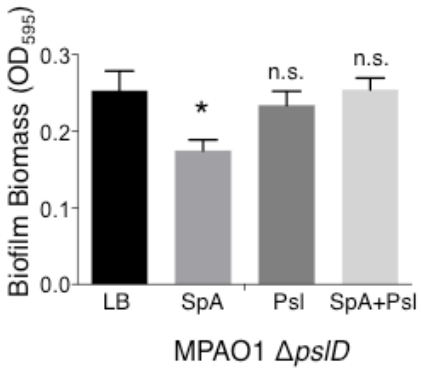

Figure 10. (a) *P. aeruginosa* isolates collected from patient 102 over 8.3 months displayed a total of three different PFGE patterns. Earlier isolates exhibited pattern 1; subsequent isolates displayed patterns 2 and 3, which differed according to the presence

or absence of larger DNA fragments. (b) Map of chromosomal deletions in 102-2 (PFGE pattern 1), 102-26 (pattern 2), and 102-21/102-30 (pattern 3), relative to the PAO1 genome, from whole-genome sequencing data. The entire Psl operon is deleted in pattern 3 isolates. (c) Psl dot blot assay results, showing that isolates with patterns 1 and 2 produce Psl (102-2 and 102-26), whereas two isolates with pattern 3 do not (102-21 and 102-30). (d) Crystal violet assay results, demonstrating that an MPAO1 Δ*pilA* mutant was not inhibited by *S. aureus* cell-free culture supernatant, whereas a Psl mutant in the same genetic background (MPAO1 Δ*pslD*) was inhibited. Crystal violet-stained biofilms indicate results after 4 h of growth. For each pair of bars in the graph, the left bar shows growth in LB and the right bar shows growth in SA113 supernatant. (e) Psl protects *P. aeruginosa* MPAO1 Δ*pslD* from SpA-mediated biofilm inhibition. Crystal violet assay results demonstrated that preincubation of 10 μg/ml purified SpA with 100 μg/ml purified Psl abrogated the biofilm-inhibitory effect of SpA on *P. aeruginosa* Δ*pslD*. SpA-only and Psl-only controls included concentrations of 10 μg/ml and 100 μg/ml, respectively. *, $P < 0.05$ compared to biofilm biomass in the LB control; n.s., no statistically significant difference in biofilm biomass relative to the LB control.

Table 2: Four hour biofilm formation as measured by crystal violet assay for Patient 102 isolates, isolates from 8 additional CF patients, and wild type and isogenic *pslD* mutants from the four biofilm matrix usage classes defined by Colvin *et al.,* 2011. Roman numerals in parentheses next to strain name indicate matrix usage class for defined strains.

Isolate ID	Makes Psl?***	Biofilm Formation (OD595)					
		in LB	(SD)	in *S. aureus* Supernatant	(SD)	T test	Fold Change
102-2	Y	0.199	0.011	0.313	0.014	**	1.577
102-5a	Y	0.248	0.030	0.358	0.030	**	1.442
102-5b	Y	0.257	0.025	0.315	0.012	*	1.223
102-6	Y	0.149	0.007	0.244	0.007	**	1.635
102-7	Y	0.205	0.006	0.277	0.018	**	1.349
102-8	Y	0.157	0.017	0.286	0.017	**	1.825
102-20	Y	0.213	0.008	0.313	0.040	**	1.472
102-21	N	0.248	0.036	0.110	0.016	**	0.444
102-25	Y	0.229	0.021	0.371	0.049	**	1.623
102-26	Y	0.268	0.025	0.315	0.030	*	1.177
102-30	N	0.307	0.053	0.092	0.004	**	0.300
102-34	N	0.263	0.025	0.088	0.012	**	0.333
102-35	N	0.181	0.005	0.118	0.003	**	0.654
102-36	N	0.243	0.025	0.124	0.017	**	0.511
102-39	N	0.196	0.013	0.100	0.004	**	0.510
102-40	N	0.192	0.024	0.090	0.006	**	0.469
115-7	Y	0.420	0.026	1.050	0.085	**	2.500
151-10	Y	0.424	0.054	0.823	0.128	**	1.942
159-1	Y	0.204	0.012	0.359	0.017	**	1.764
71-22	Y	0.110	0.021	0.224	0.010	**	2.029
200-4	N	0.432	0.030	0.147	0.017	**	0.340
134-2	Y	0.102	0.012	0.316	0.027	**	3.093
141-2	N	0.276	0.037	0.086	0.009	**	0.311
166-1	Y	0.672	0.066	0.910	0.033	**	1.355
PA14 (I)	N	0.578	0.085	0.157	0.038	**	0.272
Wild type MPAO1 (II)	Y	1.480	0.401	2.613	0.514	*	1.766
MPAO1Δ*pslD*	N	0.588	0.122	0.237	0.025	**	0.403
Wild type E2 (II)	Y	1.827	0.216	2.424	0.361	*	1.327
E2 Δ*pslD*	N	0.622	0.038	0.333	0.085	*	0.535
Wild type MSH3 (III)	Y	1.866	0.141	2.694	0.256	**	1.444
MSH3 Δ*pslD*	N	1.152	0.170	0.799	0.193	*	0.693
Wild type CF127 (IV)	Y	2.814	0.264	0.288	0.007	*	0.102
CF127 Δ*pslD*	N	0.501	0.090	0.288	0.007	*	0.574

* $p < 0.05$
** $p < 0.001$
***detected by Psl immunoblot

Table 3: Four hour biofilm formation as measured by crystal violet assay for a representative *P. aeruginosa* clinical isolate (102-21), showing that the biofilm inhibition phenotype occurs in supernatant from multiple common lab strains and clinical isolates of *S. aureus*. SA102-10 and SA102-12 are *S. aureus* clinical isolates that were collected from Patient 102, from whom the *P. aeruginosa* isolate 102-21 was also collected.

	102-21			
Grown in:	Mean Biofilm (OD595)	SD	T test	Fold Change
LB-MOPS	0.268	0.013	--	--
SA113	0.112	0.013	**	0.418
ATCC29213	0.148	0.014	**	0.552
Newman	0.13	0.009	**	0.486
SA47-34	0.143	0.006	**	0.533
SA102-10	0.175	0.02	**	0.653
SA37-12	0.15	0.018	**	0.559
SA134-5	0.121	0.014	**	0.45
SA102-12	0.122	0.015	**	0.457
SA23-71	0.145	0.028	**	0.541
SA200-3	0.105	0.008	**	0.394

* $p < 0.05$
** $p < 0.001$

CHAPTER II

Characterization of PA2582, a putative c-di-AMP-binding post-transcriptional regulator

Introduction

We had previously identified SpA as a protein produced by *S. aureus* that inhibits biofilm formation by *P. aeruginosa* strains that do not produce the Psl polysaccharide. Interestingly, we found that Psl-producing *P. aeruginosa*, including the lab strain MPAO1 (referred to as PAO1), displayed enhanced biofilm formation when grown either in co-culture with *S. aureus* or in *S. aureus* cell-free culture supernatant. We sought to identify the biofilm-stimulatory factor present in *S. aureus* culture supernatant. Initial characterization of this factor led us to investigate *S. aureus* secreted compound, c-di-AMP. This also led to a collaboration with the laboratory of Dr. Joshua Woodward, who is interested in c-di-AMP produced by *S. aureus*.

Nucleotide signaling pathways are ubiquitous across all kingdoms of life (50, 138). Bacteria use nucleotide-based second messengers to regulate a variety of physiological processes in response to environmental cues both outside and inside of the cell. While the best-studied second messenger in bacteria is c-di-GMP, used by Gram-negative bacteria and some Gram-positive species to rapidly respond to external stimuli, many additional nucleotide-based second messengers have been identified. The stringent response alarmones guanosine tetra- and pentaphosphate ((p)ppGpp) serve to mediate a global physiological response to amino acid depletion and other stresses (139). Cyclic adenosine monophosphate (cAMP) is a signaling molecule produced by both eukaryotic cells and bacteria. In bacteria, cAMP signaling plays diverse roles in carbon catabolite repression (140), as well as regulation of biofilm formation though modulating the activity of diguanylate cyclases (141, 142), type III secretion, environmental sensing, and manipulation of host cAMP levels (143).

Cyclic di-AMP was discovered serendipitously in 2008 when researchers studying DNA damage checkpoint initiation in *Bacillus subtilis* crystalized DisA, a DNA-binding protein found to be involved in the regulation of sporulation (144). The crystal structure of DisA revealed a molecule of c-di-AMP bound to its nucleotide-binding domain, and DisA was found to have diadenylate cyclase activity that was suppressed by the presence of DNA damage in the form of Holliday junctions and stalled replication forks. Since 2008, genes encoding predicted diadenylate cyclase synthases have been identified in the genomes of representatives of nearly all classes of bacteria

(145). However, strikingly, within the phylum Proteobacteria, only δ-Proteobacteria are predicted to produce c-di-AMP. Diadenylate cyclases synthesize c-di-AMP from two ATP molecules at the dimer interface of their DisA_N domains, which typically contain RHR (Arg-His-Arg) and DGA (Asp-Gly-Ala) motifs (144). To date, two major classes of c-di-AMP phosphodiesterases have been identified, the DHH-DHHA1- and HD-domain phosphodiesterases, that catalyze the hydrolysis of c-di-AMP into 5'-pApA (145). The structure and amino acid sequences of these c-di-AMP catalytic domains share no homology to diguanylate cyclases or c-di-GMP-specific phosphodiesterases (146).

Cyclic di-AMP binds a wide array of protein and riboswitch targets. Unlike the structurally-similar second messenger c-di-GMP, which regulates conditional and nonessential cellular processes such as motility and biofilm formation, c-di-AMP has thus far been found to mainly regulate essential cellular processes. It is therefore not surprising that c-di-AMP is the only essential cyclic dinucleotide identified to date. For example, c-di-AMP regulates cell wall homeostasis, potassium and carnitine transport in response to osmotic stress, acid stress resistance, and DNA repair in a variety of mainly Gram-positive bacteria (147). In contrast to diguanylate cyclases, of which *P. aeruginosa* encodes as many as 33 (48), bacteria typically encode one or very few diadenylate cyclases. Also, in contrast to the relatively subtle effects of c-di-GMP overproduction on individual cells, overproduction of c-di-AMP has deleterious effects on cells (145). While c-di-AMP and c-di-GMP are structurally similar molecules, there is no evidence of cross-talk between these two signaling networks, despite the fact that several bacterial species produce both molecules (including *Bacillus*, *Listeria*, and *Mycobacterium*) (50).

S. aureus is known to encode one diadenylate cyclase (DacA) (148), two cyclic diadenylate phosphodiesterases (GdpB and Pde2), and at least 5 c-di-AMP binding effectors with either RCK_C or USP domains (149, 150). Intracellular concentrations of c-di-AMP in *S. aureus* are estimated to be between 2-8μM (148, 151), and *S. aureus* biofilm cells have been shown to undergo autolysis, releasing 30 to 50% of the total c-di-AMP produced by the population into the extracellular milieu (152). While extracellular c-di-AMP is well-known to influence the host immune response (153, 154), whether and how c-di-AMP may influence other bacterial species in polymicrobial environments remains unknown. In this chapter, I describe how c-di-AMP stimulates biofilm formation

in *P. aeruginosa,* and I characterize a putative *P. aeruginosa* c-di-AMP-binding protein that likely plays a role in regulating a number of sRNA's.

Results

C-di-AMP stimulates *P. aeruginosa* biofilm formation

We had previously evaluated Psl production by a variety of clinical *P. aeruginosa* isolates collected from the sputum of pediatric cystic fibrosis patients, including a series of 15 clonally-related isolates collected over a 2 year period from Patient 102 (25). We subjected cell-free supernatant to a variety of chemical and physical treatments and screened samples for loss of biofilm stimulatory property in a crystal violet assay with the Psl-producing clinical isolate 102-2, in order to characterize the biofilm-stimulatory molecule(s) present in *S. aureus* supernatant (Figure 2a). The biofilm stimulatory factor was heat-stable, resistant to digestion by proteinase K, Dnase I, Rnase, smaller than 3 kDa, and soluble in methanol (Figure 2b). One such molecule that is abundant in both CF patient sputum (25-900nM) and in our SA113 culture supernatant (10μM) is c-di-AMP (Joshua Woodward, unpublished). We found that low micromolar levels of purified c-di-AMP added into LB were sufficient to stimulate biofilm formation of the lab strain PAO1 (Figure 3) and 102-2 (data not shown).

In order to determine whether *P. aeruginosa* forms increased biofilm in response to c-di-AMP specifically or to cyclic di-nucleotides in general, we tested the ability of other purified nucleotide analogs to stimulate *P. aeruginosa* biofilm formation and found that the only other molecule with biofilm-stimulatory activity was cyclic di-inosine monophosphate (c-di-IMP; Figure 4). Because c-di-IMP is a synthetic analog of c-di-AMP, we interpreted these data to indicate that *P. aeruginosa* responds specifically to c-di-AMP to increase biofilm formation.

Removal of Cyclic di-AMP from *S. aureus* supernatant abrogates biofilm stimulatory activity

Because diadenylate cyclases are typically essential proteins in bacterial species that produce c-di-AMP, we were unable to delete *dacA* from SA113 to analyze for a loss of biofilm stimulatory activity. Instead, we hydrolyzed c-di-AMP from *S. aureus*

supernatant and from LB containing 10μM c-di-AMP using a phosphodiesterase purified from *Listeria monocytogenes*, PdeA (gift from Dr. Joshua Woodward). We found that incubation with PdeA was able to fully abrogate the activity of purified c-di-AMP in LB. PdeA addition also significantly reduced the biofilm stimulatory activity of SA113 culture supernatant; however, biofilm levels were still elevated after PdeA treatment relative to levels formed in LB (Figure 5), suggesting that *S. aureus* supernatant likely contains molecules in addition to c-di-AMP that stimulate *P. aeruginosa* biofilm formation.

PA2582 binds c-di-AMP

We reasoned that the phenotypic response of *P. aeruginosa* to c-di-AMP was mediated by binding of c-di-AMP to either a cell-surface or intracellular *P. aeruginosa* receptor. Therefore, we sought to identify c-di-AMP binding proteins in *P. aeruginosa* by performing an coprecipitation of PAO1 lysate with c-di-AMP-coupled beads followed by protein identification by LC-MS/MS. While this analysis identified many components of the transcriptional machinery, including proteins in both the 50S and 30S ribosome subunits, the most abundant protein precipitated by c-di-AMP relative to bead-only controls was PA2582, with a normalized spectral abundance factor (131) (NSAF) of 0.055 in the co-precipitation and 0.001 in the control. PA2582 is annotated as a gene of unknown function in *P. aeruginosa*. It is predicted to localize to the cytoplasm, with homology to *E. coli*'s ProQ (E value = 1×10^{-8}) and the *E. coli* repressor of F plasmid transfer, FinO (E value = 0.013). PA2582 is predicted to have a mass of 19.4kDa, which corresponds to a large band present in coomassie-stained SDS-PAGE gels of the coprecipitation sample, but absent from those of the control sample (Figure 6).

To confirm that PA2582 binds to c-di-AMP, we purified PA2582 and probed for direct c-di-AMP binding with an established measure known as the differential radial capillary action of ligand assay (DRaCALA). Using ^{32}P-labeled c-di-AMP, we determined that PA2582 interacts with c-di-AMP with a K_D of 2.6μM ± 0.3 (Figure 7a). To determine the specificity of this interaction, we repeated this analysis in the presence of a variety of non-radiolabeled nucleotides, cyclic nucleotides, and cyclic dinucleotides. Of these, only unlabeled c-di-AMP could compete with ^{32}P-labeled c-di-AMP, suggesting

that PA2582 binds c-di-AMP specifically (Figure 7b). We purified two PA2582 homologs from other bacterial species (*Achromobacter xylosoxidans* and *Pseudomonas putida*), but results were inconclusive as to whether these proteins bound c-di-AMP by DRaCALA (data not shown). The *A. xylosoxidans* homolog shared 46% amino acid identity with the *P. aeruginosa* PA2582 protein sequence, with an E value of 5×10^{-37}, while the *P. putida* homolog shared 60% amino acid identity with PA2582 and had an E value of 3×10^{-61}. (DRaCALA assays were performed by Dr. Kamakshi Sureka in the laboratory of Dr. Joshua Woodward.)

PA2582 is required for *P. aeruginosa* biofilm response to c-di-AMP

To determine whether PA2582 is required for induction of biofilm formation in response to c-di-AMP and *S. aureus* supernatant, we constructed a clean deletion of PA2582, PAO1 Δ*PA2582*. We performed a growth curve to confirm that PAO1 Δ*PA2582* did not exhibit a growth defect relative to wild type PAO1 (data not shown). In a crystal violet biofilm assay, PAO1 Δ*PA2582* no longer responded to purified c-di-AMP, although it still responded to SA113 cell-free culture supernatant (Figure 8). Interestingly, PAO1 Δ*PA2582* tends to form more biofilm biomass than wild type PAO1 in LB. We complemented the PAO1 Δ*PA2582* mutant by providing PA2582 *in trans* (under control of its native promoter) at a neutral site on the chromosome and found that this strain responds to c-di-AMP and forms an amount of biofilm biomass similar to when grown in LB. Thus PA2582 is required to mediate *P. aeruginosa*'s response to c-di-AMP, but *S. aureus* supernatant stimulates biofilm formation in *P. aeruginosa* through at least one other mechanism.

Characterization of PA2582 in *P. aeruginosa*

The structure of PA2582 is predicted by the structural threading algorithm Phyre2 to be six alpha helices arranged in an irregular bundle, with a small beta hairpin, similar to the FinO crystal structure (ProQ has not been crystalized; Figure 9). PA2582 is highly conserved among sequenced *P. aeruginosa* isolates, and the PA2582 gene in the four genomes we sequenced in the SpA study have 100% sequence identity to that of PAO1. The synteny of PA2582 is highly conserved as well and while it is not predicted to be in

an operon with any other genes, it is consistently located adjacent to a predicted sensor kinase/response regulator (PA2583 in PAO1) and at least one tRNA gene. The transcription start site is predicted to be located 90 nucleotides upstream of the start codon (155).

ProQ in *Salmonella* was recently shown to be a major RNA-binding post transcriptional regulator that binds many highly structured sRNAs (156). We therefore hypothesized that PA2582 functions as a post-transcriptional regulator of *P. aeruginosa* biofilm formation in response to c-di-AMP. We performed an immunoprecipitation of VSV-G-tagged PA2582 and used LC-MS/MS to identify bound proteins. As expected based on reports of ProQ's association with translation machinery, we found that PA2582 coprecipitated with components of the 30S and 50S ribosomes, regardless of whether c-di-AMP was added to the growth media (Table 2). Thus, similar to ProQ, PA2582 likely interacts with translation machinery, potentially as an RNA chaperone or RNA-binding post-transcriptional regulator.

Identification of PA2582's RNA targets

To identify the full scope of RNAs bound by PA2582 in the presence and absence of c-di-AMP, we performed separate crosslinking immunoprecipitation sequencing (CLIPseq) analyses under two conditions. First, we crosslinked PAO1 supernatant with VSV-G-tagged PA2582 without c-di-AMP using formaldehyde (referred to as "minus c-di-AMP"), and the second approach we took was to use UV irradiation as a crosslinker for PAO1 grown in the presence and absence of 1μM c-di-AMP. RNA sequencing has not been performed on the UV-crosslinked PA2582 grown without c-di-AMP or its uncrosslinked control, so only the results from RNAseq on the sample to which c-di-AMP was added will be discussed (referred to as "plus c-di-AMP"). RNA sequencing was performed twice on UV crosslinked PA2582 plus c-di-AMP during the process of methods development, before and after a cDNA size exclusion step intended to reduce the number of rRNA reads. The formaldehyde-based CLIPeq "minus c-di-AMP" returned mostly reads that mapped antisense to PAO1 genes. One possibility is that these antisense reads represent sRNA's. For example, the most abundant RNA mapped antisense to PA0587. Deletion of the PA0588-PA0584 gene cluster is known to have an indirect,

positive effect on expression of the sRNA's rsmY and rsmZ; however, the role of these genes in production of rsmY/Z remains unclear (157). Three predicted RNA's that were abundant in the PA2582 CLIPseq minus c-di-AMP mapped antisense to genes known to be involved in biofilm formation: *pslA*, *mucA*, and *algJ.* Aside from the reads mapping antisense to PAO1 genes, the top hits from CLIPseq minus c-di-AMP were tRNA's, *rpoB*, PA5403, PA1414, the sRNA rsmY, and *rsmA*. The most abundant RNAs from CLIPseq experiment plus c-di-AMP were also many RNA's associated with translating ribosomes, as well as a variety of known sRNA's including rsmY and rsmZ. These data suggest that PA2582 likely associates with many RNA's and sRNA's, including rsmY/Z and the mRNA transcript for RsmA. These results must be confirmed with target-specific assays.

PA2582 is required for increased Psl production in response to c-di-AMP

Because rsmY/Z regulate activity of the Psl biosynthetic operon, we hypothesized that PA2582 is involved in post-transcriptional regulation of the Psl operon. We compared Psl levels by Psl immunoblot in wild type PAO1 and PAO1 Δ*PA2582* grown to stationary phase in the presence and absence of 10μM c-di-AMP. We found that wild type PAO1 produced more than twice as much Psl when grown with c-di-AMP, whereas there was no significant difference in the amount of Psl produced by PAO1 Δ*PA2582*. However, PAO1 Δ*PA2582* grown in the absence of c-di-AMP produced twice as much Psl as wild type PAO1 grown without c-di-AMP, suggesting that PA2582 may be a repressor of Psl production.

Cyclic di-AMP interferes with *P. aeruginosa* phosphate metabolism

Cyclic-di-AMP is known to regulate a variety of phenotypes in the bacteria that produce them including responses to specific environmental stresses. We wondered whether exposure of *P. aeruginosa* to cyclic-di-AMP (produced by other species) would similarly result in phenotypic and/or stress responses beyond biofilm induction. To survey for such phenotypic effects, we performed Biolog phenotypic microarrays on wild type PAO1 in the presence and absence of 5μM c-di-AMP. In particular, metabolic activity (as monitored by reduction of a tetrazolium dye during Biolog assays) of wild

type PAO1 in the presence of 5μM c-di-AMP was inhibited under numerous conditions where single phosphate sources were tested on plate PM4A (Phosphorus and Sulfur Sources) compared to wild type PAO1 grown without c-di-AMP. PAO1 was metabolically inactive when incubated without added phosphate (well A1 on the PM4A plate), regardless of whether c-di-AMP was present, suggesting that PAO1 cannot use c-di-AMP as a phosphate source. Furthermore, when phosphate was added (well A2), metabolic activity of PAO1 was not affected by addition of c-di-AMP, suggesting that c-di-AMP itself does not inhibit the growth of PAO1. However, in the presence of c-di-AMP, PAO1 was inhibited for metabolic activity using the following phosphorus sources: tripolyphosphate (well A5), a range of concentrations of guanosine-5'-monophosphate (wells B9-B10), guanosine-2',3'-cyclic monophosphate (2'3'-cGMP; well B11), guanosine-3'5'-cyclic monophosphate (3'5'-cGMP; B12), 6-phospho-gluconic acid (well C7), and thymidine 3',5'-cyclic monophosphate (well E12). The most severe metabolic defect occurred with the guanosine triphosphate-derived cyclic nucleotides, each of which PAO1 was completely unable to use as a phosphorus source when grown in the presence of 5μM c-di-AMP (wells B11-12). The 6-phospho-gluconic acid (well C7) condition has produced variable results in the past for PAO1 grown alone in that it occasionally displays somewhat diminished growth; however, PAO1 growth on the rest of the above phosphate sources has been consistent.

The Biolog Phenotypic Microarray also identified a few conditions under which the presence of 5μM c-di-AMP was protective for PAO1, including during growth in 10-11% sodium lactate (plate PM9; wells F10-11), as well as a range of levels of potassium chromate (plate PM13, wells C9-12) and the anti-Pseudomonal antibiotic cefsulodin (PM17, H2-4). Additionally, c-di-AMP protected PAO1 during growth at a low pH of 4.5 (PM10, A3 and B1), as well as at a high pH of 9.5 when L-leucine (plate PM10, well E11) or L-methionine (plate PM10, well F1) were present.

Deletion of PA2582 mimics the benefit of added cyclic di-AMP in pH and osmotic stress

We repeated the Biolog Phenotypic Microarray analysis with PAO1 Δ*PA2582* and found very few conditions under which this mutant differed from wild type PAO1.

Notably, however, whereas c-di-AMP inhibited the metabolic activity of PAO1 when it was grown using a variety of cyclic nucleotides as the sole phosphorus source, metabolic activity of PAO1 Δ*PA2582* was equal to that of wild type PAO1 under these conditions. Moreover, similar to PAO1 with 5μM c-di-AMP, PAO1 Δ*PA2582* was more resistant to high concentrations of sodium lactate (PM9; F10-11), than wild type PAO1. Another way in which PAO1 Δ*PA2582* resembled PAO1 + c-di-AMP was in its ability to tolerate pH stress. Like PAO1 grown with c-di-AMP, PAO1 Δ*PA2582* remained metabolically active at an acidic pH of 4.5 (PM10, A3 and B1), as well as at an alkaline pH of 9.5 when either L-leucine (PM10, E11) or L-methionine (PM10, F1) were present, whereas wild type PAO1 alone did not display metabolic activity under these conditions. Furthermore, metabolic activity of PAO1 Δ*PA2582* was higher than that of wild type PAO1 at pH 9.5 upon addition of two other amino acids on plate PM10, L-isoleucine (E10) and L-lysine (E12), whereas there was no difference under these conditions for PAO1 ± c-di-AMP. Thus, PAO1 + c-di-AMP and PAO1 Δ*PA2582* display similarly enhanced tolerance to osmotic and pH stresses.

False positive or negative reduction of tetrazolium dye under specific conditions is common with Biolog Arrays for a variety of reasons, particularly due to the varying rates at which some compounds in the plates degrade. Our analysis benefitted from three independent runs of wild type PAO1 to get a sense of each condition's inherent variability when interpreting our findings. For example, in one experiment, metabolic activity when pyruvic acid was the sole carbon source (PM1, H8) appeared to be dependent upon c-di-AMP; however, this is likely to be a false positive since PAO1 is known to grow on pyruvic acid and has grown normally under this condition in two of the three previous "PAO1 alone" runs. Similarly, c-di-AMP appeared to be protective against colistin (PM11; C7), dodine (PM20, E8), and 4-hydroxy-coumarine (PM20, F4); however, the apparent metabolic activity of wild type PAO1 under these conditions have been variable in previous runs. Future work will include specifically testing the effects of c-di-AMP and deletion of PA2582 on PAO1 growth under the pH and osmotic stresses, as well as the phosphorus limiting conditions, identified among the top Biolog hits *in vitro*.

Conclusions

We have found that *P. aeruginosa* biofilm formation is enhanced *in vitro* when cells are grown in the presence of c-di-AMP. We identified a c-di-AMP-binding protein PA2582, which shares homology to the known sRNA-binding chaperone protein ProQ carried by both *E. coli (158)* and *S. enterica (156)*, and showed that it is required for *P. aeruinosa's* biofilm response to c-di-AMP. The finding that PAO1 Δ*PA2582* produces more biofilm and more Psl polysaccharide than wild type PAO1 (Figure 7 compared to 4 LB condition, and Figure 9) suggests that PA2582 acts as a negative regulator of biofilm formation in *P. aeruginosa*.

ProQ is a 232 amino acid protein with two predicted structural domains that are connected by an unstructured linker region. The N-terminus of ProQ was modeled using the structure of FinO (159), an RNA-binding post-transcriptional regulator involved in F-plasmid transfer, and the C-terminus of ProQ was modeled using the RNA chaperone Hfq (160). Until recently, ProQ was thought to be an RNA chaperone protein that specifically binds one or very few mRNA transcripts, including that for the gene *proP* (158). In *E. coli*, ProP is a transporter that senses osmotic stress and responds by importing the compatible solutes proline and glycine betaine (161–163). ProQ is known to associate with ribosomes (158, 164), and deletion of ProQ leads to a reduction in cellular levels of ProP protein. While a role for ProQ in regulating proline transport is clear, one puzzling finding has been that ProQ homologs are present throughout the chromosomes, plasmids, and bacteriophages of α-, β- and γ-proteobacteria, but many of these bacteria do not encode *proP* (156). Recently, it was found that the role of ProQ is larger than previously proposed, and that it is a major small RNA-binding regulatory protein, similar to Hfq and CsrA (156). In *Legionella pneumophila*, a ProQ homolog was recently found to act as a chaperone for the *trans*-acting sRNA RocR, to regulate translation of mRNAs encoding genes involved in natural transformation (165). To date, only limited evidence for a role of ProQ in biofilm formation has been described: one group reported that deletion of ProQ abolished biofilm formation in *E. coli* (158).

We hypothesize, based on results of our proteomics and RNAseq experiments, that PA2582 associates with translation machinery and, similar to ProQ, likely acts as an sRNA-binding post-transcriptional regulator of a variety of cellular processes in *P.*

aeruginosa. We found that PA2582 bound a variety of sRNA's and ncRNA's, including rsmY and rsmZ, regardless of whether *P. aeruginosa* was grown with c-di-AMP. RsmY was a top hit from our formaldehyde-crosslinked CLIPseq experiment performed in the absence of c-di-AMP, whereas both rsmY and rsmZ were top hits from CLIPseq performed in the presence of c-di-AMP. Small RNA's (sRNAs) are non-coding sequences that are involved in regulation of many aspects of bacterial physiology, typically either through binding to and modulating protein activity or, more commonly, through base pairing with target mRNAs (166). In. *P. aeruginosa*, the sRNAs rsmY/Z act by sequestering the translational repressor RsmA, which binds to a GGA motif present near the Shine-Dalgarno sequence on 5' leader sequences of target mRNAs, thereby impeding translation initiation. Transcription of rsmY/Z is regulated by the GacA/GacS two component system, which itself is regulated by two histidine kinases, RetS and LadS, that can repress or activate GacS in response to environmental cues (167). When the response regulator GacA is phosphorylated by GacS, it directly binds to the promoters of rsmY and rsmZ and these sRNA's are transcribed (168). When rsmY/Z are transcribed, these sRNAs bind to RsmA and titrate it away from its target mRNAs, including transcript for the Psl operon (169). Interestingly, another abundant sRNA bound by PA2582 when grown in the presence of c-di-AMP was crcZ, which also functions by binding to and sequestering a translational repressor, Hfq (170). Thus, whereas the ProQ protein in *S. enterica* and *L. pneumophila* were recently described as stabilizing and promoting base-pairing of *trans*-encoded sRNAs with the 5' untranslated regions (5'-UTRs) of targeted mRNAs (171), our results indicate that PA2582 may bind many sRNAs that are known to exert their regulatory effects through binding to other post-transcriptional regulatory proteins.

While findings from our CLIPseq experiments should be confirmed (such as by immunoprecipitation of PA2582 grown in the presence and absence of c-di-AMP, followed by qRT-PCR to detect putative RNA targets), it is interesting to note that the presence or absence of c-di-AMP influenced whether rsmZ was associated with PA2582. Binding of c-di-AMP to PA2582 may differentially modulate PA2582's binding of rsmY/Z, leading to a downstream increase in biofilm formation; however, the mechanism by which PA2582's association with rsmY/Z may influence *P. aeruginosa* biofilm is still

unclear. We observed an increase in Psl production when *P. aeruginosa* was grown in the presence of c-di-AMP, a condition in which both rsmY and rsmZ were bound to PA2582, as well as increased Psl production when PA2582 was deleted. RsmA is known to post-transcriptionally repress Psl genes (169); therefore, if binding of PA2582 to rsmY/Z were to inactivate their effects on RsmA, one might predict the final effect would be to decrease, not increase, Psl operon expression. One possible model to explain this apparent discrepancy is that PA2582 binding to rsmY/Z in the presence of c-di-AMP stabilizes or in some way enhances their interaction with RsmA, sequestering RsmA from the Psl ribosomal binding site. In this model, PA2582 would be acting as an sRNA "chaperone", providing another layer of regulation of cellular rsmY/Z levels, either through promoting their interaction with RsmA or protecting them from degradation when they are not bound to RsmA, thereby influencing Psl production. However, this model does not explain why deletion of PA2582 leads to enhanced Psl production and biofilm formation.

In addition to rsmY/Z, we found that the mRNA transcript for RsmA was present in the CLIPseq from PAO1 grown without c-di-AMP, but absent from the immunoprecipitation of PA2582 when cells were grown with c-di-AMP. One possible explanation for why we see enhanced Psl production and biofilm formation in PAO1 when grown with c-di-AMP or in PAO1 Δ*PA2582* is that PA2582 binding to RsmA transcript may be important for either maintaining stability of the mRNA or mediating its interaction with the translation machinery. Clearly, more work should be done to evaluate whether and to what extent PA2582 influences RsmA, the interaction of rsmY/Z with RsmA, as well as whether and how c-di-AMP influences PA2582's interaction with the translational machinery in general.

In the absence of c-di-AMP, the most abundant RNA from our CLIPseq experiment mapped antisense to PA0587. Transcription of PA0587 has been shown to be strongly inhibited by the 50S ribosome-binding antibiotic azithromycin (172) and the PA0588-PA0584 gene cluster is known to have an indirect, positive effect on expression of the sRNA's rsmY and rsmZ; however, the role of this gene cluster in regulating production of rsmY/Z remains unknown (157). One possible role for the abundant read we identified as mapping antisense to PA0587 is as an sRNA that is involved in

regulation of rsmY/Z levels. Of the base-pairing sRNAs, there are two main groups: cis-encoded (antisense) and trans-encoded base-pairing sRNAs. Cis-encoded sRNAs can range in size from tens to thousands of nucleotides and typically form extended base-pairing structures with a specific mRNA target, whereas *trans*-encoded sRNAs tend to act via limited complementarity on multiple mRNA targets and require an RNA chaperone protein, such as Hfq (173). Thus, the putative sRNA mapping antisense to PA0587 could function as a *cis*-encoded sRNA that suppresses activity of the PA0588-PA0584 gene cluster in the absence of c-di-AMP (thereby leading to lower cellular levels of rsmY/Z) or a *trans*-encoded sRNA that requires PA2582 as a chaperone and acts on an unknown cellular target. In either case, considering deletion of the PA0588-PA0584 gene cluster leads to elevated cellular levels of rsmY/Z, future experiments should aim to determine whether PA2582 is involved in regulation of an sRNA encoded at this site and whether this interaction influences cellular levels of rsmY/Z.

The PA2582 homolog ProQ was originally studied in terms of its role in regulation of the *proP* transcript, which encodes a proline transport channel in *E. coli*. Interestingly, we found that both PAO1 Δ*PA2582* and wild type PAO1 grown with 5μM c-di-AMP had similar phenotypes in response to some conditions on the Biolog Osmolytes (PM9) and pH (PM10) plates. This is consistent with our observation that PAO1 Δ*PA2582* phenocopies the effect of c-di-AMP on wild type PAO1 biofilms. It is interesting to note that whereas ProQ in *E. coli* is important for production of ProP, a protein that transports compatible solutes in response to osmotic stress, PAO1 Δ*PA2582* and, to a lesser extent, PAO1 + c-di-AMP were more tolerant of pH and osmotic stress. Furthermore, whereas other Pseudomonads encode a ProP homolog, *P. aeruginosa* does not. Therefore, it is likely that while PA2582 may play a role in pH and osmotic stress response, it does so differently than ProQ in *E. coli*.

PA2582 is predicted to be a cytoplasmic protein, and our results demonstrate both that it is required for *P. aeruginosa* response to c-di-AMP and that it can bind specifically to this molecule. However, it is unknown whether and how c-di-AMP can enter into the *P. aeruginosa* cell to reach PA2582. Cyclic di-nucleotides are not thought to be freely diffusible across cell membranes. In collaboration with Dr. Joshua Woodward's lab, our attempts to demonstrate that ^{32}P-c-di-AMP can be transported into *P. aeruginosa* have

thus far been unsuccessful. However, our Biolog experiment comparing PAO1 ± 5μM c-di-AMP offers some interesting insight into the possibility that c-di-AMP could be taken up by *P. aeruginosa*. We found that whereas PAO1 is capable of using a variety of nucleotides and cyclic nucleotides as the sole phosphorous source, PAO1 could no longer use many phosphorous sources, notably the cyclic nucleotides, for growth in the presence of 5μM c-di-AMP. It is possible that c-di-AMP is interfering with a porin or transporter necessary for uptake of cyclic nucleotides during phosphorus-limited growth conditions, however further experimentation would be needed to investigate whether c-di-AMP is being transported into the cytoplasm via these mechanisms, as opposed to simply binding to and blocking or inactivating them.

Until we are able to demonstrate transport of c-di-AMP into *P. aeruginosa*, we cannot rule out the possibility that our identification of PA2582 as a protein that binds c-di-AMP *in vitro* may be a red herring. Our CLIPseq and proteomics experiments identifying RNA and protein binding targets of PA2582 suggest that PA2582 is likely a major sRNA-binding post-transcriptional regulator that could be involved in a variety of cellular processes, including biofilm formation. Deletion of PA2582 abrogated the biofilm stimulatory effect of purified c-di-AMP, leading us to conclude that PA2582 was required for the biofilm response to c-di-AMP, but this deletion mutant also displayed overall higher levels of biofilm formation compared to wild type PAO1. If PA2582 is not the target of c-di-AMP and c-di-AMP does not get transported into the cytoplasm, then one possibility is that c-di-AMP interacts with a receptor on the cell surface or in the periplasm and stimulates biofilm through a separate mechanism. The apparent requirement of PA2582 could therefore be due to the PA2582 deletion stimulating biofilm formation either downstream of the c-di-AMP receptor in the same pathway or through a separate pathway that has a dominant effect over the effect of c-di-AMP. While we found that PA2582 bound c-di-AMP specifically (other cyclic nucleotides and dinucleotides could not compete with ^{32}P-c-di-AMP by DRaCALA), the predicted structure of PA2582 is suggestive of one way in which this protein could have been identified as a false positive in both the initial c-di-AMP bead experiment and the follow up DRaCALA experiments. Proteins belonging to the ProQ/FinO family contain a large patch of positively charged residues on the concave surface of their helical bundle that is

predicted to be involved in RNA-binding and many proteins in this family (including the predicted structure of PA2582) contain multiple additional patches of positively charged residues on the convex surface of the bundle that are thought to allow the protein to interact with multiple RNA targets. It is possible that these patches of positively charged residues supported binding of c-di-AMP *in vitro*; however, it is unclear why c-di-AMP but not additional cyclic dinucleotides would bind nonspecifically in this manner. Another possibility is that PA2582 contains a binding site that is specific for c-di-AMP *in vitro*, but *in vivo* this site mediates interaction of sRNAs or mRNA transcripts to PA2582. The protein ligand docking software SwissDock identified two potential sites on PA2582 where a molecule of c-di-AMP would be most likely to bind. Future work should aim to mutate residues at these sites to disrupt c-di-AMP binding, in order to gain further insight into whether and how c-d-AMP may bind to PA2582. Furthermore, it is possible that our preparation of PAO1 cell lysate for the c-di-AMP bead experiment biased against identification of membrane-associated proteins. This experiment should be repeated using membrane fractions in order to identify any membrane-associated c-di-AMP receptors.

Materials and Methods

Bacterial strains and growth conditions.

The strains, plasmids, and primers used in this study are listed in Table 1. *E. coli* and *P. aeruginosa* strains were routinely grown in Luria–Bertani (LB) medium and on LB agar at 37°C. *S. aureus* was grown on LB or PN media and on LB agar at 37°C. Antibiotics were supplied where necessary at the following concentrations: for *E. coli*, 100 μg/mL ampicillin, 50 μg/mL carbenicillin, 10 μg/mL gentamicin, and 10 or 60 μg/mL tetracycline; for *P. aeruginosa*, 300 μg/mL carbenicillin, 100 μg/mL gentamicin, and 100 μg/mL tetracycline.

To construct PAO1 Δ*PA2582,* a 343bp fragment upstream and a 357bp fragment downstream of PA2582 were amplified from PAO1 genomic DNA using primers PA2582UpF01-GWB1, PA2582UpR01, PA2582DownF01, and PA2582DownR01-GWB2. These attB-flanked fragments were used to construct a PA2582 deletion allele containing a 63 nucleotide scar by SOE-PCR, cloned into pDONRPEX18-Gm using Gateway technology, and transformed into *E. coli* DH5α. Colonies were sequenced by

GeneWiz using primers M13F(-21) and M13R, and pDONRPEX18-Gm::Δ*PA2582* was transformed into *E. coli* S17.1. The mutant PAO1 ΔPA2582 was generated using two-step allelic exchange following conjugation of wild type PAO1 with *E. coli* S17.1 harboring the PA2582 deletion allele as previously described(174). PAO1 Δ*PA2582* was identified by colony PCR using primers PA2582F01-Seq and PA2582R01-Seq, PCR products were purified from 1% agarose Tris-acetate-EDTA (TAE) plus 1mM guanosine gel and sequenced with PA2582F01-Seq and PA2582R01-Seq (GeneWiz). PAO1 Δ*PA2582* is an in-frame deletion that produces a 21 amino acid scar peptide.

PAO1 Δ*PA2582* was complemented with its native promoter at the attTn7 site as previously described (175) using pUC18-miniTn7T-Gm. From genomic PAO1 DNA, PA2582 was cloned using primers BamH1-PPA2582-F and HindIII-PA2582-R, which included 198 nucleotides upstream of the PA2582 coding region. The PCR product was column purified, then both the PCR product and pUC18-miniTn7T-Gm were doubly digested with BamH1/HindIII. Digested pUC18-miniTn7T-Gm was treated with Antarctic phosphatase, then both the PCR product and the vector were column purified again with the MinElute PCR cleanup kit (Qiagen) to remove BamH1. The PA2582 complementation allele was ligated into digested pUC18-miniTn7T-Gm, then transformed into *E. coli* DH5α. Plasmids from transformants were sequenced using primers pUC18miniTn7T-Seq and attB2-Seq (GeneWiz), then purified and electroporated along with pTNS3 into PAO1 Δ*PA2582*. Transformants were selected from LBGm30 plates and colony PCR was performed using primers P_{Tn7R} and $P_{glmSdown}$ as previously described(175) to identify an insertion at the attTn7 site on the PAO1 chromosome. Finally, the miniTn7 backbone was removed by electroporation of pFLP2 and growth on LB with 300μg/mL carbenicillin. Colonies were then patched on LB with 30μg/mL gentamycin (LB Gm30) and LB with 300μg/mL carbenicillin (LB Carb300). A colony that was carbenicillin resistant, but gentamycin sensitive was streaked onto LB agar without salt (NSLB) plus 15% sucrose to cure the strain of pFLP2. Finally, colonies were patched onto NSLB with 15% sucrose, LB Gm30, and LB Carb300 and only colonies that were resistant to sucrose, but sensitive to both antibiotics were PCR checked with P_{Tn7R} and $P_{glmSdown.}$

A construct containing C-terminally VSVG-tagged PA2582 under control of an IPTG-inducible promoter was constructed in pPSV39CV(176). From PAO1 genomic DNA, PA2582 was cloned using primers SacI-PA2582RBS-F and XbaI-PA2582RBS-R, which include the native ribosomal binding site and exclude PA2582's stop codon. The PCR product and pPSV39CV were doubly digested by SacI/XbaI, and pPSV39CV was treated with Antarctic phosphatase before the PA2582 allele was ligated into the vector and transformed into *E. coli* DH5α. The plasmid was purified from transformants growing on LB Gm10 and checked by sequencing with primer pPSV39CV_seq_rev (GeneWiz). Finally, pPSV39CV-PA2582 was electroporated into PAO1 ΔPA2582 and colonies were selected from LBGm100 plates to confirm IPTG-dependent production of PA2582-VSVG by Western blot using α-VSV-G antibody (Abcam).

Bioassay guided fractionation of *S. aureus* SA113 supernatant

To generate *S. aureus* supernatant, SA113 overnight cultures grown shaking at 37^{o}C in either LB broth or PN media were back diluted and grown to midlog, shaking at 37^{o}C. Midlog cells were used to inoculate 100mL flasks of LB broth or PN media at a final OD_{600} of 0.05 and flasks were grown shaking at 37^{o}C for 6 hours. After 6 hours, both LB and PN media cultures had reached early stationary phase. *S. aureus* cell free culture supernatant was harvested, subjected to boiling, Dnase I, Rnase, proteinase K, and fractionation by molecular weight cutoff filter alongside clean LB controls, and each sample was used in a crystal violet assay with PAO1 to track the activity of the biofilm-stimulatory molecule(s) as previously described(25). Additionally, molecules soluble in methanol were extracted by mixing equal volumes of either cell free SA113 supernatant grown in minimal media (PN media) or clean PN media (control) with methanol on a rotator for 10 minutes, followed by static incubation at room temperature for 1 hour. The methanol phase was removed, dried by speedvac, and resuspended as a concentrate in PBS. The methanol extract was added back into LB broth at 1x final concentration and filter sterilized before use in a crystal violet assay as previously described(25).

Crystal violet assays with purified c-di-AMP and c-di-AMP analogs

Purified 50-100mM stocks of c-di-AMP in PBS were a gift from the laboratory of Dr. Joshua Woodward and were enzymatically synthesized from ATP (Perkin-Elmer) as previously described (177). Purified 2,3- and 3,3-cyclic guanosine monophosphate-

adenosine monophosphate (2,3-cGAMP and 3,3-cGAMP), cyclic di-inosine monophosphate (c-di-IMP), cyclic adenosine monophosphate (cAMP), and cyclic di guanosine monophosphate (c-di-GMP) were gifts from the laboratory of Dr. Joshua Woodward. C-di-AMP and the nucleotide analogs were added into LB at 1μM final concentration. Additional conditions in the experiment were *S. aureus* cell free culture supernatant and 10μM c-di-AMP. The crystal violet assay was performed as previously described with plates harvested at 2, 4, and 6 hours (25). Data presented is after 4 hours, but the trend was the same across all three timepoints.

Hydrolysis of c-di-AMP from *S. aureus* culture supernatant

Purified PdeA from *L. monocytogenes* was a gift from the laboratory of Joshua Woodward. *S. aureus* cell free culture supernatant, LB with 10μM c-di-AMP, and LB was buffered with 100mM Tris pH 8.3, 20mM KCl, and 1mM $MnCl_2$ and filter sterilized. Purified PdeA was added to a final concentration of 1μM to each sample and incubated with rotation at 37^{o}C for 1 hour. Crystal violet assays were performed with buffered LB, *S. aureus* supernatant, and LB with 10μM c-diAMP with and without incubation with PdeA. The crystal violet assay was performed as previously described with plates harvested at 2, 4, and 6 hours (25).

Identification of c-di-AMP binding proteins in *P. aeruginosa*

P. aeruginosa PAO1 was grown to OD_{600} = 0.5 in LB, cells were pelleted by centrifugation, resuspended in TNT lysis buffer (0.1 M Tris-HCl [pH 7.5], 150mM NaCl, 0.1% v/v Tween-20) with 1mM PMSF, and lysed three times by sonication for 10 seconds, followed by 10 seconds of incubation on ice. Cellular debris was pelleted from the lysate by centrifugation in a swinging bucket centrifuge at 15,000 rpm for 45 minutes. Expoxy-activated sepharose beads to which cyclic di-AMP had been conjugated (cda beads) or control beads conjugated with ethanolamine (control beads) were prepared as previously described (178). *P. aeruginosa* cell lysate was incubated with 200μl of PBS-washed cda beads or control beads for 2 hours on a rotator at 4^{o}C. Beads were pelleted by brief centrifugation at 3,000rpm, supernatant was removed, and beads were washed 3 times with 5mL cold PBS. Beads were resuspended in 1mL PBS and transferred to a microscentrifuge tube, where they were pelleted and the remaining PBS was removed.

Proteins were eluted from the beads by two rounds of heating at 56^{o}C for 10 minutes in 100µL Laemmli buffer and eluents were pooled for a final volume of 200µl per sample.

Protein samples were run on a 12.5% SDS-PAGE gel (BioRad) at 90V for 120 minutes and stained with the mass spectrometry-compatible SilverQuest Silver Stain (Invitrogen), 8 gel slices were cut per sample to capture the whole well, and then slices were destained by following the manufacturer's instructions. Proteins were digested using in-gel protein digests and LC-MS/MS was performed on tryptic peptides in collaboration with the laboratory of Dr. Michael MacCoss, as previously described (25). Peptides were identified using a *P. aeruginosa* PAO1 FASTA database. Proteins present in the cda bead pulldown with an NSAF score greater than 0.01, but absent or detected in only trace amounts in the control beads were considered a potential c-di-AMP target.

Identification of PA2582 binding proteins in *P. aeruginosa*

P. aeruginosa Δ*PA2582* harboring pPSV39CV-PA2582 was grown to mid-log in LB with or without the addition of 10µM c-di-AMP. Cells were lysed and lysates were harvested as described above for identification of c-di-AMP binding proteins. Immunoprecipitation of PA2582 was performed using 50 µl of anti-VSV-G beads (Sigma Aldrich) and incubated for 2 hrs at 4°C on a rotator. After incubation, the beads were separated by centrifugation at 700 rpm for 2 minutes and the unbound lysate was removed carefully. The beads were washed 3 times with Tris-buffered saline (TBS) plus 0.1% Tween and resuspended in Laemmli buffer. Proteins were eluted from the beads by boiling and samples were run on a 12.5% SDS-PAGE protein gel (BioRad). Bands were cut from the gel and LC-MS/MS was performed on in-gel digested tryptic peptides in collaboration with the laboratory of Dr. Michael MacCoss, as previously described (25).

Expression of PAO1 *PA2582* in *E. coli* and purification

The gene *PA2582* was cloned from MPAO1 genomic DNA using primers PA2582ExpressF and PA2582ExpressR, which excluded the PA2582 stop codon, double digested with NdeI/XhoI, and column purified. The expression vector pET20(b) was purified from *E. coli* XL1-Blue (Novagen), double digested with NdeI/XhoI and treated with Antarctic Phosphatase. The PA2582 fragment was ligated into digested pET20(b) to make pET20b-PA25826xHis, a vector containing C-terminally 6xHis-tagged PA2582 with a glycine-serine-serine (GSS) linker between PA2582 and the 6xHis tag, under

control of a T7 promoter. The PA25826xHis expression vector was transformed into *E. coli* Rosetta pLysS, and colonies were checked by purification of pET20b-PA25826xHis and sequencing with T7 forward and reverse primers (GeneWiz). To purify 6xHis-tagged PA2582, an overnight culture of *E. coli* Rosetta pLysS pET20b-PA25826xHis back diluted to OD600 0.05 in LB with 35 mg/L kanamycin and 35 mg/L chloramphenicol. Once the culture had reached OD600 0.5, cells were induced for 14 hrs with 1 mM Isopropyl β-D-1-thiogalactopyranoside (IPTG) at 20°C. Cells were harvested by centrifugation and lysed in PBS with 1mM PMSF, then soluble protein was purified by Ni-NTA agarose (Qiagen) chromatography. An aliquot of purified His-tagged PA2582 protein was run on an SDS-PAGE gel and stained with Coomassie to confirm the size and to check for purity. PA2582 homologs from *Achromobacter xylosoxidans* and *Pseudomonas putida* were cloned into pET20b as described above. The *A. xylosoxidans* PA2582 homolog (AX27061_2971) was amplified from ATCC strain 27061 (179) genomic DNA using primers AX2971ExpressF and AX2971ExpressR. The *P. putida* PA2582 homolog (Pput_2182) was amplified from strain KT2440 (180) genomic DNA using primers Pput2182ExpressF and Pput2182ExpressR.

DRaCALA on His-tagged PA2582

DRaCALA was performed by TuAnh Huynh in the laboratory of Joshua Woodward as previously described (177) using purified 6xHis-tagged PA2582, and the PA2582 homologs AXY2971 and PPUT2182.

Formaldehyde and UV-crosslinking CLIPseq's on PA2582-associated RNA

For CLIPseq of PA2582-associated RNA in the absence of c-di-AMP, separate cultures of PAO1 ΔPA2582 or PAO1 ΔPA2582 harboring pPSV39CV-PA2582 were grown to mid log phase in LB with 1μM IPTG and 100μg/mL gentamycin, then cells were pelleted and treated with 1% formaldehyde in 10mM sodium phosphate buffer (pH 7.0) for 30 minutes at room temperature. Glycine was added to 125 mM final concentration, and the cultures were incubated for an additional 5 min before cells were washed twice with PBS (pH 7.3). Cell pellets were stored at – 80 °C. To immunoprecipitate VSVG-tagged PA2582 along with its bound RNA, cells were thawed on ice and resuspended in 250 μl of lysis buffer (20 mM Tris-HCl [pH-7.5], 150 mM NaCl, 2 % Glycerol, 0.2 % Triton X100, protease inhibitor and Rnase inhibitor). Cells

were lysed in a bath sonicator as well as lysed with a probe sonicator for 3 seconds at a minimum power setting. After lysis, cell debris was removed by centrifugation at 13,000 rpm for 30 minutes, and the cell lysates were separated from the pelleted debris. The cell lysates were spiked with 30 µl of anti-VSVG beads and incubated for 2 hrs at 4°C on a rotator. After incubation, the beads were separated by centrifugation at 700 rpm for 2 minutes and the unbound lysate was removed carefully. The beads were washed 3 times in 10mL of cold lysis buffer on a rotator, then pelleted and transferred to a new tube. To reverse formaldehyde-induced crosslinks and elute RNA from the beads, the immunoprecipitated samples were incubated at 65°C for 2 hrs. The samples were then centrifuged and the supernatants were transferred to a new tube and treated with 150µl of Tris-EDTA buffer (TE) containing glycogen (0.27 mg/ml) and proteinase K (100 µg/ml) at 37°C for 2 hours. Then, RNA was purified by phenol-chloroform extraction, precipitated with isopropanol, washed with 70% ethanol, resuspended in water, and treated with DNase treated using the Ambion TURBO DNasekit. DNAse-treated RNA was ethanol precipitated, resuspended in molecular grade water, and used for cDNA preparation with the Ovation Complete Prokaryotic RNA-seq DR Multiples system (Nugen). The formaldehyde-based CLIP to identify RNA bound to VSVG-tagged PA2582 in the absence of c-di-AMP was performed in collaboration with Kamakshi Sureka in the laboratory of Joshua Woodward, and the subsequent RNAseq was performed through a collaboration of Dr. Joshua Woodward with the Fred Hutchinson Cancer Research Center Genomics & Bioinformatics Shared Resource.

PAO1 ΔPA2582 pPSV39CV grown in the presence of 10µM c-di-AMP was used in a CLIPseq experiment that used *in vivo* UV-crosslinking instead of formaldehyde crosslinking, based on a protocol developed by Dr. Erik Holmqvist in the laboratory of Dr. Jörg Vogel(181) and with significant help from Dr. Maureen Thomasson in the laboratory of Dr. Pete Greenberg. Overnight cultures of PAO1 ΔPA2582 pPSV39CV were diluted to an OD600 of 0.01 in 200mL LB media and grown at 37°C with shaking in two separate flasks. At OD_{600} of 0.15, 0.5mM IPTG was added to each to induce PA2582-VSVG expression. To one flask, 3ul purified cda was added to a final concentration of 1uM. At OD600 0.45, 100mL of each sample was removed and transferred to two 50mL conical tubes on ice (non-UV crosslinked controls), whereas the

other 100mL of cells was transferred to a plastic tray (22x22cm). Samples were crosslinked using a UV Stratalinker at 800mJ (setting is "8000" on Stratalinker display; approximately 5 minutes). The crosslinked samples were transferred to two 50mL conical tubes on ice. Crosslinked and non-crosslinked cells were pelleted by centrifugation at 4150 rpm and 4°C for 40 min, then supernatant was removed and cell pellets were stored at -80°C. To lyse cells an immunoprecipitate VSVG-tagged PA2582, pellets were resuspended in 800uL ice cold Buffer NP-T (50mM NaH2PO4, 300mM NaCl, 0.05% Tween20, pH 8.0 plus 8µl Halt Protease inhibitor and 2µL RNaseOUT RNase inhibitor [Invitrogen]). Two milliliter Eppendorf tubes were filled with 1mL glass beads and 800µL cell suspension, cells were lysed in a bead beater at 30Hz for 10 minutes at 4^{o}C, and tubes were centrifuged at 13,000rpm for 15 minutes at 4^{o}C to separate supernatant from beads. Supernatant was transferred to a new tube and 50µL of each sample was mixed with 2X Laemmli buffer and stored at -20^{o}C for Western blot analysis of VSVG-tagged PA2582. The rest of the cell lysate was diluted 5x in NP-T buffer and 400µL of PBS-washed anti-VSVG agarose beads (Sigma Aldrich) were added. Samples were incubated for 1 hour on a rotator at 4^{o}C, the beads were washed twice with 1mL High Salt Buffer (50mM NaH2PO4, 1M NaCl, 0.05% Tween20, pH 8.0) followed by two washes with 1mL NP-T buffer. Contaminating DNA and unbound RNA was digested by resuspending the beads in a benzonase mixture (999ul NP-T with 1mM $MgCl_2$ and 1µL benzonase [250U/ul]) and incubating for 10 minutes at 37^{o}C, with agitation at 900rpm and occasional low speed vortexing. Beads were chilled on ice for 2 minutes, the following washes were performed: once with high salt buffer, twice with NP-T buffer, once with high salt buffer, and twice with NP-T buffer. Beads were resuspended in 20µL Laemmli buffer, incubated at 95^{o}C for 5 minutes, then centrifuged and supernatant was transferred to new tubes. Samples were run at 40mA on a 10% SDS-polyacrylamide gel, with an empty well between each sample to avoid cross-contamination, then transferred to a nitrocellulose membrane at 4^{o}C. The membrane was stained with Ponceau S and the one band of the gel, which correspond to PA2582-VSVG was cut out, cut into 8 smaller pieces, and treated with 400µL proteinase K solution (200 µl 2X PK Buffer [100mM Tris-HCl, pH 7.9, 10mM EDTA, 1% SDS], 20µL Proteinase K [20mg/mL], 1µL RNase Inhibitor, 179µL RNase-free H_2O) for 1 hour at 37°C with 1000 rpm agitation and

occasional low speed vortexing. Then, 100µl 1xPK buffer with 9M Urea was added and samples were incubated for 1 hour at 37°C and 1000 rpm agitation. RNA was extracted by combining 450µL of proteinase K-treated samples with 450ul phenol:chloroform:IAA in a Pellet Phase Lock Gel tube. Samples were shaken to mix and incubated at 30^{o}C for 5 minutes, then centrifuged for 12 minutes at 13000 rpm and 4^{o}C. Supernatant containing RNA was transferred to a new 2mL tube and RNA was precipitated by combining with 1µL glycogen, 40µL 3M NaOAc (3M, pH 5.0), and 1200µL 100% EtOH. Samples were vortexed and incubated overnight at -20°C. RNA was pelleted by centrifugation for 30 minutes at 13,000 rpm and 4°C. Supernatant was removed and the pellet was washed with 800µl of 70% ethanol. The samples were centrifuged for 30 min at 13,000 rpm and 4°C, supernatant was removed, and the pellets were allowed to air dry at room temperature. Pellets were resuspended in 10µL RNase-free water, then heated at 65°C for 5 minutes with vortexing to fully resuspend the precipitated RNA. These samples were then used to prepare a cDNA library using the TruSeq Stranded RNA HT following manufacturers instructions. The adaptors for our four samples are located in wells D2-D5 (D2: D702 and D504, D3: D703 and D504, D4: D704 and D504, D5: D705 and D504). Our final cDNA library samples were: 1) UV-crosslinked VSVG-tagged PA2582 without c-di-AMP, 2) non-crosslinked VSVG-tagged PA2582 without c-di-AMP (control), 3) UV-crosslinked VSVG-tagged PA2582 with 1µM c-di-AMP, 4) non-crosslinked VSVG-tagged PA2582 with 1µM c-di-AMP (control). Sample number 3 was sequenced twice in collaboration with Hillary Hayden in the UW CF RDP sequencing core by Illumina MiSeq. In an attempt to reduce the number of rRNA reads, size purification was performed by excising bands from samples run on a 6% polyacrylamide/7M urea gel (Novex) to select for cDNA between 25-140bp (fragments that were protected from benzonase digestion due to being bound by PA2582), cDNA was precipitated, 6 rounds of PCR were performed using primers TruSeq_adapterF and TruSeq_adapterR that bound to the adapters as previously described(181), and DNA was precipitated again. Then, sample numbers 3 and 4 were sequenced once together by Illumina MiSeq.

Psl immunoblots

Psl production was detected by Psl immunoblot using α-Psl monoclonal antibodies (MedImmune) as previously described(25).

Biolog Phenotypic Microarrays

Biolog Phenotypic Microarrays were performed on wild type MPAO1 and MPAO1 Δ*PA2582* using plates 1-5, 9-13, and 15-20 (Biolog, Hayward, CA) and following the manufacturer's protocol. For the runs with added c-di-AMP, the same Biolog plates were run with wild type MPAO1, but c-di-AMP was spiked into the Biolog growth media at a final concentration of 5μM prior to beginning the assay.

Figures

Table 1. Strains, primers, and plasmids used in Chapter 2.

***P. aeruginosa* Strains**		**Reference**
MPAO1	wild-type	Jacobs, 2003
P. aeruginosa 102-2	Psl-producing clinical isolate	Armbruster, 2016*
MPAO1 ΔPA2582	In-frame deletion of *PA2582*	This study
MPAO1 ΔPA2582	pPSV39CV-PA2582	This study
MPAO1ΔPA2582 Tn7::PA2582	PA2582 mutant complemented with PA2582 under control of its native promoter at att site	This study
***E. coli* Strains**		
E. coli Rosetta pLysS pET20b-PA2582	Cloning strain with IPTG-inducible, c-terminally 6x His-tagged PA2582	This study
E. coli Rosetta pLysS pET20b-AXY2971	Cloning strain with IPTG-inducible, c-terminally 6x His-tagged AXY2971	This study
E. coli Rosetta pLysS pET20b-PPUT2182	Cloning strain with IPTG-inducible, c-terminally 6x His-tagged PPUT2182	This study
E. coli DH5α pDONRPEX18-Gm::ΔPA2582	*E. coli* cloning strain harboring Gateway cloning vector containing PA2582 deleltion allele	This study
E. coli S17.1 pDONRPEX18-Gm::ΔPA2582	Conjugation-proficient E. coli strain harboring Gateway cloning vector containing PA2582 deletion allele	This study
E. coli DH5a pPSV39CV-PA2582	*E. coli* cloning strain harboring vector containing C-terminally VSVG-tagged PA2582	This study
E. coli DH5a pUC18-miniTn7T-Gm::PA2582	E. coli harboring PA2582 complementation allele	This study
Other bacterial Strains		
S. aureus	wild type, SA113	Iordanescu, 1976
Achromobacter xylosoxidans	wild type, ATCC 27061	Yabuuchi, 1971
Pseudomonas putida	wild type, KT2440	Nelson, 2002
Primers		
PA2582ExpressF	GATACTCATATGATGGGTTTTGAACAACTTG	This study
PA2582ExpressR	AGTATCCTCGAGGCTGCTGCCGTTCGCCTCGGGGCTCGC	This study
AX2971ExpressF	GATACTCATATGTTGAAGCAGGCTCCCGA	This study
AX2971ExpressR	AGTATCCTCGAGGCTGCTGCCGTCGGCGCTCTGGGTGT	This study

Pput2182ExpressF	GATACTCATATGATGGGTTTTGAACAAC TAG	This study
Pput2182ExpressR	AGTATCCTCGAGGCTGCTGCCGTCGGTA GACTGCACCG	This study
PA2582UpF01-GWB1	GGGGACAAGTTTGTACAAAAAAGAGGC TACGATGGATGGCTACGAGCTGG	This study
PA2582UpR01	CTCGGGGCTCGCTTCGGT CTCGGCAAGTTGTTCAAA	This study
PA2582DownF01	ACCGAAGCGAGCCCCGAG	This study
PA2582DownR01-GWB2	GGGGACCACTTTGTACAAGAAAGCTGG GTACGGATTTGCAATCCGGTG	This study
M13F(-21)	TGTAAAACGACGGCCAGT	GeneWiz
M13R	CAGGAAACAGCTATGAC	GeneWiz
PA2582F01-Seq	GCGAGGAAGCATTCGAACG	This study
PA2582R01-Seq	GAGACCGTAAAAGTATGAAAGCG	This study
BamH1-PPA2582-F	CATGGATCC GCTGCCGGCATGGACCGGGTCC	This study
HindIII-PA2582-R	CATAAGCTT TCAGTTCGCCTCGGGGCTCGC	This study
P_{Tn7R}	CACAGCATAACTGGACTGATTTC	Choi, 2006
$P_{glmSdown}$	GCACATCGGCGACGTGCTCTC	Choi, 2006
SacI-PA2582RBS-F	GATACT GAGCTC CTCTCGCAGAAATGAACC	This study
XbaI-PA2582RBS-R	AGTATCTCTAGAGCTGCTGCCGTTCGCC TCGGGGCTC	This study
pPSV39CV_seq_rev	CCCGTTTAGAGGCCCC	This study
T7	TAATACGACTCACTATAGGG	GeneWiz
T7_term	GCTAGTTATTGCTCAGCGG	GeneWiz
TruSeq_adapterF	AATGATACGGCGACCACCG	This study
TruSeq_adapterR	CAAGCAGAAGACGGCATACG	This study
Plasmids		
pET20b-PA2582	vector containing IPTG-inducible, c-terminally His-tagged PA2582	This study
pET20b-AXY2971	vector containing IPTG-inducible, c-terminally His-tagged AXY2971	This study
pET20b-PPUT2182	vector containing IPTG-inducible, c-terminally His-tagged PPUT2182	This study
pDONRPEX18-Gm::ΔPA2582	PA2582 deletion allele	This study
pPSV39CV-PA2582	vector containing IPTG-inducible, c-terminally VSVG-tagged PA2582	This study
pUC18-miniTn7T-Gm::PA2582	PA2582 complementation vector	This study

*Collected from subjects enrolled in an ongoing, IRB-approved study (methods)

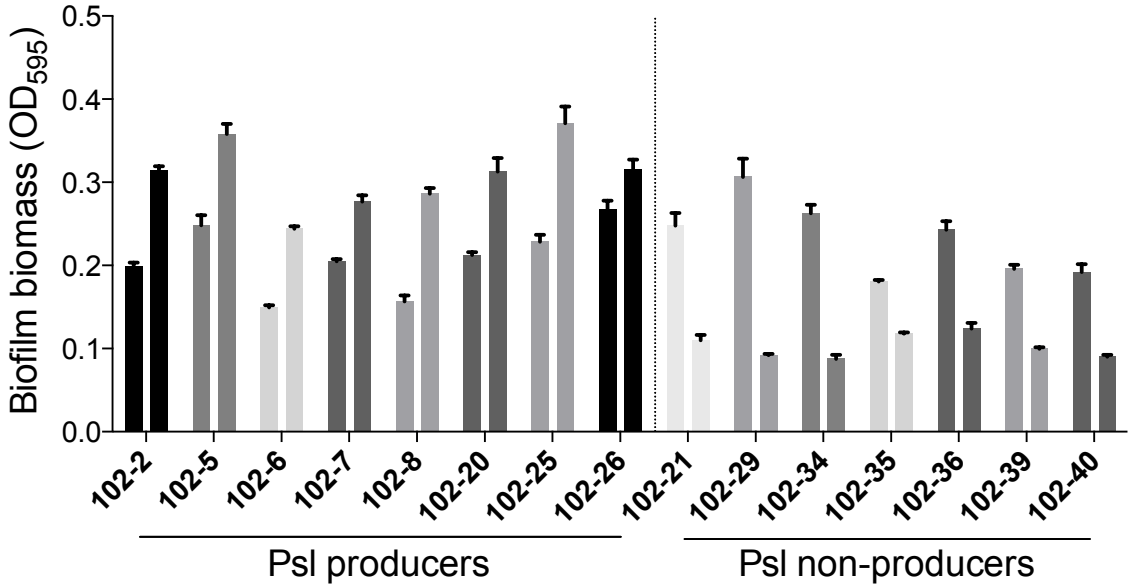

Figure 1. Psl-producing *P. aeruginosa* isolates from CF patient sputum display elevated levels of biofilm when grown in *S. aureus* cell-free culture supernatant compared to when grown in LB. Four hour biofilm formation as measured by crystal violet assay for clonally-related Patient 102 isolates. For each isolate, the left bar is growth in LB and the right bar is growth in *S. aureus* cell-free culture supernatant.

a)

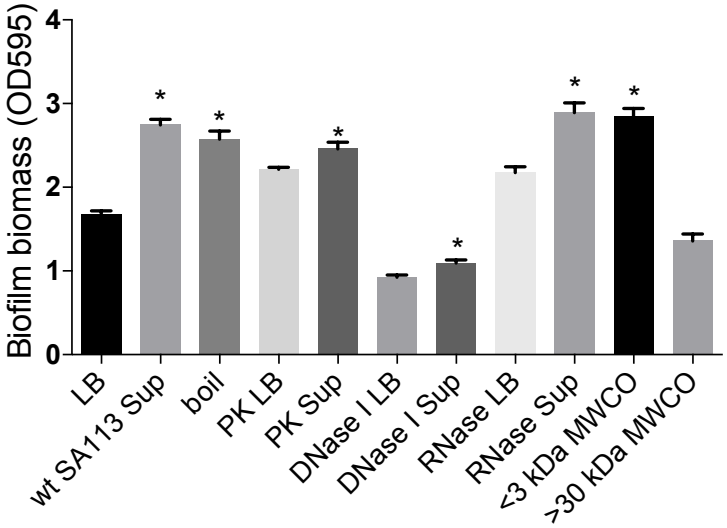

b)

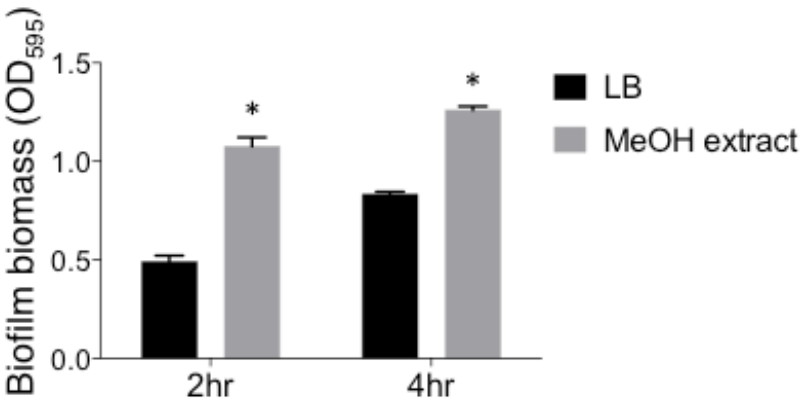

Figure 2. a) Analysis of SA113 supernatant by chemical and physical treatments indicate that biofilm induction activity is due to a heat stable molecule smaller than 3kDa. In each case, treated supernatants were added to a Psl+ CF clinical isolate (102-2) and biofilm formation was measured by crystal violet assay. PK is proteinase K. b) Biofilm formation by *P. aeruginosa* clinical isolate 102-2 during growth in LB or in LB with the addition of methanol-extracted SA113 supernatant. Asterisks indicate statistically significant increases in biofilm biomass compared to growth in the equivalent treated LB ($p < 0.05$)

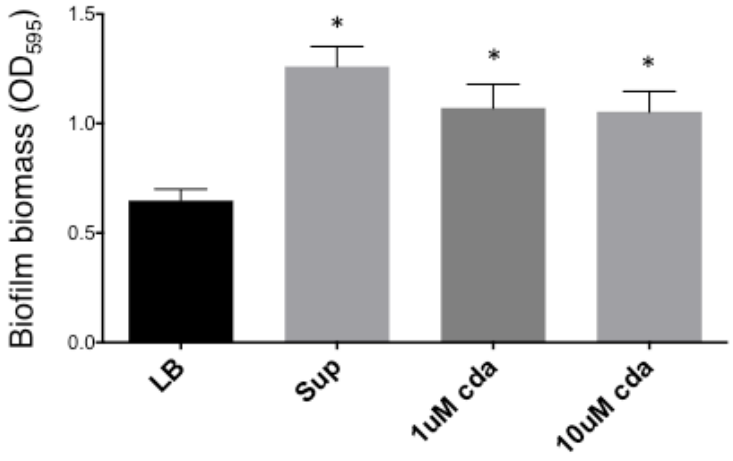

Figure 3. *P. aeruginosa* biofilm formation is enhanced by *S. aureus* cell-free culture supernatant (Sup) and low micromolar levels of purified c-di-AMP (cda). Crystal violet assay was performed after 4 hours of static growth of *P. aeruginosa* lab strain PAO1. Sup = *S. aureus* SA113 cell-free supernatant, cda = purified c-di-AMP added into LB. Asterisks indicate statistically significant increases in biofilm biomass compared to growth in LB ($p < 0.05$)

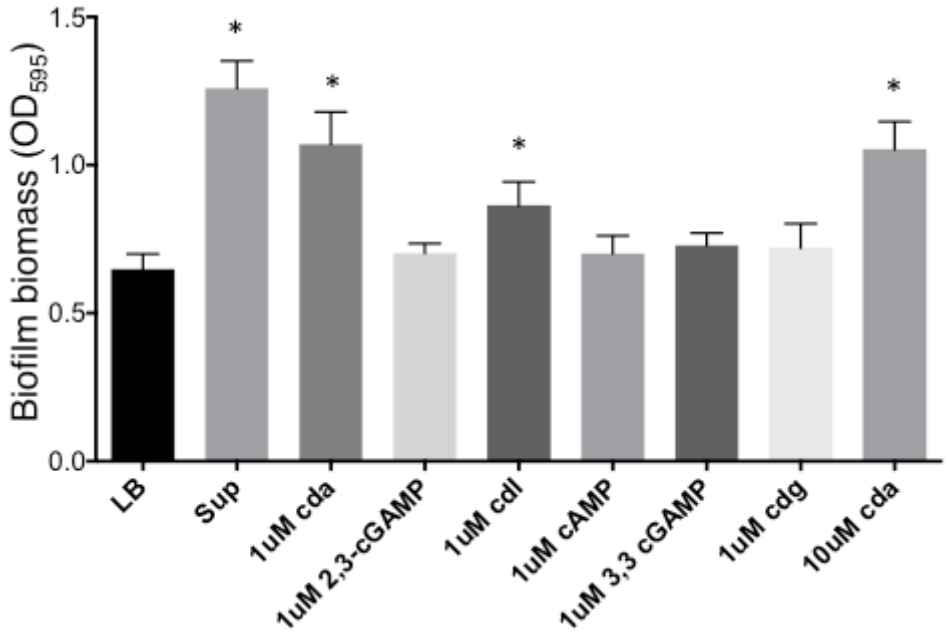

Figure 4. *P. aeruginosa* forms elevated biofilm biomass in response to purified c-di-AMP, but not other purified cyclic nucleotide analogs. Crystal violet assay was performed after 4 hours of static growth of *P. aeruginosa* lab strain PAO1. Purified cyclic nucleotides or cyclic di-nucleotides were added into clean LB media at the indicated concentrations. Sup = *S. aureus* SA113 cell-free supernatant, cda = purified c-di-AMP added into LB, cdI = c-di-IMP, cdg = c-di-GMP. Asterisks indicate statistically significant increases in biofilm biomass compared to growth in LB ($p < 0.05$)

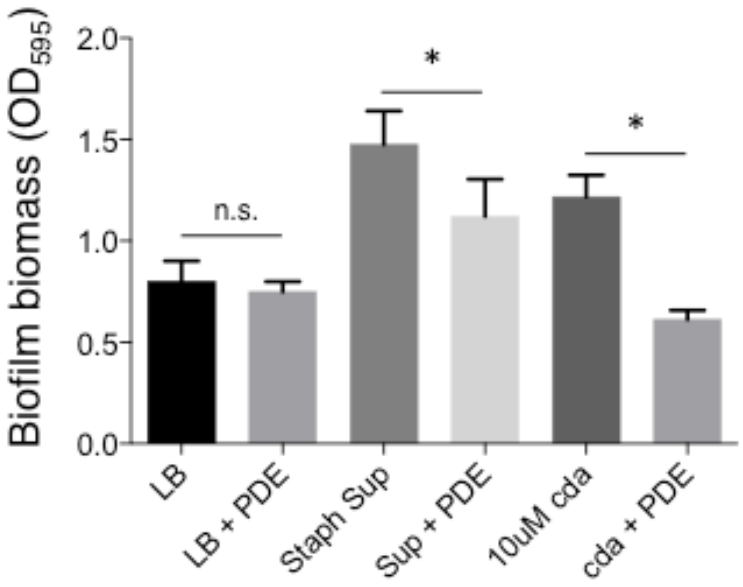

Figure 5. Hydrolysis of c-di-AMP from SA113 supernatant using purified phosphodiesterase indicates that *P. aeruginosa* biofilm formation is stimulated by c-di-AMP (cda) present in *S. aureus* cell free culture supernatant (Sup), as well as potentially an additional molecule(s) that is insensitive to hydrolysis by the phosphodiesterase (+ PDE). Crystal violet assay was performed after 4 hours of static growth of *P. aeruginosa* lab strain PAO1. Asterisks indicate statistically significant differences in biofilm biomass compared to the same condition without phosphodiesterase treatment ($p < 0.05$). n.s. indicates no statistically significant difference by t test ($p > 0.05$).

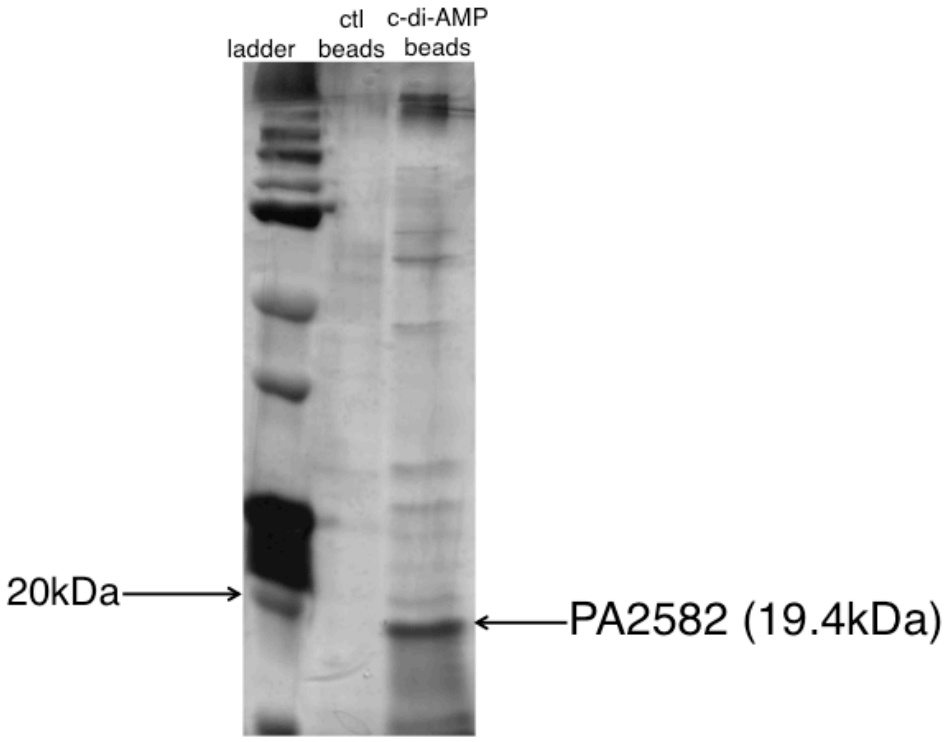

Figure 6. Silver stained SDS-PAGE protein gel comparing proteins bound to c-di-AMP-coupled sepharose beads (c-di-AMP beads) versus proteins bound nonspecifically to empty beads ("ctl beads" blocked with ethanolamine groups). "Ladder" = Dual color Precision Plus Protein ladder (Biorad). The arrow indicates the band where the 19.4kDa protein PA2582 was detected.

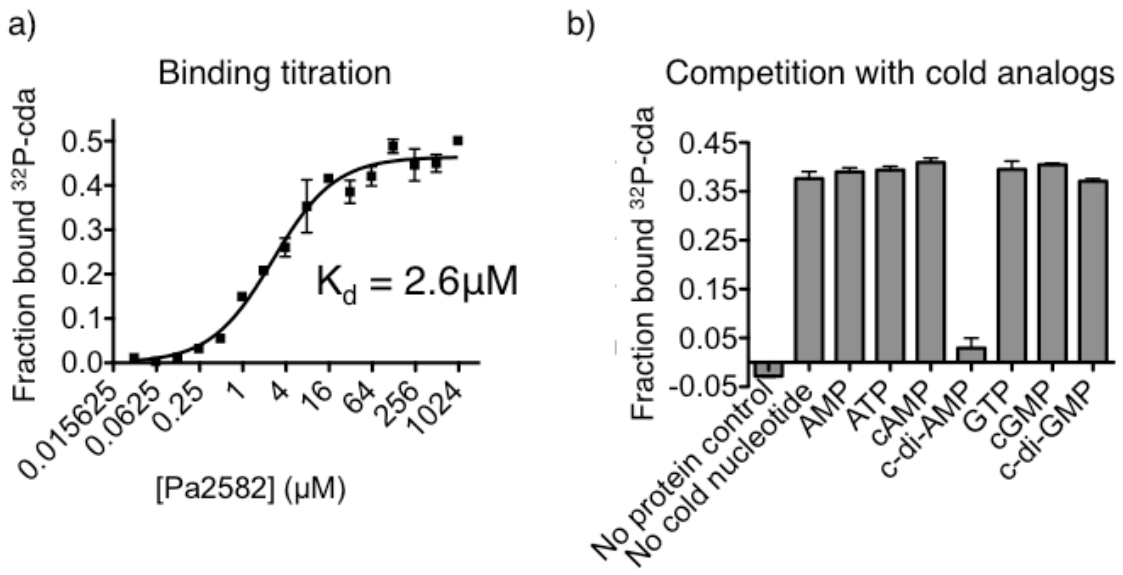

Figure 7. PA2582 binds c-di-AMP. a) Binding titration performed by differential radial capillary action of ligand activity (DRaCALA) with ^{32}P-c-di-AMP and purified, 6x-His-tagged PA2582 indicating that the dissociation constant is 2.6 μM. b) Competition of ^{32}P-c-di-AMP binding to PA2582 with 200 μM non-radioactive nucleotides ("cold" nucleotide), cyclic nucleotide, and cyclic di-nucleotide analogs demonstrates that PA2582 binds specifically to c-di-AMP and not broadly to other similar nucleotide-based molecules. Values are averages of densitometry values from at least three independent samples per condition.

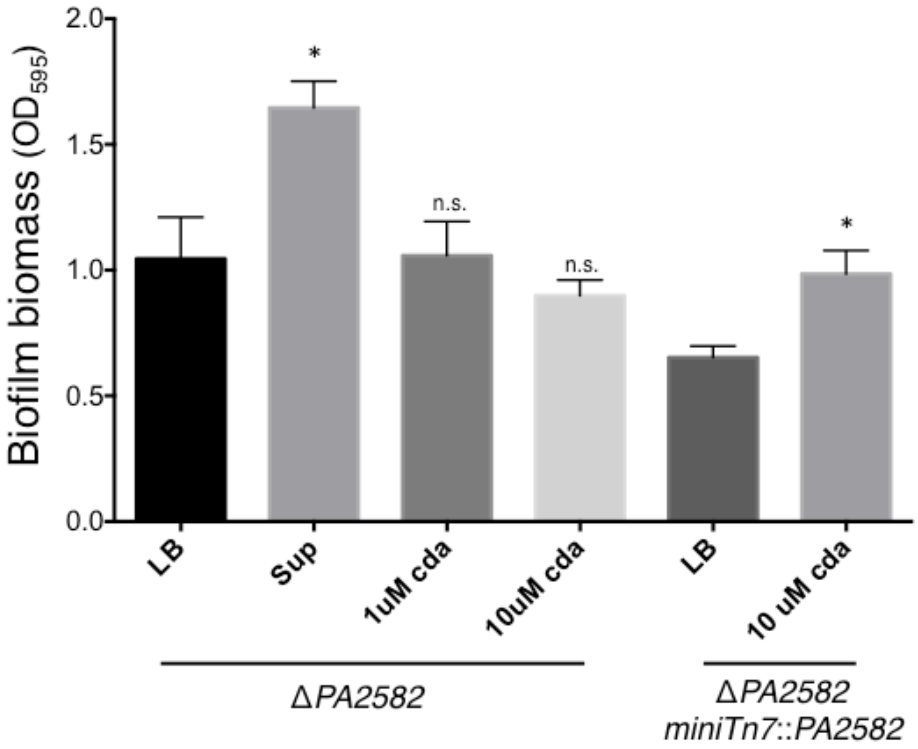

Figure 8. PA2582 is required for enhanced biofilm formation in response to purified c-di-AMP. Crystal violet assay was performed after 4 hours of static growth of PAO1 Δ*PA2582* or the same mutant complemented with PA2582 from its native promoter at a neutral site on the chromosome, PAO1 ΔPA*2582* miniTn7::*PA2582*. Asterisks indicate statistically significant differences in biofilm biomass compared to growth in LB ($p < 0.05$). n.s. indicates no statistically significant difference by t test ($p > 0.05$).

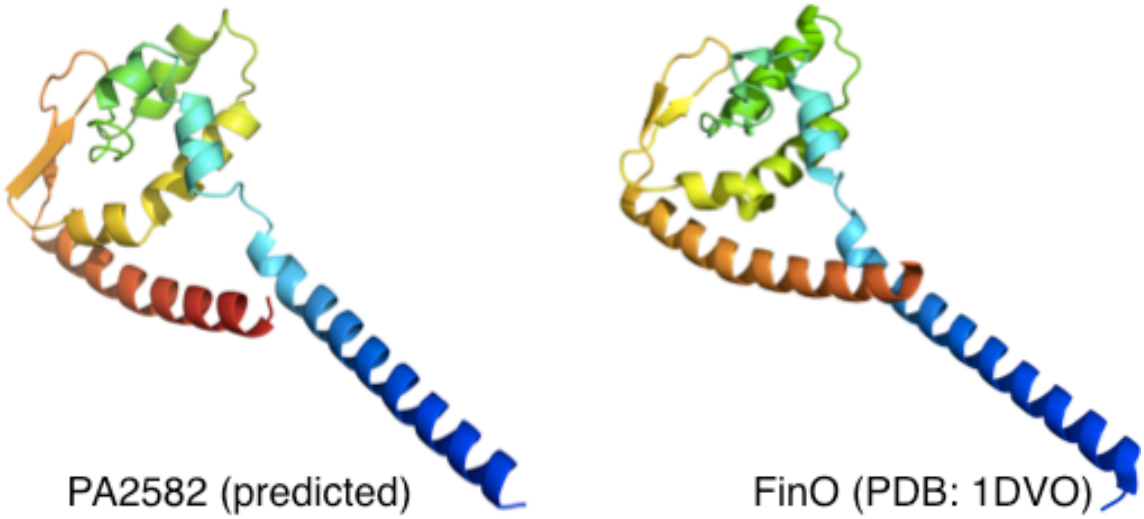

Figure 9. The structure of *P. aeruginosa* hypothetical protein PA2582 (predicted by Phyre2) compared to the crystal structure of the *E. coli* protein FinO. Each protein is colored in PyMol, from the N-terminus starting with blue, ending at the C-terminus with red.

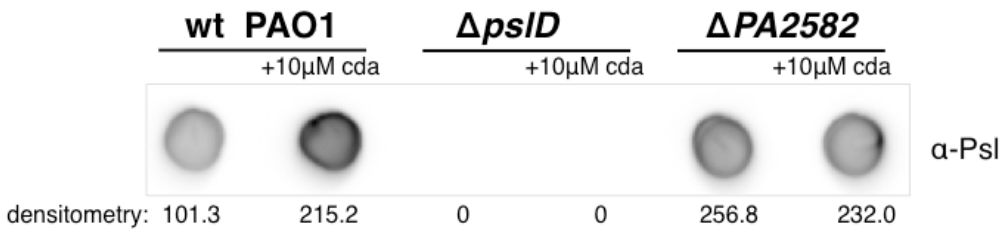

Figure 10. *P. aeruginosa* produces more Psl in a PA2582-dependent manner, in response to growth in the presence c-di-AMP. Psl immunoblot assay results for wild type PAO1, PAO1 Δ*pslD*, and PAO1 ΔPA2582 grown to early stationary phase in LB, in the presence or absence of 10μM c-di-AMP and normalized to OD_{600} prior to supernatants being harvested for Psl immunoblot. PAO1 Δ*pslD* is a control to confirm that the α-Psl antibody (MedImmune) is specific for Psl. Densitometry values are displayed below the corresponding immunoblot.

Table 2. Proteins identified as binding partners of PA2582, +/- addition of 10μM c-di-AMP. The normalized spectral abundance factor (NSAF) is a measure of the relative abundance of proteins in the sample. The five most abundant proteins identified by LC-MS/MS, aside from PA2582 and contaminating reads, were the same regardless of whether c-di-AMP was present during growth and are all components of translational machinery.

	Normalized spectral abundance factor (NSAF)	
Gene	plus c-di-AMP	no c-di-AMP
PA4239|30S	0.028373	0.02881
PA3162|30S	0.022699	0.028516
PA4273|50S	0.021409	0.026258
PA4267|30S	0.021295	0.021328
PA4241|30S	0.018275	0.020783

CHAPTER III

A division of labor during surface sensing influences *Pseudomonas aeruginosa* biofilm formation

Introduction

The second messenger signaling molecule cyclic diguanylate monophosphate (c-di-GMP) drives the transition from planktonic to the biofilm mode of growth in a variety of bacterial species. While factors contributing to the formation of mature biofilms have been well-characterized, early biofilm formation, when a bacterium first senses a surface and transitions from a planktonic state to a surface-attached state, remains poorly understood. *P. aeruginosa* has at least two "surface sensing" systems with homology to bacterial chemosensory signal transduction complexes that produce c-di-GMP in response to surface contact; the Wsp system and the Pil-Chp system. We sought to identify the relative contributions of these two signal transduction systems to c-di-GMP production during early biofilm formation in *P. aeruginosa*.

In response to surface contact, the Wsp system senses an unknown signal (recently proposed to be membrane perturbation (43)) through WspA, a membrane-bound receptor homologous to methyl-accepting chemotaxis proteins (MCPs), transducing a signal to the CheA homolog, WspE. Upon autophosphorylation, the sensor kinase WspE activates the diguanylate cyclase WspR through phosphorylation of a conserved aspartate residue on its receiver domain. Phosphorylation of WspR leads to the formation of large subcellular WspR-P aggregates that synthesize c-di-GMP (182). The Wsp system is known to regulate biofilm matrix production through the transcription factor FleQ, a c-di-GMP-binding transcription factor that acts in complex with FleN to inversely regulate transcription of genes involved in flagellar biosynthesis and biofilm matrix production (183). When cellular levels of c-di-GMP are high, such as during growth on a surface, FleQ binds c-di-GMP and derepresses transcription of genes encoding the Pel and Psl polysaccharide biosynthetic machinery, as well as the adhesin CdrA (183–186). Binding of c-di-GMP to FleQ occurs with a lower affinity (K_D = 15-25μM (183, 186)) compared other c-di-GMP binding effectors in *P. aeruginosa* (such as the type IV pilus assembly regulator FimX, K_D = 125nM) (55), thus ensuring that transcription of genes associated with biofilm matrix production generally occurs at higher cellular c-di-GMP levels than those that lead to earlier stages in biofilm formation, including suppression of flagellar- and type IV pilus-mediated surface motility.

The Pil-Chp system is another chemosensory-like two-component system that is known to regulate twitching motility (187) and levels of cellular cyclic adenosine monophosphate (cAMP) (188), potentially through Type IV pilus-mediated sensing of mechanical tension during surface attachment (189). In work published simultaneously with the mechanosensory findings, the role of the Pil-Chp complex was expanded to include c-di-GMP signaling and biofilm regulation (142). The Pil-Chp system was proposed to initiate a hierarchical cascade of second messenger signaling in response to growth on a surface (142). First, an increase in cellular cAMP levels occurs through activation of the adenylate cyclase CyaB by the chemotaxis-like Pil-Chp complex. The transcriptional regulator Vfr binds cAMP and, in concert with the FimS-AlgR two component system, activates transcription of genes leading to type IV pilus biogenesis, including *pilY1*. PilY1 is localized to the cell surface through an unknown mechanism that requires the type IV pilus, where it is proposed to signal through the type IV pilus alignment complex proteins (PilMNOP) to activate the membrane-bound diguanylate cyclase SadC to produce c-di-GMP (142). Unlike the Wsp system, which has been shown to localize laterally along the cell (190), PilY1 is required to be associated with polarly-localized type IV pili in order to stimulate c-di-GMP production (142, 191), indicating that *P. aeruginosa* employs both polar and laterally localized surface sensing systems.

While the Wsp and Pil-Chp systems have individually been characterized extensively, much remains unknown regarding whether and how these systems coordinate the series of physiological changes that occur when *P. aeruginosa* first senses a surface. One challenge to interpreting the relative contributions of these two systems to surface sensing is that they have largely been characterized in different lab strains; Wsp in PAO1 and Pil-Chp in PA14. The Pil-Chp system has recently been proposed to become activated prior to Wsp, with evidence of type IV pilus production being stimulated within 120 minutes of surface contact (142). Additional evidence in support of this model includes the observation that high c-di-GMP levels suppress cAMP (192, 193), and that while a functional Wsp system contributes to biofilm macrocolony development, reports vary as to whether a WspR diguanylate cyclase mutant (Δ*wspR*) is defective for initial surface attachment (48, 194, 195).

Here, we examined the dynamics of c-di-GMP production at the single cell level during surface sensing and early biofilm formation. We used a plasmid-based, transcriptional reporter of intracellular c-di-GMP and a microscopy-based approach to follow the downstream fate of cells producing varying levels of c-di-GMP in response to surface attachment. We compared both surface sensing systems, Wsp and Pil-Chp, in two lab strains (PAO1 and PA14) in order to provide a comprehensive analysis of the relative roles of each system temporally for each strain. Within a clonal population of *P. aeruginosa*, we found that levels of c-di-GMP vary among individual cells as they sense a surface, leading to physiological differences between cells. We propose that these subpopulations of cells with high and low c-di-GMP levels represent a division of labor in the behaviors associated with early biofilm formation: surface exploration and polysaccharide production. Additionally, we demonstrate a role for the Wsp system in initiating early c-di-GMP signaling after surface attachment and we demonstrate how the dynamics of c-di-GMP production during surface sensing differ significantly by strain.

Results

Cellular c-di-GMP levels rapidly increase when upon surface attachment

In order to quantitate cellular levels of c-di-GMP change during surface sensing, we used LC-MS/MS to compare levels of c-di-GMP in mid-log *P. aeruginosa* PAO1 cells growing attached to a silicone tube under constant flow for 4 hours to the same quantity of bacteria grown planktonically in static liquid culture for 4 hours. We observed that PAO1 cellular c-di-GMP levels are 4.4-fold higher (+/−0.78) after 4h of growth attached to a surface compared to planktonic growth (Figure 1a). The Pel polysaccharide operon is regulated by a c-di-GMP-binding transcription factor, FleQ, and high cellular levels of c-di-GMP leads to FleQ-dependent transcription of Pel genes (183, 186). Pel production has previously been shown to be elevated in tube biofilms after 48 hours (21). Because direct measurement of c-di-GMP by LC-MS/MS is limited by our ability to generate enough biomass during very early surface attached growth, we used qRT-PCR to monitor Pel transcript levels as a marker of increased c-di-GMP during surface sensing in tube biofilms. We found that after just 30 minutes of surface attachment, *pelA*

transcript levels had increased almost 10-fold compared to planktonically grown cells (Figure 1b).

The P$_{cdrA}$::*gfp* reporter detects changes in c-di-GMP during surface sensing

We used a plasmid-based transcriptional reporter, pP$_{cdrA}$::*gfp*$_{\mathrm{ASV}}$ (53), to monitor c-di-GMP production at the single cell level by confocal microscopy during surface sensing and early biofilm formation in a flow cell system. *P. aeruginosa* cells were grown to planktonically to mid-log, a condition in which cellular levels of c-d-GMP are relatively low (56) and the pP$_{cdrA}$::*gfp*$_{\mathrm{ASV}}$ reporter is expected to be inactive. We imaged PAO1 pP$_{cdrA}$::*gfp*$_{\mathrm{ASV}}$ hourly for up to 6 hours after surface attachment in a flow cell (Figure 2 and 3b). As expected, we saw very minimal GFP fluorescence at the 0 hour time point (right after surface attachment). However, by 1 hour, the pP$_{cdrA}$::*gfp*ASV reporter was activated in a subset of surface attached cells, as defined by GFP fluorescence greater than twice that of background levels. Between 4 and 6 hours post inoculation, we consistently observed that the c-di-GMP reporter was active in 40-60% of surface attached PAO1 cells.

The Wsp system is required for surface sensing

We evaluated the relative contributions of both the Wsp and Pil-Chp chemosensory systems to surface-induced c-di-GMP production in PAO1. In response to an unknown signal during surface contact, the Wsp system is activated to produce c-di-GMP through phosphorylation of the diguanylate cyclase, WspR (194). Deletion of WspR results in inactivation of the Wsp system, whereas deletion of the gene encoding the methylesterase, *wspF*, locks the system into the active state, regardless of whether cells are surface-associated. As expected, we found that PAO1 Δ*wspR* harboring the pP$_{cdrA}$::*gfp*$_{\mathrm{ASV}}$ reporter had very low levels of reporter activity during the first 6 hours of surface sensing (Figure 3). Complementation of PAO1 Δ*wspR* with *wspR* provided *in trans* from the Wsp operon's native promoter restored wild type levels of pP*cdrA*::*gfp*$_{\mathrm{ASV}}$ reporter activity at all time points (Figure 4). Conversely, PAO1 Δ*wspF* had a greater percentage of cells with high reporter activity, even at the 0 hour time point, which was expected because this strain has constitutive Wsp system activity, resulting in high cellular levels of c-di-GMP (194) (Figure 3). We repeated these experiments using Wsp system mutants in the PA14 genetic background and saw a similar trend, although the

wild type PA14 displayed much lower levels of pP_{cdrA}::gfp_{ASV} reporter activity compared to wild type PAO1, with only 10% of cells showing induced reporter activity over 6 hours (Figure 5). Similar to PAO1, deletion of *wspR* in PA14 lead to a reduction in pP_{cdrA}::gfp_{ASV} reporter activity and deletion of *wspF* lead to a higher number of cells with pP_{cdrA}::gfp_{ASV} reporter activity (Figure 5). Thus, the pP_{cdrA}::gfp_{ASV} reporter is responsive to Wsp-dependent variation in cellular c-di-GMP levels upon surface attachment in both PAO1 and PA14.

To investigate if c-di-GMP reporter activity correlated with the capacity of strains to attach and form biofilm, we performed crystal violet attachment assays using Wsp system mutants and observed that a PAO1 Δ*wspR* mutant was defective for biofilm formation relative to wild type PAO1 after 2, 4, and 6 hours of attachment (Figure 6a). Furthermore, while PAO1 Δ*wspR* has a defect in early biofilm formation, this mutant displayed biofilm formation capacity similar to wild type levels by 24 hours (Figure 6a). Complementation of PAO1 Δ*wspR in trans* with *wspR* expressed from the *wsp* operon's native promoter restored wild type levels of biofilm formation (Figure 6b). When we imaged wild type PAO1 and PAO1 Δ*wspR* biofilms 12 to 24 hours after surface attachment, we saw that both strains had a greater percentage of active cells than at earlier time points (Figure 7b), but wild type PAO1 was the most active (Figure 7a). Finally, to confirm that the promoter of *cdrA* is representative of FleQ-regulated gene expression, we replaced P_{cdrA} with the promoter of *siaA*, a gene that is known to be highly expressed under conditions of high c-di-GMP (120) and that has recently been suggested to be regulated transcriptionally by FleQ (185). We found that pP_{siaA}::gfp_{ASV} reporter activity resembled that of pP_{cdrA}::gfp_{ASV} and was Wsp-dependent (Figure 8). Together, these data suggest that the Wsp system rapidly responds to surface contact to generate elevated levels of c-di-GMP during surface sensing and early biofilm formation, but other mechanisms contribute to full biofilm capability by 24 hours.

Interestingly, mutants in the Pil-Chp chemosensory system had less severe defects in surface sensing activity than equivalent Wsp system mutants. Whereas the pP_{cdrA}::gfp_{ASV} reporter was active in only active in fewer than 10% of Wsp system diguanylate cyclase mutant (PAO1 Δ*wspR*) cells during the first 6 hours of surface sensing, deletion of the diguanylate cyclase activated by the Pil-Chp system (PAO1

Δ*sadC*) had a very mild defect (Figure 9a,b). Similarly, a deletion in a gene encoding a protein thought to activate the diguanylate cyclase SadC in response to surface attachment (PAO1 Δ*pilY1*) was only partially defective for pP_{cdrA}::gfp_{ASV} reporter activity. Whereas both the SadC and PilY1 mutants displayed wild type levels of pP_{cdrA}::gfp_{ASV} reporter activity by 6 hours, a mutant lacking the main Type IV pilus filament protein (PAO1 Δ*pilA*) was the most defective of all Pil-Chp system mutants tested (Figure 9b). Complementation of PAO1 Δ*sadC* with SadC provided *in trans* with its native promoter restored wild type levels of pP*cdrA*::gfp_{ASV} reporter activity at all time points (Figure 4).

Previous work has demonstrated that SadC contributes to exopolysaccharide production and the transition to irreversible surface attachment during early biofilm formation in PA14 (196). We performed a crystal violet attachment assay to determine whether the SadC diguanylate cyclase was important for early biofilm formation in PAO1 and found this mutant to have a similar level of defect to the WspR diguanylate cyclase mutant (Figure 6a). Additionally, a double mutant of these two cyclases (PAO1 Δ*sadC* Δ*wspR*) had an additive defect during early biofilm formation, suggesting that both WspR and SadC proteins play pivotal roles at early stages of biofilm formation. Complementation of PAO1 Δ*sadC in trans* with SadC expressed from its native promoter restored wild type levels of biofilm formation (Figure 6b). Together, our data suggest that both the Wsp and Pil-Chp systems contribute to surface induced increases in c-di-GMP during early biofilm formation, and that mutants in the Wsp system have the greatest impact on initiation of c-di-GMP signaling during surface sensing.

Heterogeneity in c-di-GMP levels among cells correlates with Wsp system activity

To identify sources of heterogeneity in c-di-GMP production among cells during surface sensing, we first evaluated the role of DipA (Pch), a phosphodiesterase known to be involved in generating nanomolar levels of c-di-GMP heterogeneity during planktonic growth in PA14 that influences flagellar motility (197). While DipA is known to play a role in dispersal of mature biofilms (52), it is unknown whether this protein contributes to surface sensing in any way. We evaluated c-di-GMP reporter activity in PAO1 Δ*dipA* and found that this deletion did not affect variation in cellular c-di-GMP levels during the first 6 hours of surface sensing (Figure 10). Thus, the heterogeneity generated in c-di-

GMP levels during surface sensing is due to a separate mechanism than the nanomolar levels of heterogeneity generated by unequal partitioning of the DipA phosphodiesterase during cell division in planktonic growth.

Because our data suggest that surface sensing in PAO1 is dependent on activity of the Wsp system, we evaluated whether variability in Wsp system activity leads to the heterogeneity we observed in c-di-GMP production with cells harboring the P_{cdrA}::*gfp*$_{ASV}$ reporter. Through studies of Wsp system subcellular localization dynamics, the laboratory of Dr. Caroline Harwood has observed that Wsp complex formation and clustering of the WspR diguanylate cyclase occurs in only a subset of cells during growth on agar pads (a surface) (182, 190, 198). After 20 hours of growth on an agar surface, WspR-YFP clusters are visible in 29.7% (±2.9) of wild type PAO1 cells and 59.8% (±11.8) of PAO1 Δ*wspF* cells(198). We constructed a version of the c-di-GMP reporter that expresses mTFP1 instead of GFP to avoid the issue of spectral overlap with *wspR*-YFP (pP_{cdrA}::*mTFP1*). Using an arabinose-inducible WspR strain (PAO1 Δ*wspR* att::P_{BAD}-*wspR*-eYFP (182)), we found that pP_{cdrA}::*mTFP1* reporter was significantly increased when this strain was grown on LB agar with 1% arabinose compared to LB agar without arabinose, as expected (Figure 11a). We similarly monitored pP_{cdrA}::*mTFP1* activity in two point mutants of WspR that have been previously shown to form large subcellular WspR clusters, PAO1 Δ*wspR* att::P_{BAD}-*wspR*[L170D]-eYFP and PAO1 Δ*wspR* att::P_{BAD}-*wspR*[E253A]-eYFP. The WspR[L170D] protein is highly active for c-di-GMP production and cells expressing this allelic variant grow as rugose small colony variants, whereas the WspR[E253A] point mutation abolishes diguanylate cyclase activity (182). As expected, when these two strains were grown in the presence of 1% arabinose, we observed a large increase in pP_{cdrA}::*mTFP1* activity in the strain that produces c-di-GMP (WspR[L170D]), but not in the strain with an inactive WspR (WspR[E253A]; Figure 10a,b).

We used these two WspR point mutants that form highly visible subcellular WspR foci to determine whether heterogeneity in pP_{cdrA}::*mTFP1* activity is related to WspR clustering. When grown on an agar surface with 1% arabinose for 20 hours, we saw that many cells from each strain contained large clusters of WspR-eYFP, however only the WspR[L170D] strain displayed high levels of pP_{cdrA}::*mTFP1* reporter activity, as

expected (Figure 12a). Furthermore, we found that pP$_{cdrA}$::*mTFP1* activity was significantly higher in cells with at least one subcellular WspR-eYFP focus in the WspR[L170D] strain, but not in the WspR[E253A] strain (in which the WspR protein cannot produce c-di-GMP; Figure 12b). Thus, we found that heterogeneity in pP$_{cdrA}$::*mTFP1* levels was dependent on WspR activity and associated with WspR-eYFP cluster formation.

Cyclic di-GMP heterogeneity leads to phenotypic diversification at early stages of biofilm formation.

We wanted to confirm that cells exhibiting wither reporter on or off activity correlated to expected changes in cellular physiology. To determine whether subpopulations of surface attached *P. aeruginosa* cells with high and low c-di-GMP reporter activity are physiologically distinct from one another, we sought to correlate P*cdrA*::*gfp*$_{\mathrm{ASV}}$ reporter activity with stable downstream indicators of high c-di-GMP using flow cytometry. We used PAO1 cells that did not express GFP (wild type PAO1; Figure 13a) or constitutively expressed GFP (PAO1 Tn7::P(A1/04/03)::GFPmut; Figure 12b) to define a gate for high GFP fluorescence. We validated this gate using a strain in which we expect very high levels of reporter activity (surface grown PAO1 Δ*wspF*Δ*pelA*Δ*pslBCD* harboring pP*cdrA*::*gfp*$_{\mathrm{ASV}}$) and saw that 91.6% of cells had high GFP levels (Figure 13c), in agreement with our flow cell characterization of this strain (Figure 8b). After 4 hours of attachment to glass in a static biofilm system, the pP$_{cdrA}$::*gfp*$_{\mathrm{ASV}}$ reporter was active in an average of 56.6% of PAO1 cells, in agreement with the percentage of cells with high reporter activity after 4 hours in the flow cell biofilm system (Figure 13d). Similarly, reporter activity of wild type PA14 grown in LB resembled that of our flow cell experiments (12.8% of cells with reporter "on", Figure 13e). We grew PA14 in Jensen's minimal media with glucose, a condition in which Pel production is enhanced relative to growth in LB, and saw that the pP$_{cdrA}$::*gfp*$_{\mathrm{ASV}}$ reporter displayed greater activity in this media (31.9%; Figure 13F), suggesting that the growth medium can impact c-di-GMP levels during PA14 surface sensing.

Pel and Psl polysaccharide production are both known to be upregulated under conditions of high c-di-GMP (35). We used TRITC-labeled lectins specific for either Psl or Pel polysaccharides (24, 199) to identify polysaccharide-producing cells. We

determined gating for TRITC using cells that had not been stained with TRITC-conjugated lectin (Figure 14a), as well as two strains that overproduced either Psl (Figure 14b) or Pel (Figure 14c) that were stained with the appropriate TRITC-conjugated lectin. Our flow cytometry gating procedure accurately gated 99.7% of wild type PAO1 cells (without the P*cdrA* reporter or lectin-staining) as low GFP and low TRITC (Figure 14d). After 4 hours of attachment to glass, we stained PAO1 and PA14 pP_{cdrA}::gfp_{ASV} reporter cells with TRITClabeled lectins specific for Psl or Pel polysaccharides (24, 199), respectively. As expected for both PAO1 and PA14, we observed an enrichment of TRITC-conjugated lectin staining in the population of cells with high c-di-GMP reporter activity (Figure 14e and f), suggesting that the subpopulation of cells with high c-di-GMP is producing more polysaccharide than their low c-di-GMP counterparts.

Finally, we separated 4 hour surface grown PAO1 pP_{cdrA}::gfp_{ASV} reporter cells into two populations depending on their level of GFP fluorescence using flow assisted cell sorting, and used qRT-PCR to compare Pel and Psl transcript levels in these two populations. Gating for GFP was determined similar to the lectin flow cytometry experiments, using wild type PAO1 cells (Figure 15a), PAO1 constitutively expressing GFP (Figure 15b), and PAO1 ΔwspFΔpelΔpsl pP*cdrA*::gfp_{ASV} (Figure 15c). As expected, wild type PAO1 pP_{cdrA}::gfp_{ASV} reporter cells that had been harvested after 4 hours of surface attachment to glass in static LB liquid culture displayed subpopulations of high GFP, reporter "on" cells (30.8% of the population) and "off" (57.2%) cells (Figure 15d), whereas this same strain grown to mid-log planktonically in LB displayed mostly reporter "off" cells (Figure 15e). We used flow assisted cell sorting (FACS) on the four-hour surface-attached sample, then performed qRT-PCR to determine expression levels of polysaccharide genes. As expected, both the Pel and Psl operons were transcriptionally upregulated in the population of cells with high pP_{cdrA}::gfp_{ASV} reporter activity (Figure 16). These data suggest that the populations of PAO1 cells with high and low c-di-GMP levels that emerge during surface sensing are physiologically distinct, and that the population with high c-di-GMP produces more polysaccharide.

Cyclic di-GMP heterogeneity leads to diversification in surface exploration prior to irreversible attachment

While the subpopulation of cells with high c-di-GMP during surface sensing appears to specialize as early polysaccharide producers, we hypothesized that cells with low pP$_{cdrA}$::*gfp*$_{ASV}$ reporter activity would correlate with increased surface motility. *P. aeruginosa* has a single polar flagellum and polar Type IV pili (Tfp) that are involved in initial surface attachment(30) and surface exploration (200, 201). Flagellar motility is inhibited under conditions of high c-di-GMP (202) and there is evidence that the assembly and activity of Type IV pili is also influenced by cellular c-di-GMP levels (203). Using flow cells, we tracked P$_{cdrA}$::*gfp*$_{ASV}$ reporter activity and type IV-mediated surface motility for 40 hours across multiple generations of cells during surface sensing in wild type PAO1 pP$_{cdrA}$::*gfp*$_{ASV}$ and found an inverse correlation between P$_{cdrA}$::*gfp*$_{ASV}$ reporter activity and surface motility (ρ -0.4644, $p < 0.001$; Figure 17). Cells with the highest levels of c-di-GMP (GFP fluorescence above 250RFU) displayed a complete lack of surface motility (0% of lifetime with Tfp activity). In contrast, cells that displayed the most type IV pili-mediated surface motility (50% or more of their lifetime with Tfp activity) had the lowest levels of c-di-GMP. Thus, heterogeneity in cellular levels of c-di-GMP generated by the Wsp system in response to surface sensing leads to a division of the labor of early biofilm formation and surface exploration among a genetically homogenous population of cells.

Conclusions

Cyclic di-GMP is generally appreciated to be a master regulator of the transition between motile and sessile lifestyles in many bacterial species. However, the variety of c-di-GMP-regulated bacterial behaviors occurring during surface sensing that lead to downstream biofilm development remains understudied. We provided the first evidence that physiologically distinct subpopulations of *P. aeruginosa* emerge during early biofilm formation, allowing for the specialization of cells toward either surface exploration or beginning the process of microcolony formation. We propose that this division of labor represents an important step in early biofilm formation that occurs during the transition from reversible to irreversible attachment. Current anti-biofilm strategies have focused on targeting polysaccharide production to prevent biofilm formation (204), but our work suggests that development of additional materials or small molecule inhibitors that

disrupt type IV pili-mediated surface motility may be essential in prevention of early biofilm formation.

Phenotypic heterogeneity is a common phenomenon in bacteria that is thought to be beneficial at the population level by allowing a single genotype to survive sudden environmental changes and by promoting a division of labor between costly behaviors that support the growth and survival of the population . Heterogeneity in cellular c-di-GMP at the nanomolar level has been observed in *P. aeruginosa* PA14 during planktonic growth, due to the unequal partitioning of the phosphodiesterase DipA, resulting in a diversity of swimming motility phenotypes . However, we found that heterogeneity in c-di-GMP concentrations among cells during early biofilm formation does not require DipA or cell division. Instead, we found that c-di-GMP heterogeneity during surface sensing mirrored the heterogeneity observed in clustering of Wsp system proteins during surface growth (182, 190, 198). Cells with at least one subcellular WspR cluster displayed higher levels of c-di-GMP reporter activity than cells of the same genetic background that did not have a visible WspR focus. Two defining characteristics of the Wsp system are the instability (relative to chemotaxis chemoreceptors) of the laterally-localized proteins of the Wsp complex and the dynamic activity of the diguanylate cyclase WspR, which is potentiated by oligomerization. Interestingly, mutations that resulted in polarly-localized and more stable Wsp complex clusters were defective for activation of WspR, suggesting that the inherent instability and lateral localization of the Wsp complex are important features of surface sensing through Wsp. Therefore we have identified an additional mechanism by which heterogeneity in cell-to-cell c-di-GMP levels can be generated. We hypothesize that the rates of cluster formation and dissolution of both the Wsp surface sensing receptor, WspA, and the diguanylate cyclase WspR introduce heterogeneity in cellular c-di-GMP levels during surface sensing.

We found that c-di-GMP increases rapidly in *P. aeruginosa* during surface sensing. Pel polysaccharide transcription increased over almost 10-fold within 30 minutes of PAO1 attachment to a silicone tube. In flow cells, the p*P*$cdrA$::gfp_{ASV} reporter was activated in a subset of both PAO1 and PA14 cells within 1 hour following attachment to glass. However, the p*P*$cdrA$::gfp_{ASV} reporter was activated in a greater percentage of PAO1 cells than PA14. The FleQ proteins in PAO1 and PA14 are identical at the

nucleotide sequence level, thus we do not expect variation in reporter activity due to differences in FleQ derepression of this promoter. One possible explanation for differences in the percentage of cells with high pP_{cdrA}::gfp_{ASV} reporter activity between PAO1 and PA14 is that fewer PA14 cells reach the high levels of c-di-GMP needed to derepress FleQ from the *cdrA* promoter. One major difference between PAO1 and PA14 biofilm formation is that PA14 does not produce Psl and instead forms a Pel-based biofilm. In contrast, PAO1 makes comparatively little Pel and relies primarily on the Psl polysaccharide (21, 35). Pel is known to be both transcriptionally (through FleQ) and post-translationally (through PelD) regulated by cellular levels of c-di-GMP. The affinity of PelD for c-di-GMP is much greater than FleQ (K_D = 104.2 nM) (205); thus, lower cellular levels of c-di-GMP are needed to initiate Pel production. While PA14 is known to make CdrA, the role of this protein outside of the context of its interaction with the Psl polysaccharide is unknown (184). While high levels of c-di-GMP during surface sensing may be important for PAO1 in order to begin transcribing Psl and CdrA through their FleQ-regulated promoters, these high levels of c-di-GMP may not be essential for PA14 during surface sensing.

Additionally, we found that deletion of genes required for proper functioning of the Wsp surface sensing system had a greater impact on p*PcdrA*::gfp_{ASV} reporter activity compared to equivalent Pil-Chp mutants during the first 6 hours of surface attachment in PAO1. The Pil-Chp system was previously proposed to act upstream of Wsp to stimulate c-di-GMP production during surface sensing; however, our data suggest that the Wsp system is active in surface sensing within 1 hour of attachment. In support of a role for the Wsp system in surface sensing during initial attachment, the Wsp system is known to be constitutively expressed in PAO1 ((206), Caroline Harwood, unpublished), whereas expression of PilY1, the protein required for Pil-Chp mediated signaling to activate the diguanylate cyclase SadC and is surface contact-dependent. Therefore, one interpretation of our findings is that activation of the Pil-Chp surface sensing system to produce c-di-GMP is delayed relative to the Wsp system.

An additional interpretation of these data is that our reporter, which relies on derepression of the *cdrA* promoter by FleQ, is more sensitive to deletion of genes whose products act upstream of WspR activation (compared to genes that activate SadC) if

WspR contributes higher levels of c-di-GMP than SadC during surface sensing. Due to the low affinity of FleQ for binding c-di-GMP, cells must achieve high levels of c-di-GMP for our reporter to be activated. If this is the case, a c-di-GMP reporter with a greater dynamic range, may be able to detect a reduction in cellular c-di-GMP due to SadC, in the presence of functional WspR. Finally, one hypothesis as to how *P. aeruginosa* achieves c-di-GMP signaling specificity despite having approximately 40 proteins potentially involved in c-di-GMP production/degradation and numerous c-di-GMP receptors is through subcellular, localized pools of c-di-GMP (56–58). In this case, it would be possible that the P_{cdrA} reporter could be biased toward detecting Wsp-dependent changes in cellular c-di-GMP levels if c-di-GMP from WspR, but not SadC, derepresses FleQ. However, our demonstration that P_{cdrA} reporter reporter activity correlates with c-di-GMP-dependent physiological changes in both polysaccharide production and surface motility provides strong evidence against this interpretation. Additionally, our study is not the first to observe that deletion of PilY1 does not affect cellular c-di-GMP levels. In a study of c-di-GMP-mediated repression of swarming motility in PA14, PilY1 was found to repress the hyper-swarming phenotype of a phosphodiesterase mutant, but deletion of PilY1 in the phosphodiesterase mutant background did not alter cellular levels of c-di-GMP or *pelA* gene expression (191). The authors suggest that either PilY1 may regulate SadC activity independently of altering global c-di-GMP levels or that that PilY1 alters SadC-mediated, localized levels of c-di-GMP.

Our work represents the most comprehensive comparison of the relative activities of the Wsp and Pil-Chp systems during surface sensing to date, but more work is needed to fully characterize the function and relative temporal activation of each system during surface sensing. Our mutational analyses suggest that both surface sensing systems are important for early biofilm formation, and it is possible that each system plays a distinct role in regulating steps in early in biofilm formation, including polysaccharide production and surface motility. One way in which these two systems could differentially regulate steps in biofilm formation is through the levels of c-di-GMP they produce. Our data suggest that WspR produces more c-di-GMP than SadC during surface sensing. The Wsp system has been shown to influence biofilm matrix production through FleQ (183),

whereas Pil-Chp has been shown to play a role in regulating both flagellar- and type IV pilus-mediated motility (142, 196). Thus, SadC could be specialized to primarily regulate surface motility through comparatively lower levels of c-di-GMP, whereas WspR may regulate polysaccharide production through production of the higher levels of c-di-GMP that are needed in order to modulate FleQ activity. Furthermore, these two systems could play distinct roles through their differing subcellular localizations; Wsp is located laterally, whereas Pil-Chp is localized along with type IV pili at the cell poles. Initial *P. aeruginosa* surface attachment is characterized by polarly attached cells (referred to as "reversibly attached"). When these polarly attached cells transition to lateral attachment, they are thought to be "irreversibly" attached to the surface and go on to participate in biofilm formation (207). Thus the polar Pil-Chp system could play a role in initial attachment, whereas the laterally-localized Wsp system could play a role in the transition to irreversible attachment. One possible model for how these two surface sensing systems mediate initial attachment and surface sensing through both their relative c-di-GMP output levels and the subcellular localization of the systems is as follows. First, a planktonic cell attaches to a surface polarly and the Pil-Chp system activates SadC, leading to a modest increase cellular c-di-GMP levels. Pel production is known to be regulated post-translationally through c-di-GMP binding to PelD (205), and SadC is known to influence Pel production post-transcriptionally (196). As the polarly attached cells produce Pel, they could transition to lateral attachment, at which point the Wsp system could be activated to produce a larger increase in c-di-GMP, leading to transcriptional activation of biofilm matrix genes that had previously been repressed by FleQ. While our study has provided new insight into the relative contributions of Wsp and Pil-Chp to surface sensing, more work is needed to understand whether and how these two systems coordinate steps in early biofilm formation.

Materials and Methods

Bacterial strains and growth conditions.

The strains, plasmids, and primers used in this study are listed in Table 1. *Escherichia coli* and *P. aeruginosa* strains were routinely grown in Luria–Bertani (LB) medium and on LB agar at 37°C. For the flow cell experiments, *P. aeruginosa* was grown in either LB

or FAB minimal medium supplemented with 10mM or 0.6mM glutamate (24) at room temperature. For flow cytometry experiments, *P. aeruginosa* was grown in either LB medium or in Jensen's defined medium with glucose as the carbon source (199). For the tube biofilm and c-di-GMP measurements, *P. aeruginosa* strains were grown in Vogel-Bonner Minimal Medium (VBMM; (208)). Antibiotics were supplied where necessary at the following concentrations: for *E. coli*, 100 μg/mL ampicillin, 10 μg/mL gentamicin, and 10 or 60 μg/mL tetracycline; for *P. aeruginosa*, 300 μg/mL carbenicillin, 100 μg/mL gentamicin, and 100 μg/mL tetracycline. P_{cdrA}::gfp_{ASV} reporter and vector control plasmids were selected with 100 μg/mL gentamicin for *P. aeruginosa* strains and 10 μg/mL gentamicin for *E. coli*.

PAO1 Δ*pilY1* was constructed using two-step allelic exchange following conjugation of wild type PAO1 with *E. coli* S17.1 harboring pENTRPEX18Gm::Δ*pilY1* (constructed by Joe Harrison) as previously described (174). PAO1 Δ*pilY1* was identified by colony PCR using primers PAO1pilY1-SEQ-F and PAO1pilY1-SEQ-R. PAO1 Δ*dipA* was constructed similarly by conjugation of wild type PAO1 with *E. coli* S17.1 harboring pENTRPEX18Gm::Δ*dipA* (constructed by Joe Harrison). PAO1 Δ*dipA* was identified by colony PCR using primers PAO1dipA-SEQ-F and PAO1dipA-SEQ-R.

Cyclic di-GMP measurement and qRT-PCR of tube biofilms

Measurement of c-di-GMP in tube biofilm cells was performed by Dr. Keiji Murakami as previously described (21). Transcriptional analysis of PelA expression in tube biofilms was performed by Dr. Keiji Murakami essentially as described in the "FACS and qRT-PCR of c-di-GMP reporter cells" section.

Crystal violet attachment assays

Crystal violet assays were performed essentially as previously described to measure biofilm biomass using gentle washing after 2-6 hours of static incubation (25). To measure biofilm biomass at 24 hours, the crystal violet assay was performed as previously described without gentle washing(35).

Flow cell time course experiments and confocal microscopy.

P. aeruginosa cells harboring the pP_{cdrA}::gfp_{ASV} reporter plasmid or a promotorless vector control (pMH489) were grown to mid-log in LB with 100 μg/mL gentamicin (Gm100) from LB Gm100 plates or from FAB + 10mM glutamate overnight broth cultures in FAB

+ 10mM glutamate. Mid-log cells were back diluted into 1% LB or FAB + 0.6mM glutamate and flow chambers were inoculated at a final OD_{600} 0.01 and inverted for 10 minutes to allow cells to attach before induction of flow. Clean media was used to wash non-attached cells by flow at 40mL per hour for 20 minutes. Flow was then reduced to a final constant flow rate of 3mL per hour and bacteria were imaged immediately on a Zeiss LSM 510 scanning confocal laser microscope (t=0hr). Flow cells were incubated at a constant flow rate at room temperature and imaged hourly for 6 hours. For every strain and time point, 5 fields of view and a minimum of 300 cells were captured using identical microscope settings to image GFP fluorescence across all experiments. Images were analyzed using using Volocity software (Improvision, Coventry, UK). Cells were counted as pP_{cdrA}::gfp_{ASV} reporter "on" if their mean GFP fluorescence intensity per pixel was greater than two-fold above the background GFP fluorescence intensity (approximately 340). Data are presented in terms of the percentage of cells with an average GFP fluorescence per pixel twofold more intense compared to the background (pP_{cdrA}::gfp_{ASV} reporter "on"). Microscopy images were artificially colored to display GFP fluorescence as green.

Construction of pP*siaA*::*gfp*

A region 259bp upstream through 21 bp into the coding sequence of *siaA* was amplified from PAO1 genomic DNA using primers BamH1-Psia-F and SiaA-BamH1-R, then gel purified using a QIAquick gel extraction kit (Qiagen, Hilden, Germany) digested with BamH1, then column purified with a QIAquick PCR purification kit (Qiagen, Hilden, Germany) to remove BamH1. The GFP expression vector pMH487, which contains the *gfp*mut3 gene with an RNase III splice site and lacking a promoter (184), was digested with BamH1, treated with Antarctic phosphatase (New England Biolabs, Ipswich, MA), then column purified with a QIAquick PCR purification kit (Qiagen, Hilden, Germany) to remove BamH1. The P*siaA* allele was ligated into digested pMH487, then transformed into *E. coli* DH5α, purified, and sequenced using primer M13F(-21) (Genewiz). The reporter pP_{siaA}::*gfp* was electroporated into *P. aeruginosa* as previously described and maintained under gentamycin selection at 100 μg/mL.

Multi-generation single cell tracking of type IV motility and c-di-GMP reporter activity

Wild type PAO1 harboring the pP_{cdrA}::*gfp*$_{ASV}$ reporter was grown shaking for 20 hours in FAB media with 6mM glutamate. The flow cell inoculum was prepared by diluting the culture to a final OD_{600} of 0.01 in FAB with 0.6mM glutamate. The flow cell inoculum was injected into the flow cell (Department of Systems Biology, Technical University of Denmark) and allowed to incubate for 10 minutes at 30^{o}C prior to flushing with media at 30mL/h for 10 minutes. Experiments were performed under a flow rate of 3mL/hour for a total of 40 hours.

Images were acquired with an Olympus microscope and Andor EMCCD camera. Bright-field images were recorded every 3 seconds and fluorescence every 15 minutes. Acquisition continued for a total recording time of 40 hours, which resulted in approximately 48000 bright-field images, and 160 fluorescence images. Images were analyzed to track bacterial family trees, GFP fluorescence, and surface motility essentially as previously described (24). Experiments and analyses were performed by Calvin Lee and Jiame DeAnda in the laboratory of Dr. Gerard Wong at UCLA.

Lectin staining and flow cytometry

Glass culture tubes were inoculated with 1mL of *P. aeruginosa* in LB or Jensen's minimal media at an OD_{600} 0.8 and incubated statically at 37^{o}C for 4 hours. Non-adhered cells were removed by washing three times with 2mL sterile phosphate buffered saline (PBS). Biofilm cells were harvested by vortexing in 1mL PBS with fluorescein-labeled lectins (WFL lectin (100 μg/mL; Vector Laboratories) for Pel, TRITC-labeled HHA (100 μg/mL; EY Laboratories) for Psl) and incubated on ice for 5 minutes. Cells were washed 3 times to remove non-adhered lectin, resuspended in PBS, and immediately analyzed for GFP and TRITC fluorescence on a BD LSRII flow cytometer (BD Biosciences). Events were gated based on forward and side scatter to remove particles smaller than a single *P. aeruginosa* cell and large aggregates.

FACS and qRT-PCR of c-di-GMP reporter cells

Static biofilm reporter cells were grown as described above and harvested without lectin staining. Cells were fixed with 6% paraformaldehyde for 20 minutes on ice, then rinsed once with sterile PBS prior to analysis with a FACSAriaII (BD Biosciences, San Jose, CA). Events were gated first to remove debris and large cellular aggregates, and then gated into cells with low and high GFP fluorescence intensity. The low GFP gate

was drawn using wild type PAO1 cells without the gfp gene and the high GFP gate was drawn using both PAO1 Tn7::P(A1/04/03)::GFPmut and PAO1 Δ*wspF* Δ*pelA* Δ*pslBCD* P_{cdrA}::gfp_{ASV} reporter. Cells were sorted at 4°C by flow assisted cell sorting (FACS) to collect 100,000 events into TRIzol LS (Thermo Fisher Scientific, Waltham, MA). RNA was extracted from sorted cells by boiling immediately for 10 minutes and following the manufacturer's instructions for RNA isolation. DNA was digested by treating with RQ1 Dnase I (Promega, Madison, WI) and samples were checked for genomic DNA contamination by PCR to detect *rplU*. Expression of *pelA*, *pslA*, and *ampR* was measured by quantitative Reverse Transcriptase PCR (qRT-PCR) using the iTaq Universal SYBR Green One-Step kit (Biorad, Hercules, CA) and a CFX96 Touch Real-Time PCR detection system (Bio-Rad, Hercules, CA). The $\Delta\Delta C_q$ was calculated for 3 independent samples of wild type PAO1 P_{cdrA}::gfp_{ASV} reporter biofilm cell sorted populations by normalizing PelA and PslA to relative levels of AmpR expression. Data were presented as the average fold change in PelA or PslA expression in the P_{cdrA}::gfp_{ASV} sorted "on" population (high GFP) relative to the "off" population (low GFP).

WspR-YFP foci and pP_{cdrA}::*mTFP1* reporter

A version of the pP*cdrA* reporter was constructed in the pBBR1MCS5 plasmid to express mTFP1 instead of GFP, for use with YFP-tagged WspR proteins. The P*cdrA* promoter and an enhanced ribosomal binding site from the gene 10 leader sequence of the T7 phage (g10L) was amplified from pUC18-miniTn7T2-P_{cdrA}-RBSg10L-gfp_{AGA} using primers SacI-PcdrA-F and SOE-PcdrA-RBSg10L-R. The primers mTFP1-F and KpnI-mTFP1-R were used to amplify the mTFP1 gene from plasmid pNCS-mTFP1 (Allele Biotech, San Diego, CA). The P_{cdrA}::RBSg10L::*mTFP1* allele was constructed by SOE-PCR using primers SacI-PcdrA-F and Kpn1-mTFP1-R, then pBBR1MCS5 and the SOE PCR product were doubly digested withSacI/KpnI. Digested pBBR1MCS5 was treated with Antarctic phosphatase, then both digests were gel purified and ligated. The ligation was transformed into *E. coli* DH5α, and plasmid from clones growing on LB with 10 μg/mL gentamycin were sequenced with primers M13F and M13F(-21) (GeneWiz). Fluorescence of the pP_{cdrA}::*mTFP1* reporter was measured in Wsp mutants in a fluorimeter (BioTek Synergy H1 Hybrid Reader, BioTek Instruments, Inc., Winooski, VT, USA) and in flow cells to confirm its activity resembled that of pP_{cdrA}::gfp_{ASV}. The

pP*cdrA*::*mTFP1* reporter was electroporated into *P. aeruginosa* strains with the native WspR deleted and harboring an arabinose-inducible copy of WspR-YFP on its chromosome (182). Cells were grown on LB agar plates with 100 μg/mL gentamycin and 1% arabinose for 10 hours, then transferred to an agar pad for imaging. WspR-YFP foci and mTFP1 fluorescence was imaged using a Nikon Ti-E inverted wide-field fluorescence microscope with a large-format scientific complementary metal-oxide semiconductor camera (NEO, Andor Technology, Belfast, United Kingdom) and controlled by NIS-Elements. WspR-YFP foci were detected as previously described (182). Images were acquired on the Nikon Ti-E in collaboration with Julie Cass in the laboratory of Dr. Paul Wiggins.

Figures

Table 1. Strains, primers, and plasmids used in Chapter 3.

***P. aeruginosa* Strains**		**Reference**
PAO1	wild-type	Holloway, 1979
PA14	wild-type	Rahme, 1995
PAO1Δ*wspF*	markerless, in frame deletion of WspF	Hickman, 2005
PAO1Δ*wspF*Δ*pelA*Δ*pslBCD*	markerless, in frame deletions of WspF, PelA, and PslBCD genes	Rybtke, 2012
PAO1Δ*wspR*	markerless, in frame deletion of WspR	Hickman, 2005
PAO1Δ*pilY1*	markerless, in frame deletion of PilY1	this study
PAO1Δ*sadC*	markerless, in frame deletion of SadC	Irie, 2012
PAO1Δ*pilA*	markerless, in frame deletion of PilA	Shrout, 2006
PAO1Δ*dipA*	markerless, in frame deletion of DipA	this study
PAO1Δ*wspR* attCTX::PwspA::*wspR*	PAO1ΔwspR complemented with WspR under control of the Wsp operon promoter and including intergenic region upstream of WspR	Yasuhiko Irie (unpublished)
PAO1Δ*sadC* attCTX::*sadC*	PAO1ΔsadC complemented with SadC under control of its native promoter	Yasuhiko Irie (unpublished)
MPAO1 attTn7::P(A1/04/03)::GFPmut	wild type MPAO1 constitutively expressive stable GFP	Boo Shan Tseng (unpublished)
PA14 Δ*wspF*	markerless, in frame deletion of WspF	Harwood Lab (unpublished)
PA14 Δ*wspR*	markerless, in frame deletion of WspR	Harwood Lab (unpublished)
PAO1Δ*wspR* attCTX::PBAD-wspR-eYFP	markerless, in frame deletion of WspR with arabinose-inducible, C-terminally eYFP-tagged wild type WspR allele	Huangyutitham, 2013
PAO1Δ*wspR* attCTX::PBAD-wspR[L170D]-eYFP	markerless, in frame deletion of WspR with arabinose-inducible, C-terminally eYFP-tagged WspR[L170D] allele	Huangyutitham, 2013
PAO1Δ*wspR* attCTX::PBAD-wspR[E253A]-eYFP	markerless, in frame deletion of WspR with arabinose-inducible, C-terminally eYFP-tagged WspR[E253A] allele	Huangyutitham, 2013
***P. aeruginosa* Reporter Strains**		
PAO1 pMH489		Rybtke, 2012
PAO1 pP*cdrA*::*gfp*ASV		Rybtke, 2012
PAO1 pP*siaA*::*gfp*ASV		this study
PA14 pMH489		this study
PA14 pP*cdrA*::*gfp*ASV		this study
PAO1Δ*wspF* pMH489		this study
PAO1Δ*wspF* pP*cdrA*::*gfp*ASV		this study
PAO1Δ*wspF* pP*siaA*::*gfp*		this study

PAO1Δ*wspF*Δ*pelC*Δ*pslD* pMH489		this study
PAO1Δ*wspF*Δ*pelC*Δ*pslD* p*cdrA*::*gfp*ASV		this study
PAO1Δ*wspR* pMH489		this study
PAO1Δ*wspR* p*cdrA*::*gfp*ASV		this study
PAO1Δ*wspR* p*siaA*::*gfp*		this study
PAO1Δ*pilY1* pMH489		this study
PAO1Δ*pilY1* p*cdrA*::*gfp*ASV		this study
PAO1Δ*sadC* pMH489		this study
PAO1Δ*sadC* p*cdrA*::*gfp*ASV		this study
PAO1Δ*pilA* pMH489		this study
PAO1Δ*pilA* p*cdrA*::*gfp*ASV		this study
PAO1Δ*dipA* pMH489		this study
PAO1Δ*dipA* p*cdrA*::*gfp*ASV		this study
PAO1Δ*wspR* attCTX::PwspA::*wspR* pMH489		this study
PAO1Δ*wspR* attCTX::PwspA::*wspR* p*cdrA*::*gfp*ASV		this study
PAO1Δ*sadC* att::*sadC* pMH489		this study
PAO1Δ*sadC* att::*sadC* p*cdrA*::*gfp*ASV		this study
PA14 Δ*wspF* pMH489		this study
PA14 Δ*wspF* p*cdrA*::*gfp*ASV		this study
PA14 Δ*wspR* pMH489		this study
PA14 Δ*wspR* p*cdrA*::*gfp*ASV		this study
PAO1Δ*wspR* attCTX::PBAD-wspR-eYFP p*cdrA*::*mTFP1*		this study
PAO1Δ*wspR* attCTX::PBAD-wspR[L170D]-eYFP p*cdrA*::*mTFP1*		this study
PAO1Δ*wspR* attCTX::PBAD-wspR[E253A]-eYFP p*cdrA*::*mTFP1*		this study
***E. coli* Strains**		
E. coli S17.1 pENTRPEX18Gm::Δ*pilY1*	conjugation proficient E. coli harboring *pilY1* deletion allele	Joe Harrison (unpublished)
E. coli S17.1 pENTRPEX18Gm::Δ*dipA*	conjugation proficient E. coli harboring *dipA* deletion allele	Joe Harrison (unpublished)
E. coli DH5α pUC18-miniTn7T2-P*cdrA*-RBSg10L-*gfp*AGA	source of PcdrA-RBSg10L	Boo Tseng and Catherine Armbruster

E. coli DH5α pBBR1MCS5-PcdrA::RBSg10L::mTFP1	referred to as "pP*cdrA*::*mTFP1*"	this study
E. coli DH5α pP*siaA*::*gfp*	plasmid-based, fluorescent *siaA* transcriptional reporter	this study
Primers		
PAO1pilY1-SEQ-F	CTACTACGAGACCAATAGCGTC	this study
PAO1pilY1-SEQ-R	GTCGATGTCCACCAGGTTCTTC	this study
PAO1dipA-SEQ-F	GATACGCTTAACTTGGGCCCTG	this study
PAO1dipA-SEQ-R	CTTTTCTTGGTGAGGATTTCAGAAC	this study
SacI – PcdrA - F	GGGGAGCTC GTATGGAAGGTTCCTTGGCGG	this study
SOE-PcdrA-RBSg10L - R	ctcctcgcccttgctcaccat GGATATATCTCCTTCTTAAAG	this study
mTFP1 - F	atggtgagcaagggcgaggag	this study
KpnI - mTFP1 – R	GGGGTACC ttacttgtacagctcgtcc	this study
BamH1-Psia-F	GGG GGATCC GGCAGCGGCAACCGCCTCTG	this study
SiaA-BamH1-R	CCC GGATCC CAACCCCCAGTTCGCCGCCAT	this study
M13F(-21)	TGTAAAACGACGGCCAGT	GeneWiz
M13R	CAGGAAACAGCTATGAC	GeneWiz
ampR-F-qPCR	GCG CCA TCC CTT CAT CG	Colvin, 2011
ampR-R-qPCR	GAT GTC GAC GCG GTT GTT G	Colvin, 2011
pslA-F-qPCR	AAG ATC AAG AAA CGC GTG GAA T	Colvin, 2011
pslA-R-qPCR	TGT AGA GGT CGA ACC ACA CCG	Colvin, 2011
pelA-F-qPCR	CCT TCA GCC ATC CGT TCT TCT	Colvin, 2011
pelA-R-qPCR	TCG CGT ACG AAG TCG ACC TT	Colvin, 2011
rplU-F-qPCR	CGC AGT GAT TGT TAC CGG TG	Colvin, 2011
rplU-R-qPCR	AGG CCT GAA TGC CGG TGA TC	Colvin, 2011
Plasmids		
pMH487	promotorless stable GFP expression vector	Rybtke, 2012
pMH489	promotorless unstable GFP (gfpASV variant) expression vector	Rybtke, 2012
pP*cdrA::gfp*ASV	PcdrA reporter with short halflife GFP	Rybtke, 2012
pENTRPEX18Gm::Δ*pilY1*	suicide plasmid containing pilY1 deletion construct for use in PAO1	Joe Harrison (unpublished)
pENTRPEX18Gm::Δ*dipA*	suicide plasmid containing dipA deletion construct for use in PAO1	Joe Harrison (unpublished)
pBBR1MCS5	broad host range vector that is stable in *P. aeruginosa*, GentR	Kovach, 1995
pUC18-miniTn7T2-P*cdrA*-RBSg10L-*gfp*AGA	source plasmid containing promoter of *cdrA* with enhanced ribosomal binding site	Boo Tseng and Catherine Armbruster
pNCS-mTFP1	source plasmid containing mTFP1	Allele Biotech
pBBR1MCS5-	teal fluorescent protein version of P*cdrA*	this study

PcdrA::RBSg10L::mTFP1	reporter	
pP*siaA::gfp*	P*siaA* reporter expressing stable GFP, constructed using pMH487 plasmid	this study

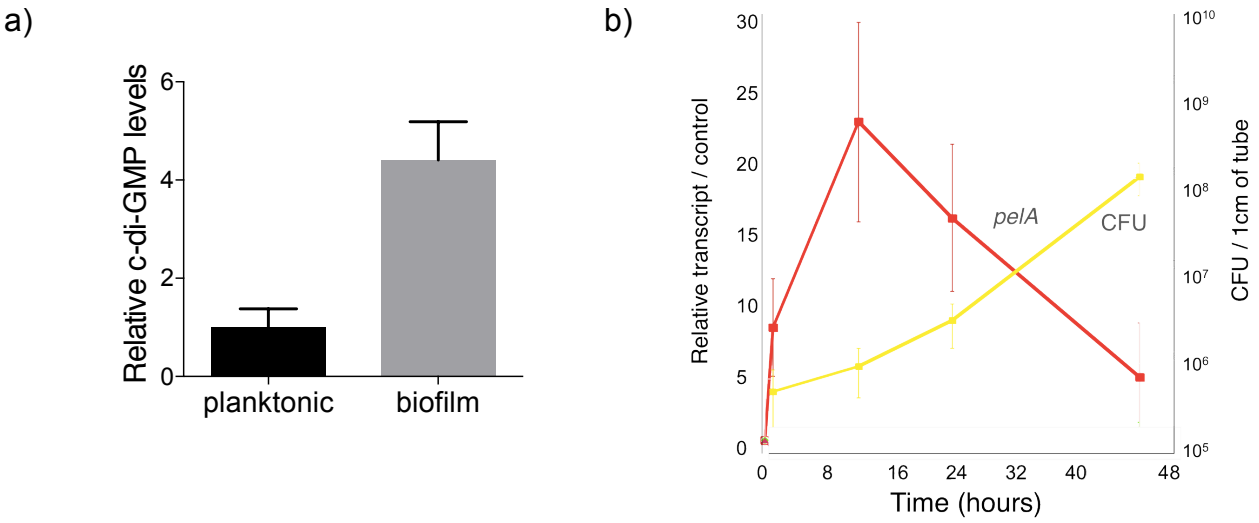

Figure 1. a) c-di-GMP levels are elevated rapidly upon association of *P. aeruginosa* cells with a surface. LC-MS/MS of intracellular levels of c-di-GMP in wild type PAO1 cells grown either planktonically or after 4 hours of attachment to a silicone tube surface. Values are normalized to the average concentration of c-di-GMP in planktonic cells, in pmol c-di-GMP/mg total protein. b) The c-di-GMP regulated promoter of the Pel polysaccharide operon is transcriptionally activated almost 10-fold compared to planktonic cells within 30 minutes of attachment of PAO1 to a silicone tube. qRT-PCR was performed to detect *pelA* transcript levels in silicone tube biofilm cells compared to planktonic cells. Biofilm transcript levels were normalized to planktonic levels at each time point.

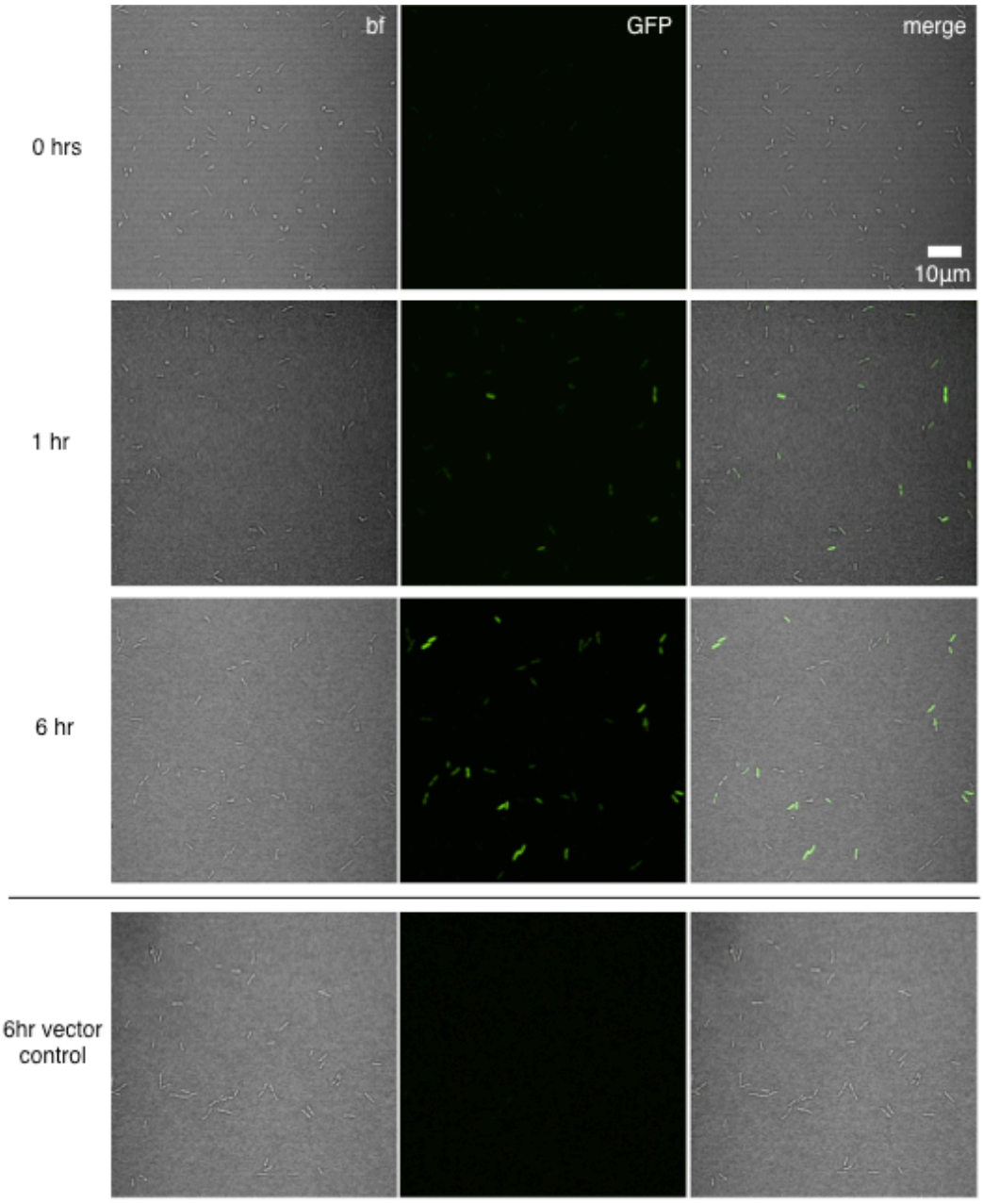

Figure 2. Representative time course images showing the c-di-GMP reporter (P_{cdrA}::gfp_{ASV}) transitioning from inactive upon initial attachment of wild type PAO1 (0 hr) to active in a subpopulation of cells between 1 and 6 hours during a flow cell experiment. A strain harboring the vector control, which encoded gfp_{ASV}, but lacks the P_{cdrA} promoter was imaged alongside each reporter strain (in the appropriate genetic background) to confirm that GFP fluorescence was not due to random expression from

the plasmid. Wild type PAO1 P_{cdrA}::gfp_{ASV} was grown in 1% LB and imaged by CSLM. bf = bright field, merge = bright field and GFP channels combined.

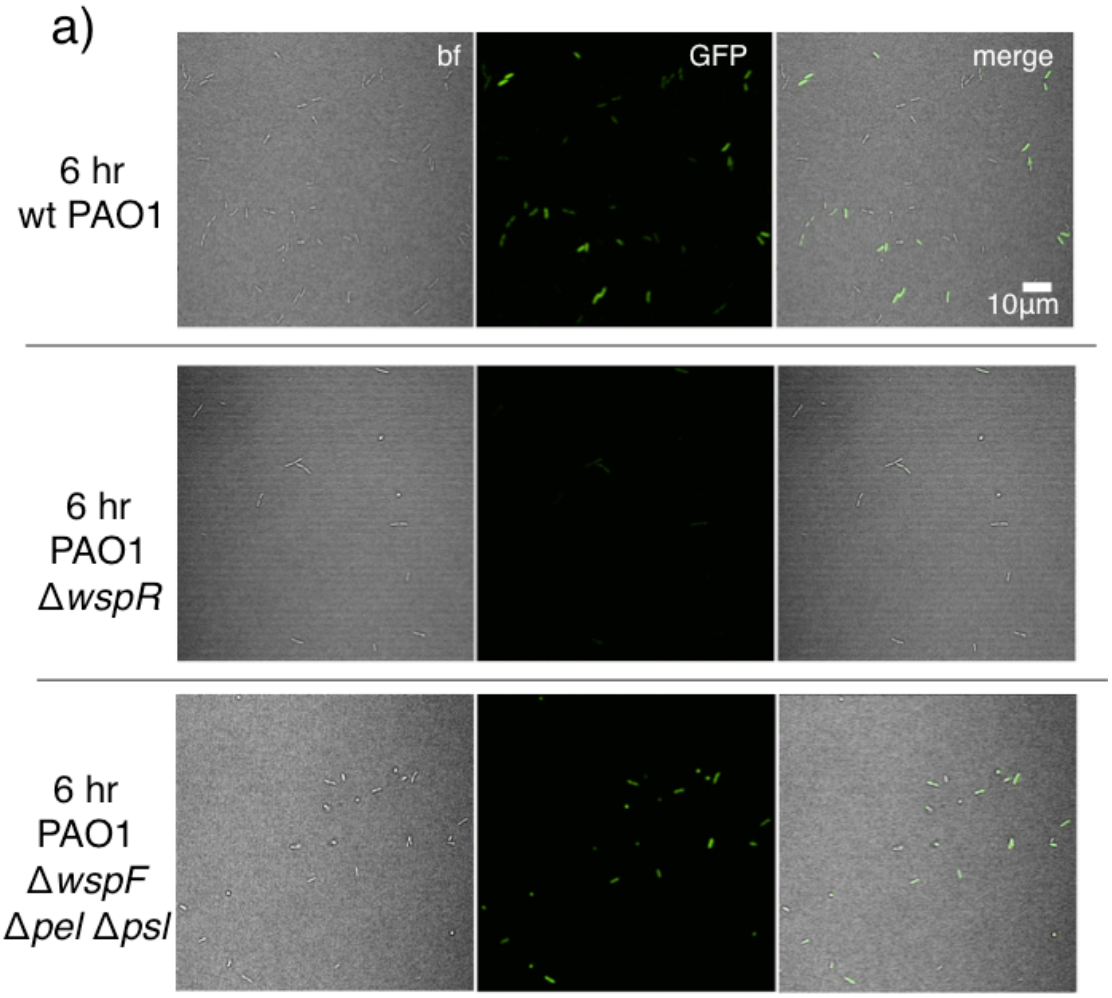
a)
bf
GFP
merge
10μm
6 hr
wt PAO1
6 hr
PAO1
ΔwspR
6 hr
PAO1
ΔwspF
Δpel Δpsl

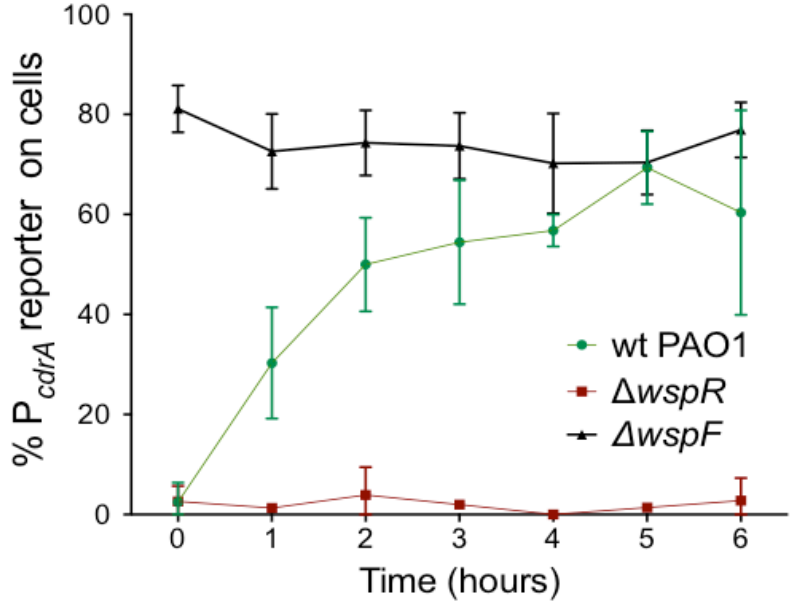
b)
% P cdrA reporter on cells
100
80
60
40
20
0
0
1
2
3
4
5
6
Time (hours)
wt PAO1
ΔwspR
ΔwspF

Figure 3. The pP_{cdrA}::gfp_{ASV} reporter is sensitive to Wsp-dependent variation in c-di-GMP during surface sensing. a) Representative images from wild type PAO1, PAO1 Δ*wspR*, and PAO1 Δ*wspF*Δ*pelC*Δ*pslD* after 6 hours of surface attachment. bf = bright field, merge = bright field and GFP channels combined. b) Six hour time course plot of the average percentage of cells from either wild type PAO1 (green), PAO1 Δ*wspR* (red), or PAO1 Δ*wspF*Δ*pelC*Δ*pslD* (black) in which the pP_{cdrA}::gfp_{ASV} reporter had turned "on" at each hour. Cells were identified as "on" if their average GFP fluorescence was greater than twice the average background GFP fluorescence of the image.

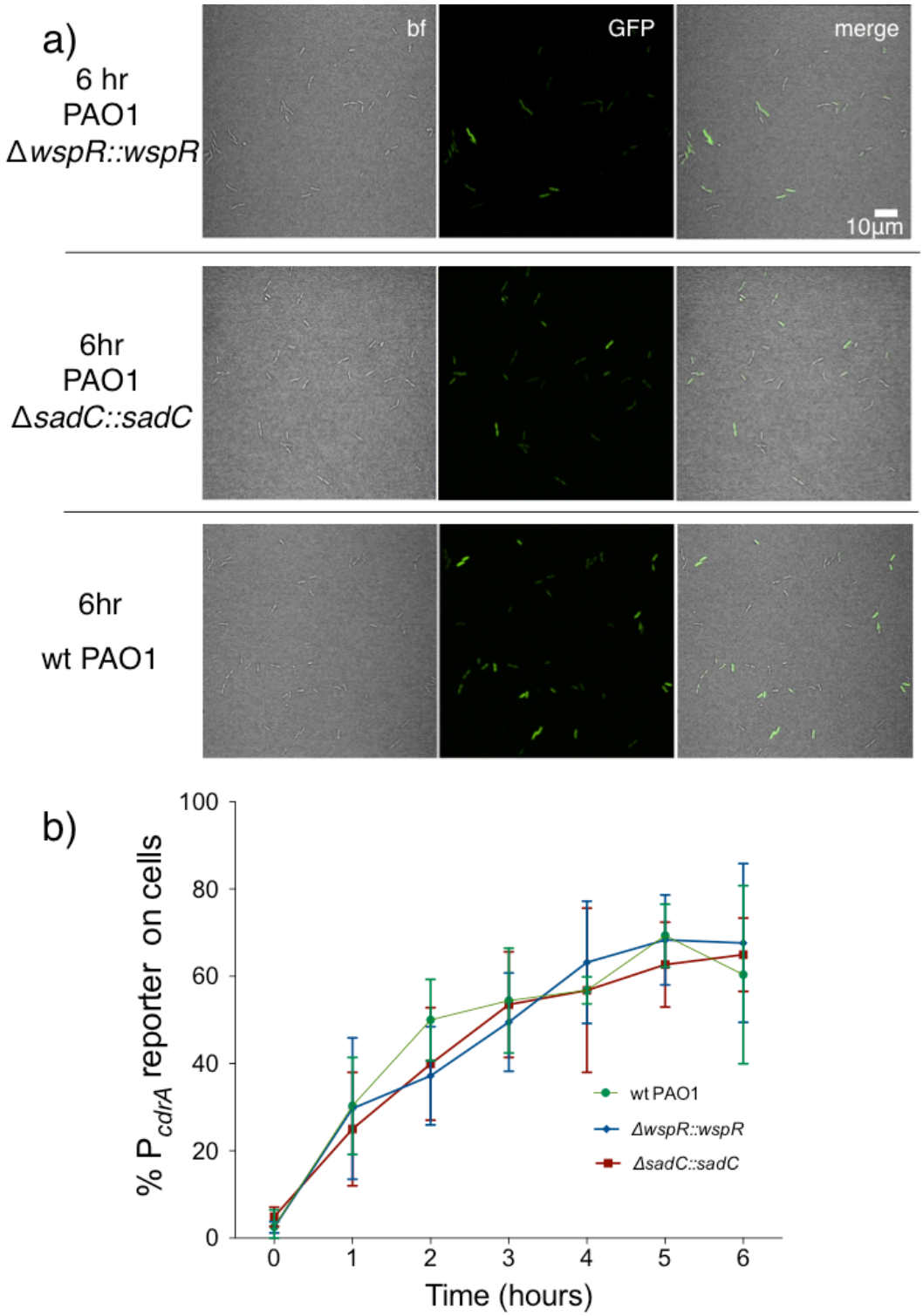

Figure 4. Complemented diguanylate cyclase mutants display wild type levels of P*cdrA*::*gfp*$_{ASV}$ reporter activity. PAO1 Δ*wspR* and PAO1 Δ*sadC* were complemented at a

neutral site on the chromosome under control of their native promoters. a) Representative images from wild type PAO1, PAO1 Δ*wspR* attCTX::*wspR* (Δ*wspR::wspR*), and PAO1 Δ*sadC* Tn7::*sadC* (PAO1 Δ*sadC::sadC*) after 6 hours of surface attachment. bf = bright field, merge = bright field and GFP channels combined. b) Six hour time course plot of the average percentage of cells from either wild type PAO1 (green), PAO1 Δ*wspR* attCTX::*wspR* (blue), or PAO1 Δ*sadC* Tn7::*sadC* in which the pP_{cdrA}::gfp_{ASV} reporter had turned "on" at each hour. Cells were identified as "on" if their average GFP fluorescence was greater than twice the average background GFP fluorescence of the image.

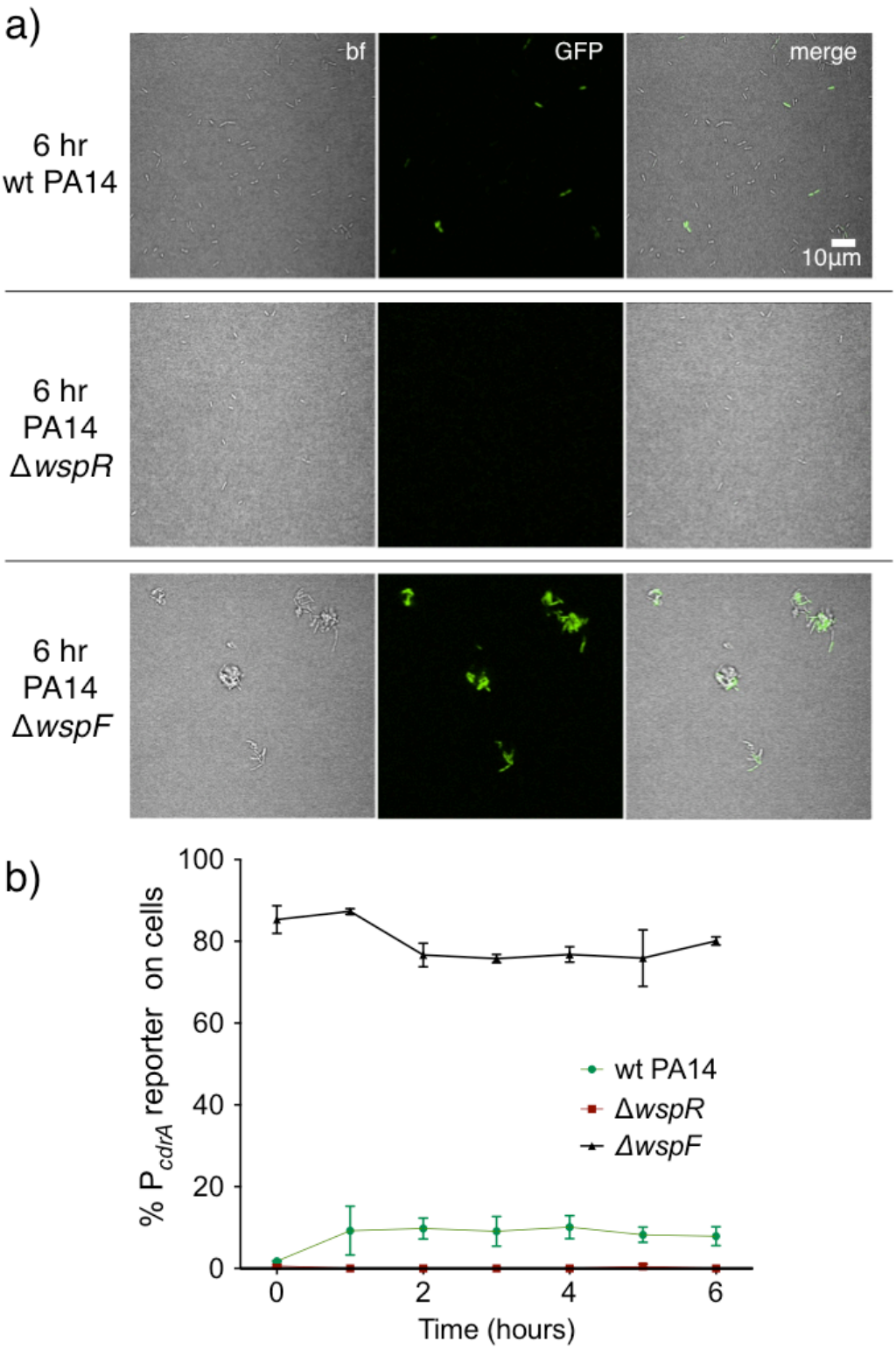

Figure 5. Activity of the pP$_{cdrA}$::*gfp*$_{ASV}$ reporter in the lab strain PA14 differs from PAO1.

a) Representative images from wild type PA14, PA14 Δ*wspR*, and PA14 Δ*wspF* after 6

hours of surface attachment. bf = bright field, merge = bright field and GFP channels combined. b) Six hour time course plot of the average percentage of cells from either wild type PA14 (green), PA14 Δ*wspR* (red), or PA14 Δ*wspF* (black) in which the pP_{cdrA}::gfp_{ASV} reporter had turned "on" at each hour. Cells were identified as "on" if their average GFP fluorescence was greater than twice the average background GFP fluorescence of the image.

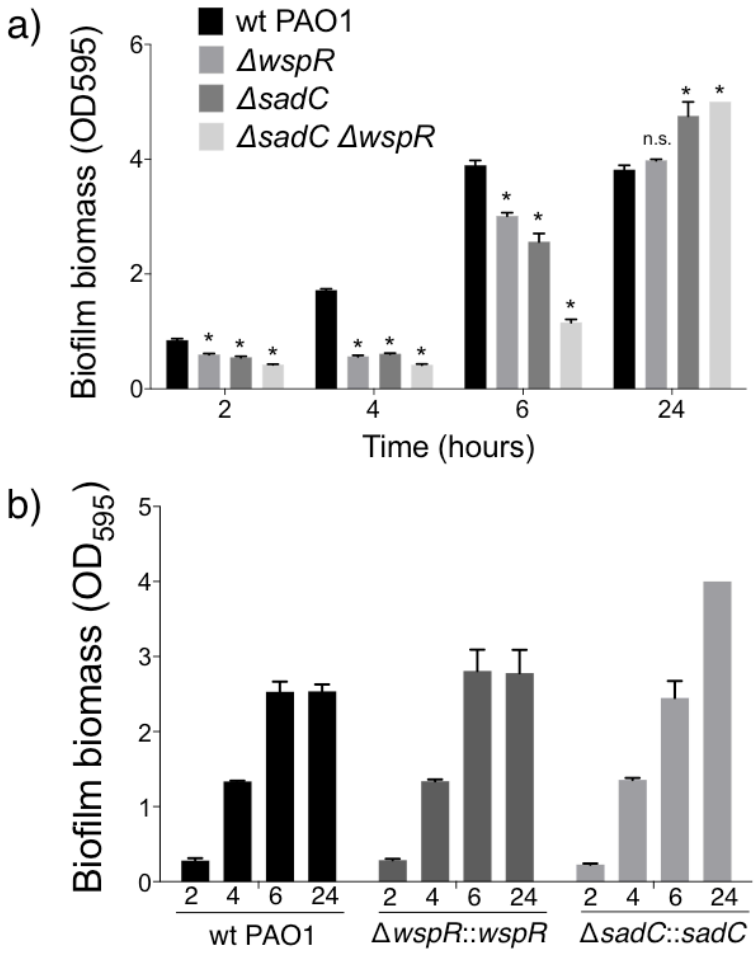

Figure 6. The diguanylate cyclases WspR and SadC are involved in early surface attachment in PAO1. a) Crystal violet assay performed in wild type PAO1, single mutants of either WspR or SadC, and a double mutant lacking both cyclases. Between 2 and 6 hours, all three mutants show defects in surface attachment and biofilm formation relative to the wild type. After 24 hours, all mutants formed either equal or greater biofilm biomass than wild type. Asterisk indicates a statistically significant change in biomass relative to wild type PAO1 at each time point ($p < 0.05$). b) Complemented mutants of WspR or SadC form wild type levels of biofilm biomass from 2-24 hours as measured by a crystal violet assay.

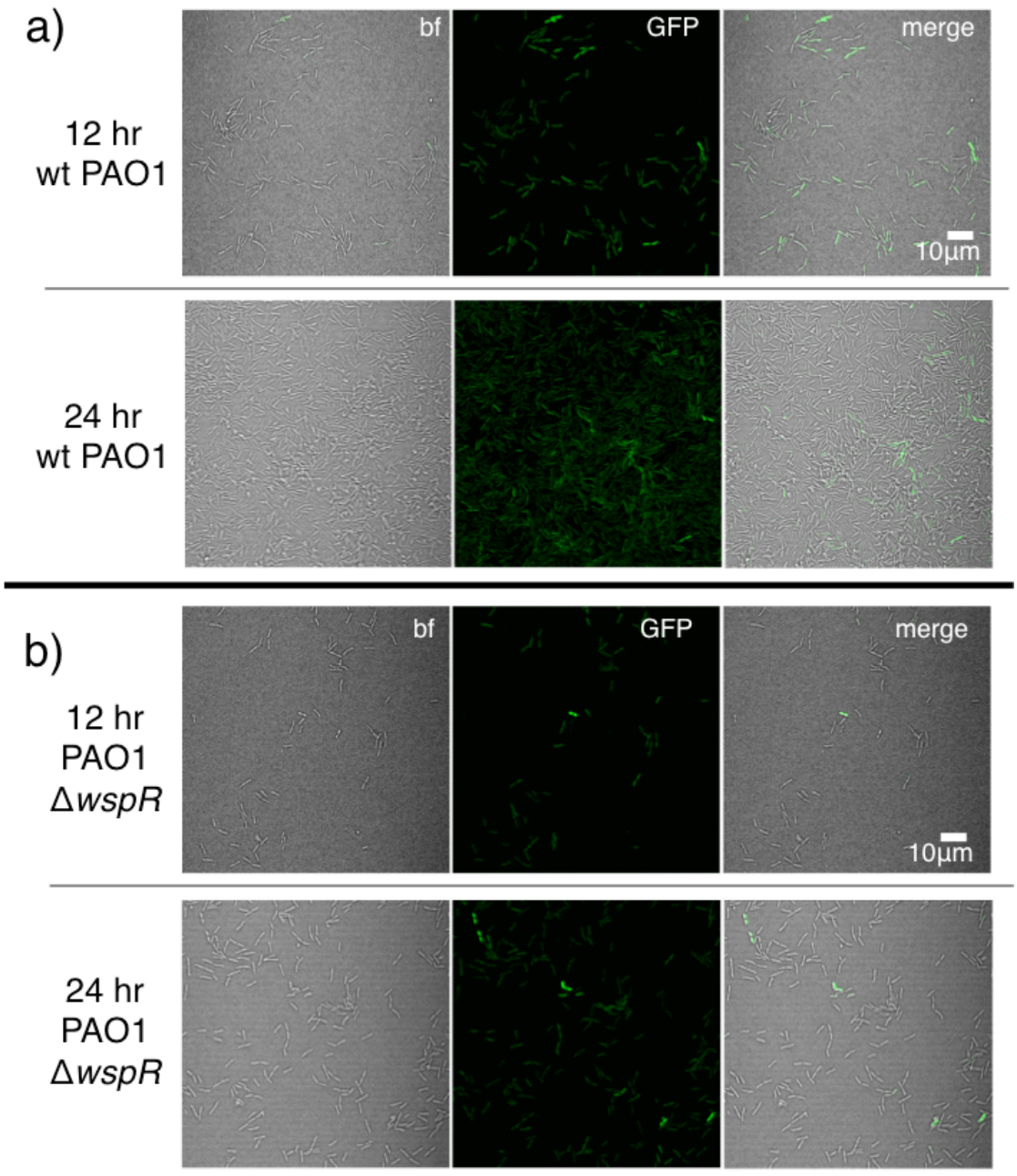

Figure 7. The pP$_{cdrA}$::*gfp*$_{ASV}$ reporter is activated at low levels in PAO1 Δ*wspR* by 24 hours. Representative images from wild type PAO1 (a) and PAO1 Δ*wspR* (b) after 12 and 24 hours of surface attachment in flow cells. bf = bright field, merge = bright field and GFP channels combined.

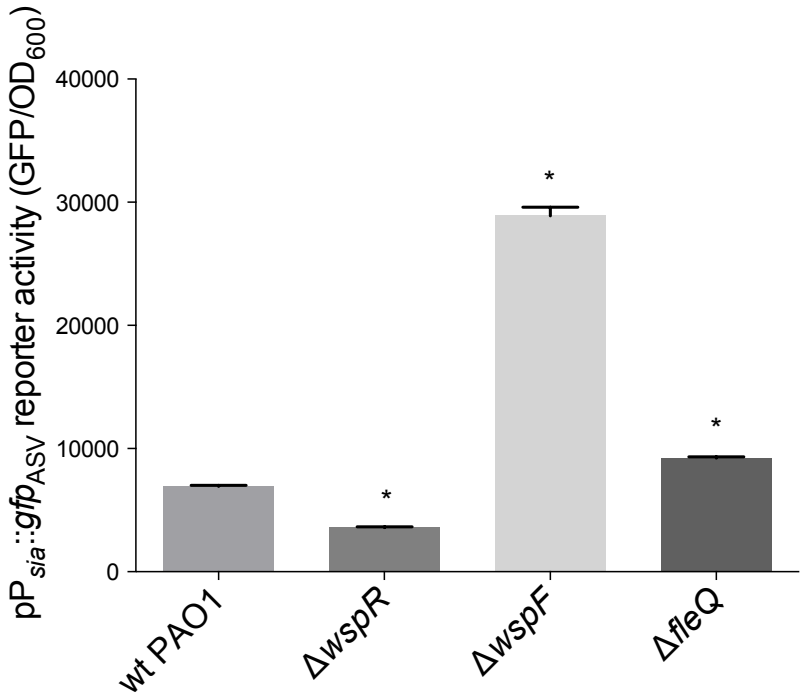

Figure 8. FleQ-regulated promoters are responsive to Wsp-dependent changes in cellular levels of c-di-GMP. Wild type PAO1 and PAO1 mutants harboring the pP$_{siaA}$::*gfp* reporter were grown for 20 hours on an LB agar surface with 100 μg/mL gentamycin, resuspended in PBS, and their GFP fluorescence and absorbance at OD_{600} was measured immediately in a spectrophotometer. Asterisk indicates a statistically significant difference in pP$_{siaA}$::*gfp* reporter activity relative to wild type PAO1 ($p < 0.05$).

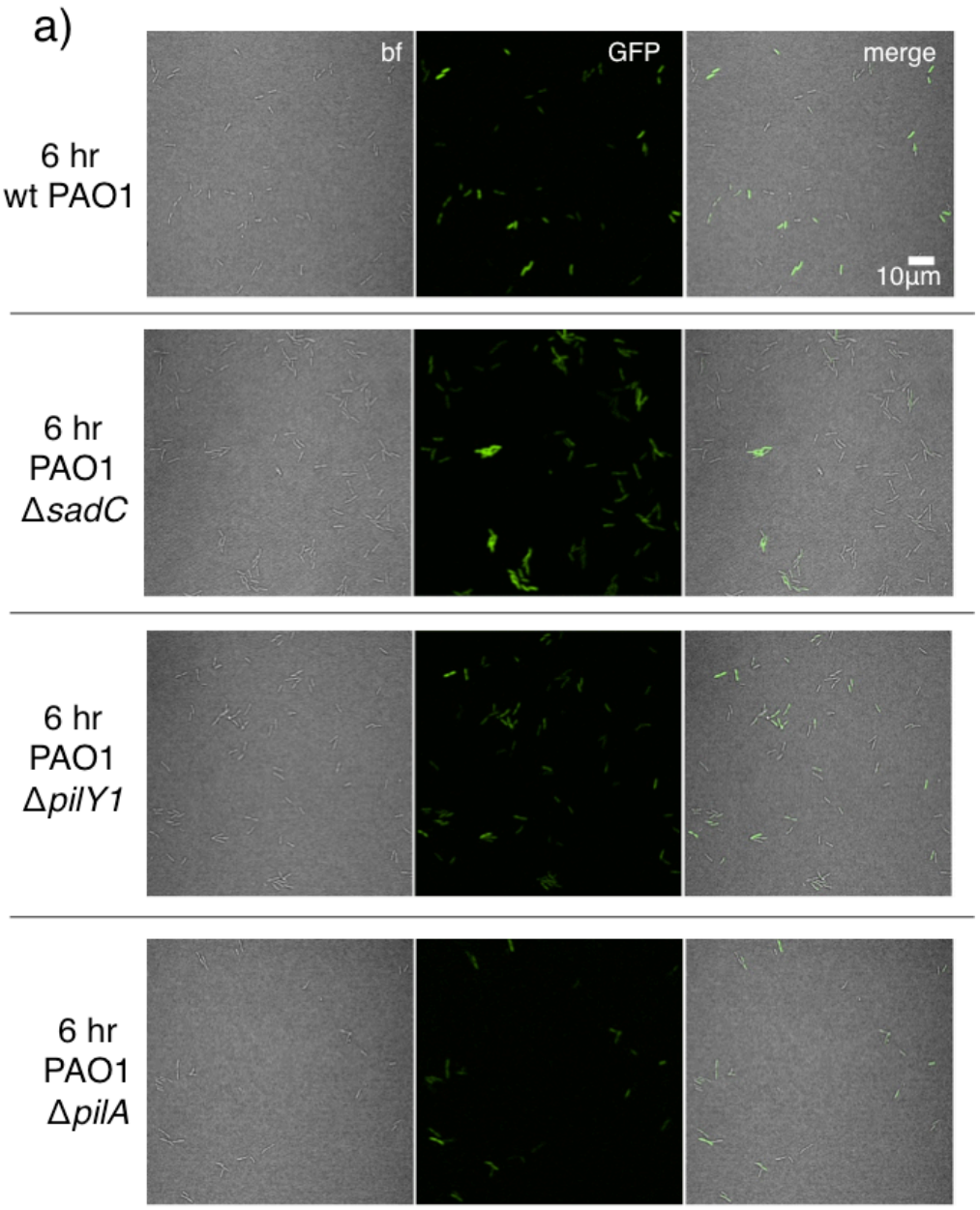
a)
bf
GFP
merge
6 hr
wt PAO1
10µm
6 hr
PAO1
ΔsadC
6 hr
PAO1
ΔpilY1
6 hr
PAO1
ΔpilA

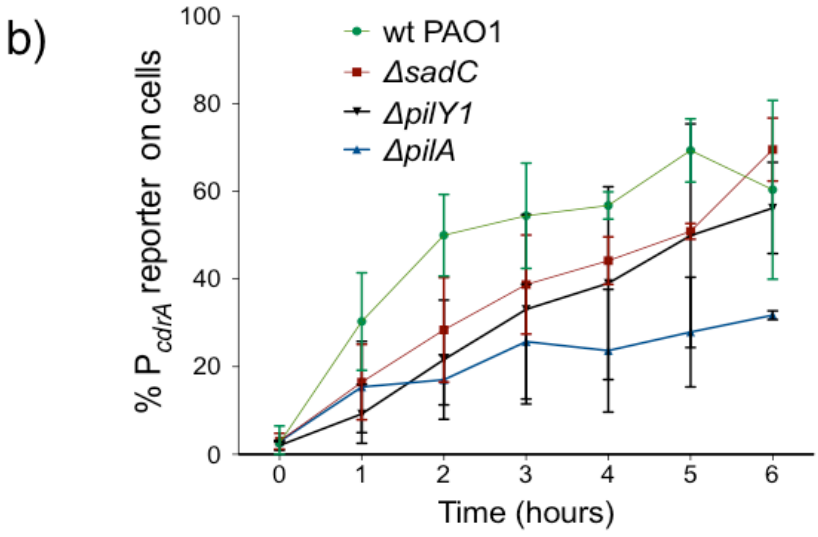
b)
wt PAO1
ΔsadC
ΔpilY1
ΔpilA
% P cdrA reporter on cells
Time (hours)
0
20
40
60
80
100
0
1
2
3
4
5
6

Figure 9. Mutants predicted to inactivate the Pil-Chp surface sensing system largely retain pP_{cdrA}::gfp_{ASV} reporter activity during the first six hours of surface sensing. a) Representative images from wild type PAO1, PAO1 Δ*sadC*, PAO1 Δ*pilY1*, and PAO1 Δ*pilA* after 6 hours of surface attachment. bf = bright field, merge = bright field and GFP channels combined. b) Six hour time course plot of the average percentage of cells from either wild type PAO1 (green), PAO1 Δ*sadC* (red), PAO1 Δ*pilY1* (black), or PAO1 Δ*pilA* (blue) in which the pP_{cdrA}::gfp_{ASV} reporter had turned "on" at each hour. Cells were identified as "on" if their average GFP fluorescence was greater than twice the average background GFP fluorescence of the image.

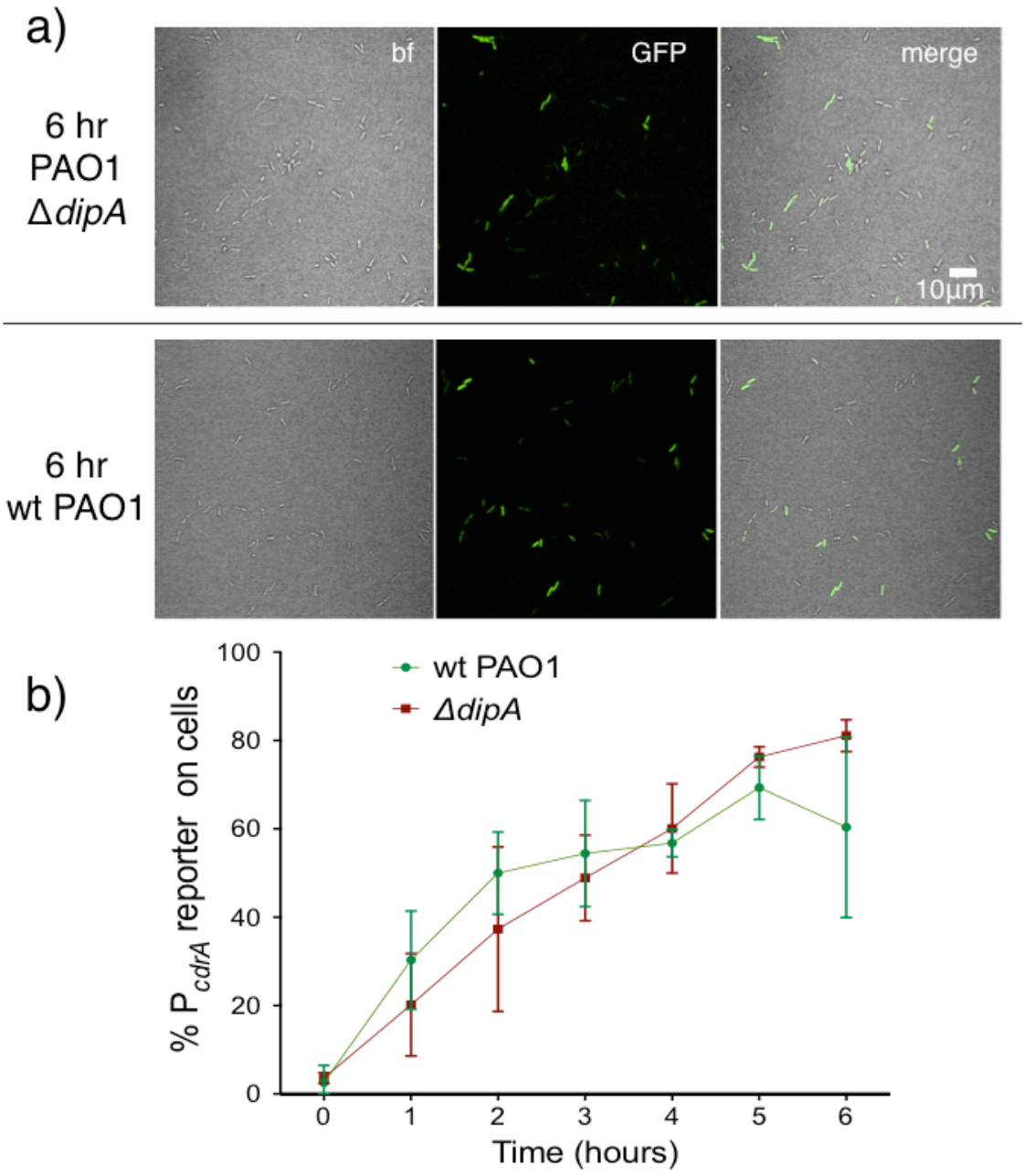

Figure 10. The phosphodiesterase DipA is not required for heterogeneity in cellular levels of c-di-GMP during surface sensing. a) Representative images from wild type PAO1 and PAO1 Δ*dipA* after 6 hours of surface attachment. bf = bright field, merge = bright field and GFP channels combined. b) Six hour time course plot of the average percentage of cells from either wild type PAO1 (green) and PAO1 Δ*dipA* (red) in which the

pP$_{cdrA}$::*gfp*$_{\mathrm{ASV}}$ reporter had turned "on" at each hour. Cells were identified as "on" if their average GFP fluorescence was greater than twice the average background GFP fluorescence of the image.

a)

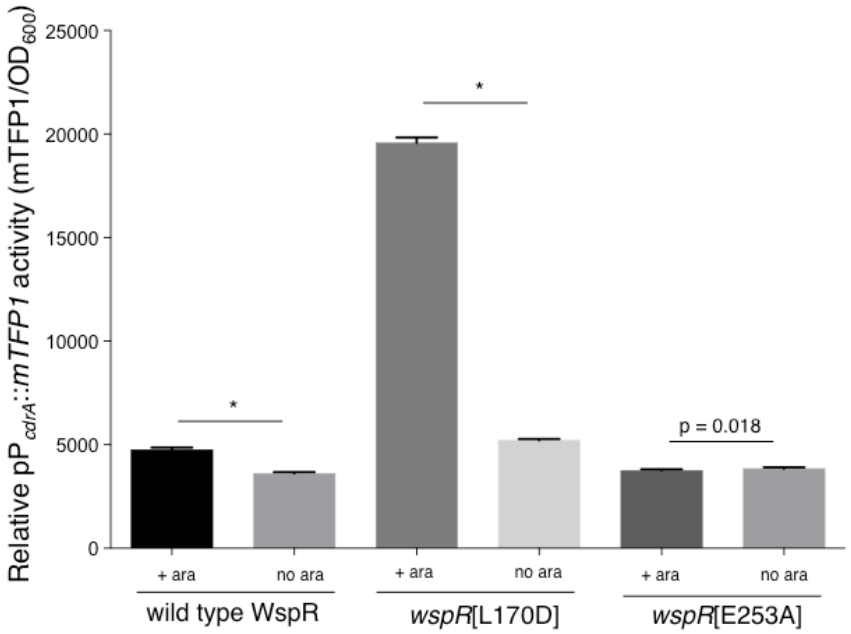

b)

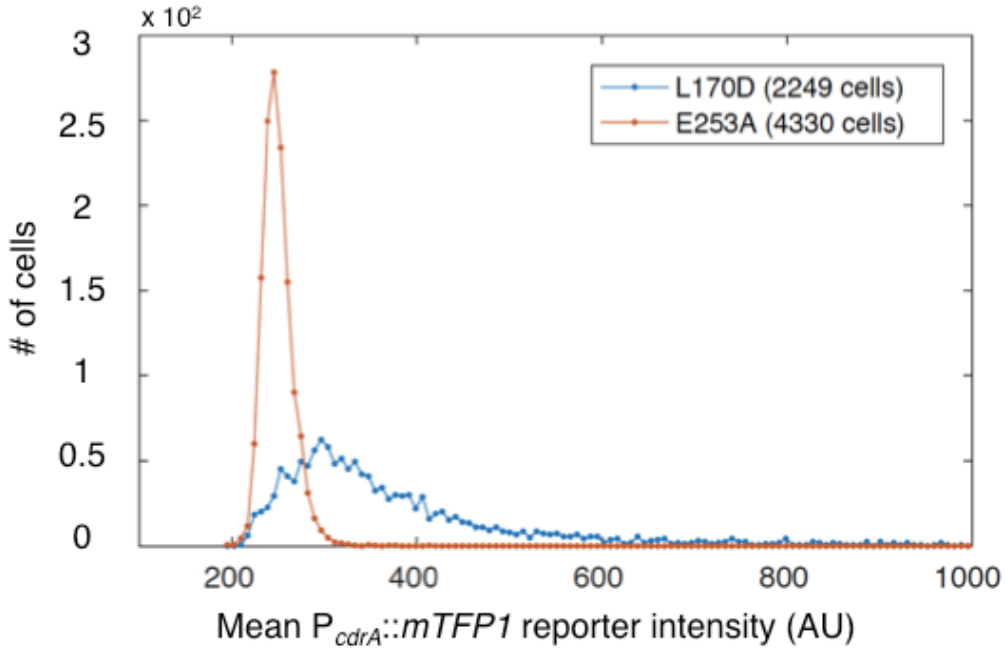

Figure 11. Activity of the pP$_{cdrA}$::*mTFP1* reporter is dependent on the ability of WspR to produce c-di-GMP. a) The pP$_{cdrA}$::*mTFP1* reporter is active in surface grown cells with functional, arabinose-inducble alleles of WspR when arabinose is added to the media.

Wild type WspR is PAO1 Δ*wspR* att::*wspR*-eYFP. *wspR*[L170D] is PAO1 Δ*wspR* att::*wspR*[L170D]-eYFP, a strain which produces large subcellular clusters of WspR and grows as rugose small colonies on LB with 1% arabinose, a phenotype that is indicative of high intracellular c-di-GMP. *wspR*[E253A] is PAO1 Δ*wspR* att::*wspR*[L170D]-eYFP cells, a strain which forms large subcellular WspR clusters, but does not produce c-di-GMP via WspR due to the point mutation located in WspR's active site. Cells were grown on LB agar plates with 100 μg/mL gentamycin, and in the presence or absence of 1% arabinose. Cells were resuspended in PBS and mTFP1 fluorescence and OD_{600} were measured. Relative pP_{cdrA}::*mTFP1* reporter activity is the level of mTFP1 fluorescence normalized to OD_{600}. Asterisk indicates statistical significance by Student's t-test ($p < 0.001$).

b) Histogram displaying the distribution of average cellular levels of mTFP1 fluorescence from expression of the pP_{cdrA}::*mTFP1* reporter in either the PAO1 Δ*wspR* attCTX::*wspR*[L170D]-eYFP (blue) or PAO1 Δ*wspR* attCTX::*wspR*[L170D]-eYFP (red) backgrounds.

a)

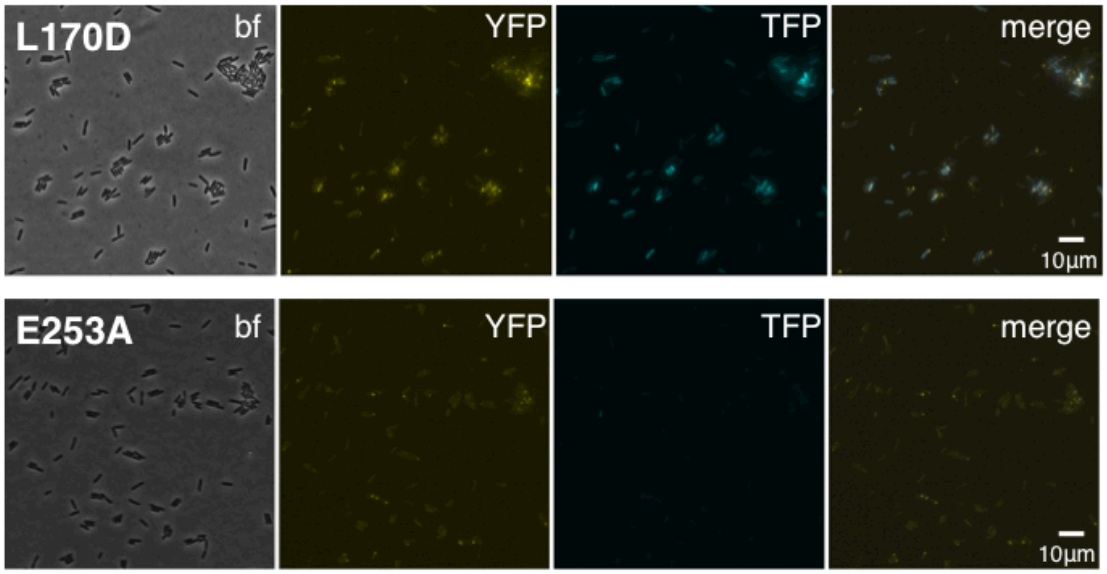

b)

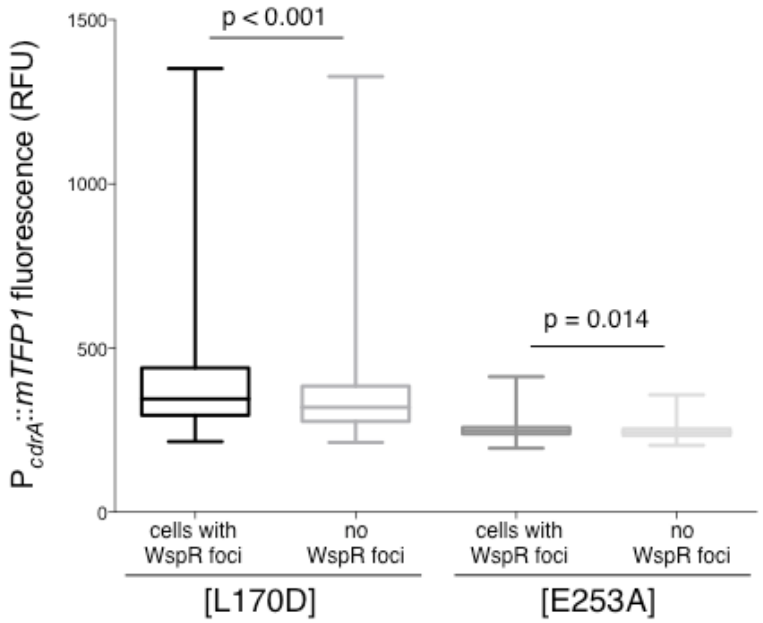

Figure 12. WspR-eYFP clustering correlates with pP$_{cdrA}$::*mTFP1* reporter activity. a) Subcellular WspR-eYFP clusters are visible in both PAO1 Δ*wspR* att::*wspR*[L170D]-eYFP and PAO1 Δ*wspR* att::*wspR*[L170D]-eYFP cells, but the pP*cdrA*::mTFP1 reporter is only active in the strain with a functional WspR (WspR[L70D]). Bf = bright field. YFP

= wspR-YFP foci. mTFP1 = pP_{cdrA}::*mTFP1* activity. PAO1 Δ*wspR* att::*wspR*[L170D]-eYFP and PAO1 Δ*wspR* att::*wspR*[L170D]-eYFP cells harboring the pP_{cdrA}::mTFP1 reporter were grown on LB agar plates with 1% arabinose and 100 μg/mL gentamycin, then spotted onto an agar pad and imaged immediately. b) PAO1 Δ*wspR* att::*wspR*[L170D]-eYFP cells with at least one WspR-eYFP focus have significantly higher pP_{cdrA}::*mTFP1* activity ($p < 0.001$). There is no significant difference in reporter activity between PAO1 Δ*wspR* att::*wspR*[E253A]-eYFP cells with and without WspR-eYFP foci ($p > 0.01$).

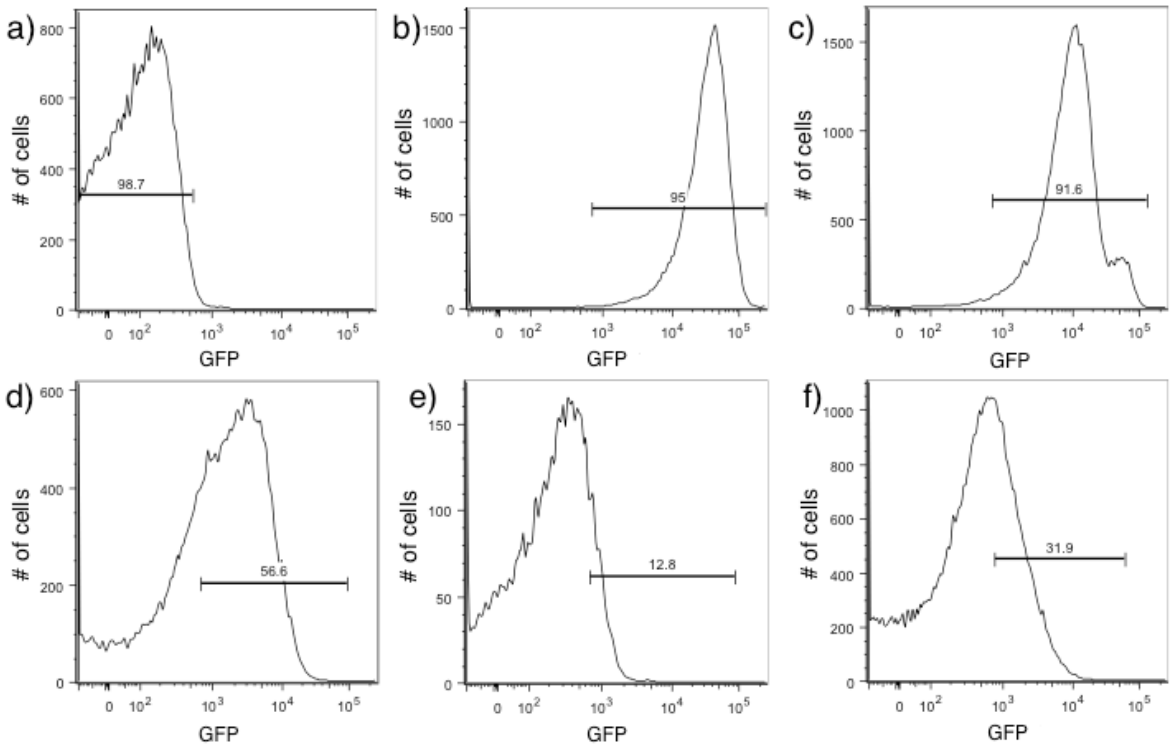

Figure 13. Development of a protocol to monitor pP$_{cdrA}$::*gfp*$_{ASV}$ using an LSRII flow cytometer. Brackets indicate gates for "on" (GFP above 1.7 x 10^2 RFU) or "off" (GFP below 1.7 x 10^2 RFU) reporter cells and the number above the bracket indicates the percentage of cells that fall within that gate. a) Wild type PAO1 cells were used to determine the background level of fluorescence on the BD Aria III for GFP measurements. The population of cells falls below 10^3 RFU. b) A *P. aeruginosa* strain constitutively expressing stable GFP (PAO1 Tn7::P(A1/04/03)::GFPmut) was used to determine gating for cells with high GFP, with the population ranging from 10^3 to 10^5 RFU. c) Surface grown PAO1 Δ*wspF*Δ*pel*Δ*psl* harboring the pP$_{cdrA}$::*gfp*$_{ASV}$ was used to draw a gate for collection of cells with high reporter activity (91.6% of the population). d) Example of gating for reporter "on" cells from wild type PAO1 pP$_{cdrA}$::*gfp*$_{ASV}$ cells that had been attached to glass in LB media for 4 hours. Approximately 56.6% of the

population falls into the reporter "on" population. e) Example of gating for "on" cells from wild type PA14 pP_{cdrA}::gfp_{ASV} cells that had been attached to glass in LB media for 4 hours prior to FACS sorting. Approximately 12.8% of the population falls into the reporter "on" population. f) Example of gating for "on" cells from wild type PA14 pP_{cdrA}::gfp_{ASV} cells that had been attached to glass in Jensen's media (a condition in which Pel is more abundantly produced than in LB) for 4 hours. Approximately 31.9% of the population falls into the reporter "on" population.

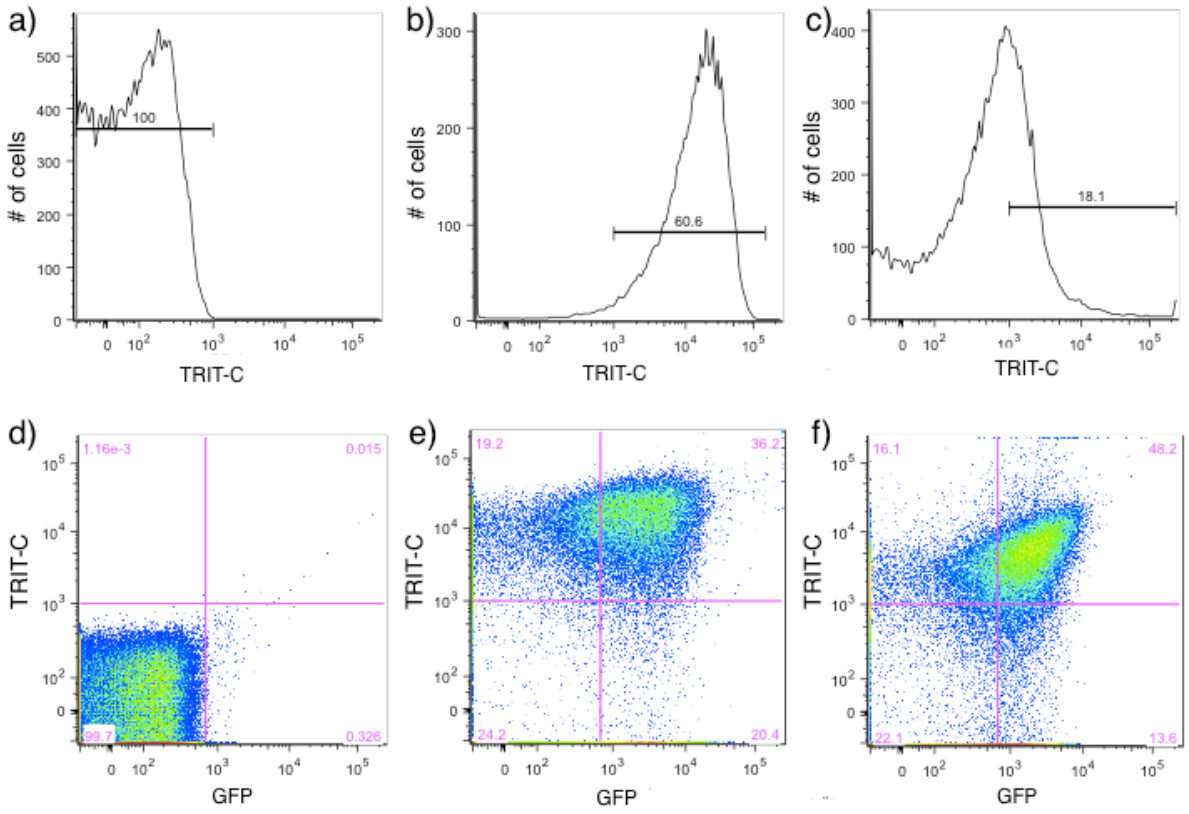

Figure 14. Psl and Pel polysaccharide production is highest in cells with high c-di-GMP as measured by the pP$_{cdrA}$::*gfp*$_{ASV}$ reporter. Brackets indicate gates for polysaccharide-producing, TRITC lectin bound cells (TRITC above 10^3 RFU) or cells without lectin bound (TRITC below 10^3 RFU) on an LSR II flow cytometer and numbers above the brackets indicate the percentage of total cells that fall within the gate. a) Determination of the background level of TRITC autofluorescence in wild type PAO1 that had not been stained with a TRITC-conjugated lectin. b) Determination of the a high level of TRITC-conjugated Psl-specific lectin binding in PAO1 P$_{BAD}$-psl grown in shaken liquid culture for 4 hours with 1% arabinose before staining with the TRITC-HHA lectin and extensive washing. Approximately 60% of the cells have TRITC-HHA lectin bound to their surface. c) Determination of the a high level of TRITC-conjugated Pel-specific lectin

binding in PAO1 P_{BAD}-*pel* grown in shaken liquid culture for 4 hours with 1% arabinose before staining with the TRITC-WFL lectin and extensive washing. Approximately 18.1% of the cells have TRITC-HHA lectin bound to their surface. d) A scatterplot of pP_{cdrA}::gfp_{ASV} reporter activity (GFP) on the x axis and Psl production (as measured by binding of TRITC-HHA lectin to the cell surface) demonstrating the specificity of GFP and TRITC gating in a negative control condition. Wild type PAO1 cells that do not contain the reporter and had not been stained with lectin mostly fall into the lower left quadrant of "off" GFP and no TRITC-lectin binding. The purple numbers in each quadrant represent the percentage of the total population that falls within that quadrant. Quadrants were drawn based on gating of pP_{cdrA}::gfp_{ASV} reporter activity "on" vs. "off" and lectin bound vs. unbound. e) Psl polysaccharide production is enriched in the population of cells with high c-di-GMP. Representative scatterplot of reporter activity versus Psl lectin binding in wild type PAO1 harboring the pP_{cdrA}::gfp_{ASV} reporter grown for four hours in LB before surface attached cells were harvested, lectin stained, washed, and counted by flow cytometry. f) Pel polysaccharide production is enriched in the population of cells with high c-di-GMP. Representative scatterplot of reporter activity versus Pel lectin binding in wild type PA14 harboring the pP_{cdrA}::gfp_{ASV} reporter grown for four hours in Jensen's minimal media plus glucose before surface attached cells were harvested, lectin stained, washed, and counted by flow cytometry.

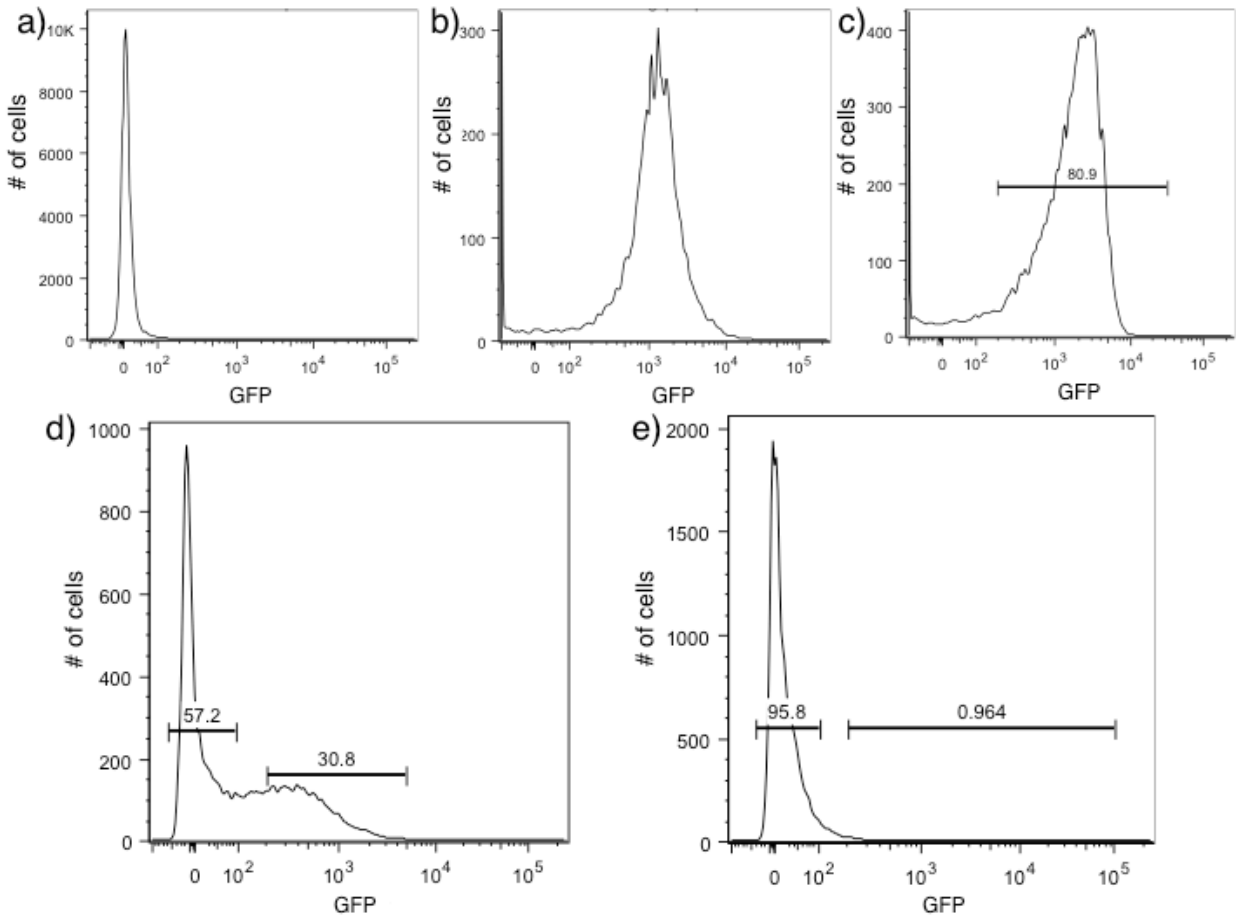

Figure 15. Development of a protocol to sort biofilm cells by pP_{cdrA}::*gfp*$_{ASV}$ using flow assisted cell sorting (FACS). Brackets indicate gates for "on" (GFP above 1.1 x 10^2 RFU) or "off" (GFP below 10^2 RFU) reporter cells on a BD Aria III flow cytometer and the number above the bracket indicates the percentage of cells that fall within that gate. a) Wild type PAO1 cells were used to determine the background level of fluorescence on the BD Aria III for GFP measurements. The population of cells centers around zero RFU. b) A *P. aeruginosa* strain constitutively expressing stable GFP (PAO1 Tn7::P(A1/04/03)::GFPmut) was used to determine gating for cells with high GFP, with the population centering around 10^3 RFU. c) PAO1 Δ*wspF*Δ*pel*Δ*psl* harboring the pP_{cdrA}::*gfp*$_{ASV}$ was used to draw a gate for collection of cells with high reporter activity

(80% of the population). d) Example of gating for reporter "off" and "on" cells from wild type PAO1 pP_{cdrA}::gfp_{ASV} cells that had been grown on a surface for 4 hours prior to FACS sorting. Approximately 30% of the population falls into the reporter "on" population. A gap was left between the sorted "off" and "on" populations to increase the stringency of the sorting. e) Example of the "off" and "on" gates drawn on wild type PAO1 pP_{cdrA}::gfp_{ASV} cells that were grown planktonically to midlog, demonstrating that the surface dependent nature of P*cdrA* reporter activity can be detected by flow cytometry.

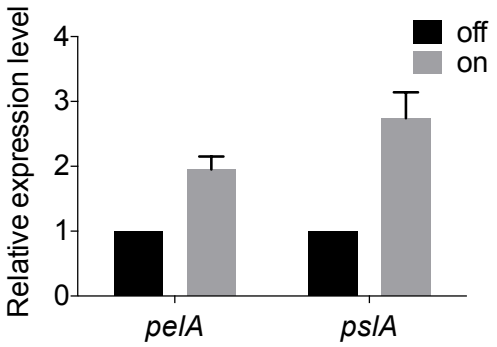

Figure 16. Subpopulations of PAO1 cells with high and low c-di-GMP reporter activity are physiologically distinct. Cells with higher c-di-GMP reporter activity have increased expression of Pel and Psl biosynthetic machinery genes. After 4 hours of attachment to glass, wild type PAO1 cells were separated by flow-assisted cell sorting (FACS) into a population of cells with high (on) and low (off) c-di-GMP reporter activity, then qRT-PCR was performed to quantify expression of Pel and Psl polysaccharide biosynthesis genes. Levels of expression of Pel or Psl mRNA were normalized to the off population.

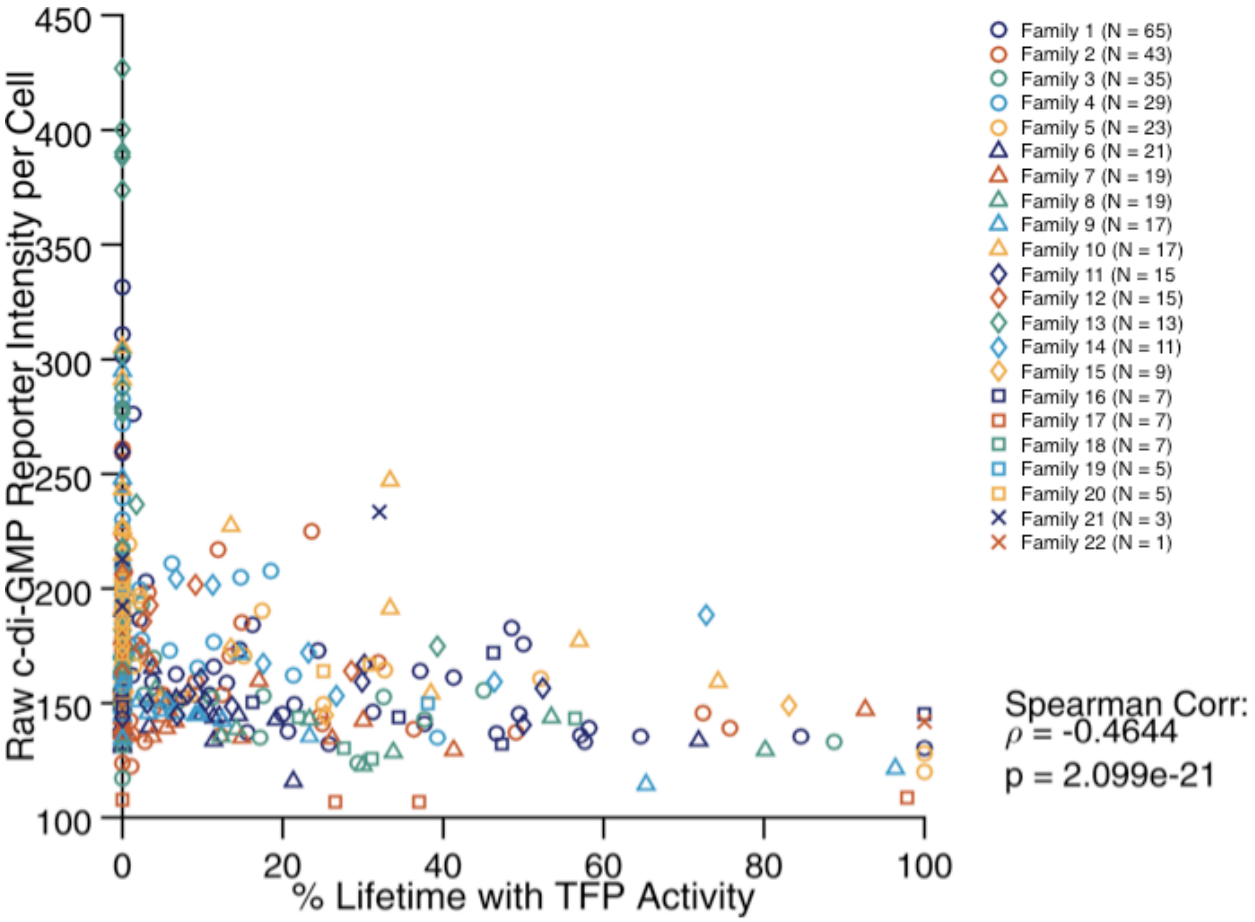

Figure 17. C-di-GMP levels within a population of surface-attached wild type PAO1 cells are inversely correlated with type IV pili-mediated surface motility (ρ -0.4644, p <0.001). Scatterplot of individual cells' percentage of lifetime spent traveling on a surface versus the average GFP fluorescence of the pP$_{cdrA}$::*gfp*$_{ASV}$ reporter across the lifetime of the cell indicating that cells with the highest level of surface motility tend to have low levels of P$_{cdrA}$::*gfp*$_{ASV}$ activity. GFP fluorescence, type IV pili-mediated surface motility, and cell divisions were tracked by taking an image every 3 seconds for 40 hours in wild type PAO1 cells harboring the pP$_{cdrA}$::*gfp*$_{ASV}$ reporter during growth in flow cells with FAB + 0.6mM glutamate. % lifetime with TFP activity refers to the percentage of time in the video that a cell moved between consecutive frames of the video. Families indicate cells

that originated from the same initial cell at the start of the experiment. N is the number of cells within each family.

CONCLUSIONS AND FUTURE DIRECTIONS

Bacteria have a huge capacity to sense, respond to, and interact with their environment and each other (2, 209, 210). The social behaviors that arise from these interactions drive microbial community composition and function. In this thesis work, I have identified inter- and intra-species interactions that influence biofilm formation by *P. aeruginosa*. In chapters I and II, I identified two molecules produced by *S. aureus* that influence *P. aeruginosa* biofilm formation. In Chapter III, I described how a genetically homogenous population of *P. aeruginosa* cells divides the labor of two of the most energetically costly behaviors of biofilm formation: surface exploration and polysaccharide production. We have only begun to scratch the surface as we seek to elucidate the diversity of social interactions that occur as bacteria encounter each other and their environment. For each chapter, multiple exciting lines of research remain to be explored.

Chapter I: *Staphylococcus aureus* Protein A Mediates Interspecies Interactions at the Cell Surface of P*seudomonas aeruginosa*

Does SpA bound to the *P. aeruginosa* cell surface perform additional functions?

In Chapter I, I described how Staphylococcal Protein A (SpA) binds to two abundant targets on the *P. aeruginosa* cell surface, the Psl polysaccharide and the PilA filament protein of type IV pili (25). SpA is the most abundantly produced *S. aureus* extracellular protein and *S. aureus* is notorious for its ability to "hide" from neutrophils due to the ability of SpA to sequester Fcγ domain of IgG antibodies, thereby interfering with antibody-mediated opsonization (211). We found that *P. aeruginosa* with SpA bound to its cell surface is resistant to IgG-mediated opsonophagocytosis by neutrophils. While our *in vitro* experiment suggests that *P. aeruginosa* can benefit from at least one important protective function of SpA, this adhesin mediates multiple interactions of *S. aureus* with the host during infection, in addition to blocking IgG-mediated opsonophagocytosis. For example, SpA bound to the cell surface of *S. aureus* mediates the interaction of *S. aureus* with red blood cells and damaged endothelial cells by binding

von Willebrand factor (vWF), a large glycoprotein produced by endothelial cells and megakaryocytes (cells that release platelets) (123). SpA binding to vWF is thought to play a role in *S. aureus* bloodstream infections and infective endocarditis (a biofilm infection of heart valves) by promoting the recruitment and adherence of *S. aureus* to collagen and sites of blood vessel damage, despite the high shear stress environment of the circulatory system (123, 212, 213). Because *S. aureus* and *P. aeruginosa* can be co-isolated from bloodstream infections (214) and endocarditis (87, 215), as well as other infections where vWF is present such as chronic wounds (216), it would be interesting to see if SpA promotes the initial adherence of *P. aeruginosa* to these same targets through binding to vWF. Endothelial cells can be cultured as monolayers in flow cells under conditions of high shear stress (217). Relative attachment of *P. aeruginosa* to endothelial cells could be evaluated during co-culture with *S. aureus* or *S. aureus* Δ*spa* in flow cells under conditions of increasing shear force, to determine whether SpA can enhance *P. aeruginosa* attachment to vWF-expressing cells.

Is SpA secretion exclusively a cooperative behavior during co-infection of *P. aeruginosa* and *S. aureus*?

While the functions of cell surface-associated SpA have been well studied for decades, recent reports have described that the *S. aureus* cell wall hydrolase LytM is responsible for cleaving a significant amount of SpA from the cell surface, resulting in its release into the extracellular milieu during growth (109). In the context of lower respiratory infections, a common site where *P. aeruginosa* and *S. aureus* co-infect, neutrophils are the most abundant phagocytic cells and a key player in the innate immune response to infection. However, B cells are a type of adaptive immune cell that are also present in airways during infection, as well as other sites where *P. aeruginosa* and *S. aureus* co-infect (such as in chronic wounds (122), endocarditis, and medical device-associated infections (214)). In addition to binding to the Fcγ domain of IgG, SpA can bind to the Fab region of some antibodies and lead to immunosuppression by at least two mechanisms. First, extracellular SpA binding to the Fab region of V_H3 clan IgM, a major class of IgM antibodies (also referred to as B cell receptors), can crosslink IgM molecules, thereby acting as a superantigen that triggers the activation, proliferative

expansion, and apoptotic collapse of B cells (211). Second, SpA's superantigen activity been suggested to impede the development of adaptive immunity during infection by inducing the affinity maturation and biasing of activated B cells (plasmablasts) exclusively toward recognition of SpA. Affinity maturation is a step in the adaptive host immune response to infection whereby B cells produce antibodies with increased affinity for a specific antigen and portion of these antigen-activated B cells differentiate into memory cells, leading to long-lasting immunity toward their specific target antigen (218). SpA's superantigenicity interferes with the ability of the host to generate B cells that target any of the multiple other virulence factors of *S. aureus*, leading not only to difficultly in clearing the current *S. aureus* infection, but also an inability to generate sufficient memory to protect against future *S. aureus* infections (219).

While this interaction of SpA with B cells is known to be protective for *S. aureus in vivo*, it is interesting to note that this process results in a large portion of B cells that specifically recognize SpA. This leads to the question of whether SpA bound to the cell surface of *P. aeruginosa* could target *P. aeruginosa* for killing by B cells following affinity maturation toward SpA. In this case, SpA would not be functioning as a "public good" to protect neighboring *P. aeruginosa* from killing by the host immune response, but instead may offer *S. aureus* a competitive advantage during co-infection. On the other hand, SpA bound to *P. aeruginosa* may retain its superantigen properties and lead to protection of *P. aeruginosa* from B cells, similar to our observation that SpA retains its protective function against neutrophils when bound to the *P. aeruginosa* cell surface. One minimally-invasive way to begin to test this hypothesis could be to see whether individuals who have experienced an acute co-infection with *P. aeruginosa* and *S. aureus* develop a less robust adaptive immune response to *P. aeruginosa* (presumably because their B cells developed a disproportionate affinity toward SpA instead of *P. aeruginosa* antigens) compared to patients who were infected with *P. aeruginosa* alone. Because SpA bound to the cell surface of *P. aeruginosa* likely mediates multiple interactions with a variety of immune cells and other host targets, *in vitro* studies of each of these individual effects of SpA on *P. aeruginosa* survival can only provide a small snapshot of the multifactorial interaction occurring between the host and bacteria within a polymicrobial community. Thus, studies employing relevant animal models would be

needed to understand whether and how secreted SpA influences *P. aeruginosa* survival and persistence during co-infection with *S. aureus*.

Does extracellular SpA broadly inhibit IgG-mediated opsonophagocytosis of bacteria during polymicrobial infections?

In addition to finding that SpA could protect *P. aeruginosa* from neutrophil phagocytosis through SpA binding to specific targets on its cell surface prior to *P. aeruginosa* being bound by IgG, we found that SpA binding to the Fc region of anti-Pseudomonal antibodies that had been allowed to bind to *P. aeruginosa* in their "correct" orientation was still hugely protective. Furthermore, this protection did not require the presence of specific SpA binding targets on *P. aeruginosa*'s cell surface (Psl and PilA). While our analysis of this interaction was limited to *P. aeruginosa*, it is possible that extracellular SpA can bind to the Fc region of any antibody bound to a neighboring bacterial cell and provide protection against IgG-mediated opsonophagocytosis, provided SpA binds to the Fc region of the IgG molecule before this Fc region is recognized by a neutrophil's Fc receptor to initiate phagocytosis. *S. aureus* is the most commonly isolated pathogen from pediatric cystic fibrosis patients; however, many other co-infecting bacteria are typically present in the lungs at this time as well, including *Haemophilus influenzae*, *Stenotrophomonas maltophilia*, and *Achromobacter* sp. (94). As with *P. aeruginosa*, the genomes of these bacteria are not predicted to encode IgG-binding proteins (as determined by a BLAST search for proteins with homology to SpA or Sbi), but it is possible that these species may also be able to benefit from the nonspecific IgG-binding activity of secreted SpA during co-infection with *S. aureus*. A broad, interesting avenue of future research will be evaluating the collective function of abundantly produced extracellular "virulence factors" within the context of polymicrobial communities, because it is apparent that the full scope of any single bacterium's pathogenesis during polymicrobial infections is likely not limited to what is encoded on its genome.

Do *P. aeruginosa* biofilms selectively retain proteins secreted by *S. aureus* and other bacteria in polymicrobial environments?

The *P. aeruginosa* biofilm extracellular matrix is beginning to be appreciated as more than simply a scaffold that provides structure and protection to a community of cells (22, 24). While only one *bona fide P. aeruginosa* biofilm matrix associated protein has been identified to date (the Psl-binding adhesin, CdrA (184)) and our description of SpA is the first description of a *P. aeruginosa* biofilm matrix molecule (Psl) binding a proteins from other bacteria, the biofilm matrix may be rife with bioactive proteins, either due to secretion, cell lysis, or outer membrane vessicle production by *P. aeruginosa* (220), or similar mechanisms from neighboring bacterial species. In particular, it would be interesting to see whether additional *S. aureus* proteins can be selectively retained by *P. aeruginosa* biofilms. *S. aureus* produces an impressively large repertoire of secreted enzymes and adhesins that play diverse and important roles in *S. aureus* pathogenesis (219) that could be retained by the *P. aeruginosa* extracellular matrix through direct binding or through charge interactions. *P. aeruginosa* produces the anionic polysaccharide alginate (221), the neutral Psl (222), and the cationic Pel (199), each of which has a distinct sugar composition, thus there is a great potential for differences in which proteins are retained in the matrix depending on which polysaccharide is produced, as well as the physiochemical properties of the environment. Furthermore, rugose small colony variants (RSCVs) are Psl over-producers that commonly evolve during chronic CF lung infection by *P. aeruginosa* (223). If an important social function of biofilm matrix polysaccharides is to retain bioactive proteins from neighboring bacteria, then these RSCVs have the potential to display enhanced retention of such proteins. Immunoprecipitation of known *P. aeruginosa* bofilm matrix components, such as the polysaccharides, from co-culture biofilms followed by LC-MS/MS is one simple approach that can be employed to identify putative *P. aeruginosa* biofilm matrix associated proteins from other bacteria.

How common are Pel-dominant biofilms in *P. aeruginosa*?

Our study was the first to explicitly identify and characterize non-mucoid *P. aeruginosa* clinical isolates that do not produce the Psl polysaccharide. Strikingly, these Psl non-producers formed Pel-dominant biofilms that were equally robust compared to their Psl-producing counterparts. The Pel-dominant biofilm of the lab strain PA14 was

thought to be atypical; most non-mucoid *P. aeruginosa* had been found to produce both Pel and Psl, although the relative contributions of the two polysaccharides to biofilm formation varied (224). While we now know that Psl non-producing *P. aeruginosa* isolates can arise within a pediatric population of children with CF, additional screening of a larger sample of isolates is required in order to describe the prevalence of Psl non-producers, as well as to determine whether there is any association of loss of Psl production with clinical outcome in CF. Interestingly, within a collection of clonal *P. aeruginosa* isolates collected from the same child over 2 years, only the latest isolates were Psl non-producers and we demonstrated that a large genomic deletion was responsible for the loss of Psl in this lineage. However, a PCR screen for presence of *pslA* in the additional Psl non-producers from other children indicated that these strains lost their ability to produce Psl through a mechanism other than genomic deletion of the Psl operon (data not shown). The emergence of this Pel-dominant biofilm phenotype in in multiple patients suggests that the pediatric CF lung environment has the potential to select for loss of Psl production. One intriguing possibility is that these Pel-dominant biofilm producing clinical isolates represent a previously unknown step in *P. aeruginosa* pathoadaptation during CF lung infections, prior to conversion to the alginate-producing "mucoidy" phenotype that is more typical of *P. aeruginosa* isolates from adult CF patients.

Chapter II: Characterization of PA2582, a c-di-AMP-binding post-transcriptional regulator

Do Proteobacteria sense and respond to cyclic di-AMP as a signal of "non-self" bacteria in their local environment?

In Chapter II, I described how *P. aeruginosa* forms elevated levels of biofilm biomass in response to cyclic di-AMP present in *S. aureus* culture supernatant. *P. aeruginosa* and other Proteobacteria (excluding δ-Proteobacteria) are not predicted to encode the diadenylate cyclases responsible for producing c-di-AMP (145). However, *P. aeruginosa* PA2582 binds c-di-AMP *in vitro* with a greater affinity than at least one known c-di-AMP binding protein in *Listeria monocytogenes* (LmPC, $K_D = 8 \pm 0.2\mu M$

(178) versus PA2582 $K_D = 2.6 \pm 0.3$ μM). PA2582 is a protein of unknown function in *P. aeruginosa* with strong homology to ProQ, an RNA chaperone present throughout Proteobacteria. The distribution of ProQ homologs throughout bacteria that are not predicted to produce c-di-AMP is intriguing and raises the question of whether ProQ is involved in sensing and coordinating a response of Proteobacteria to non-Proteobacteria. *S. aureus* is capable of producing micromolar levels of c-di-AMP during growth (152); thus, this molecule may be present throughout the environment and frequently encountered by Proteobacteria.

Can cyclic di-AMP be transported into the cytoplasm of *P. aeruginosa*?

PA2582 is predicted to be a cytoplasmic protein, yet cyclic di-nucleotides are not thought to be able to freely diffuse across bacterial cell membranes. While the mechanism of c-di-AMP secretion during *L. monocytogenes* has been shown to be dependent upon a multi-drug efflux pump, no known mechanism of bacterial uptake of c-di-AMP has been identified. Pilot experiments to demonstrate transport and accumulation of ^{32}P-c-di-AMP into *P. aeruginosa* were unsuccessful. Determining whether and how c-di-AMP can reach the P. aeruginosa cytoplasm is essential in developing a model of how c-di-AMP-binding to PA2582 influences *P. aeruginosa* biofilm formation. Interestingly, we found in a Biolog screen that *P. aeruginosa* was impaired for use of cyclic nucleotides as a sole phosphorous source when grown in the presence of 5μM c-di-AMP. One possible explanation for this defect in cyclic nucleotide metabolism is that the micromolar concentration of c-di-AMP present in the media interferes with a porin or transporter necessary for uptake of cyclic nucleotides during phosphorous-limited growth conditions. While this interference could simply be due to c-di-AMP binding to and blocking or inactivating the uptake mechanism for cyclic di-nucleotides, it is possible that c-di-AMP may be transported into the cell through these pathways as well. By identifying genes required for growth on cyclic nucleotides as a sole phosphorous source, we may identify a membrane-associated protein that is involved in transport of c-di-AMP into *P. aeruginosa*. Presumably, we could screen these putative c-di-AMP transporters by crystal violet assay for loss of elevated biofilm formation in response to growth with c-di-AMP.

Do other *S. aureus*-produced molecules stimulate *P. aeruginosa* biofilm formation?

We hydrolyzed c-di-AMP from *S. aureus* culture supernatant and observed a significant reduction in the biofilm-stimulatory activity of the supernatant; however, biofilm formation was still noticeably elevated in the hydrolyzed supernatant relative to the control LB condition. Thus, while c-di-AMP is present in *S. aureus* culture supernatant and stimulates *P. aeruginosa* biofilm formation, there is likely at least one additional heat-stable small molecule that also stimulates biofilm formation in *P. aeruginosa*. Bioassay guided fractionation of *S. aureus* culture supernatant could be employed to identify the additional biofilm-stimulatory small molecule(s).

Is PA2582 a novel sRNA chaperone in *P. aeruginosa*?

PA2582 is homologous to ProQ, which has recently been describes as representing a new class of RNA chaperones, like Hfq and RsmA/CsrA (156). Specifically, ProQ was found to bind a large number of sRNAs. When we sequenced RNA bound to PA2582, we also identified a large number of known sRNAs, as well as many putative sRNAs (reads mapping antisense to *P. aeruginosa* genes). While our CLIPseq experiments identified some interesting targets to follow up on in terms of a role for PA2582 in biofilm regulation, the experiments were hindered by a large number of rRNA reads (due to the nature of PA2582 as a ribosome-associated protein). To address the issue of abundant rRNA reads dominating CLIPseq when characterizing *Salmonella enterica*'s ProQ, the laboratory of Dr. Jörg Vogel developed a technique called GRADseq, which relied on sedimentation of cellular RNAs and their associated proteins via glycerol gradient into 20 fractions, then performing Illumina cDNA sequencing on each fraction. By separating samples into such a large number of fractions, some fractions were not dominated by abundant housekeeping RNAs. While our initial CLIPseq-based characterization of PA2582-bound RNAs likely identified many of the more abundant RNA targets (such as rsmY and rsmZ), future efforts to reduce the number of rRNA reads either by GRADseq or another technique are necessary to identify the full scope of RNAs bound by PA2582.

Chapter III: A division of labor during surface sensing influences *Pseudomonas aeruginosa* biofilm formation

Why does *P. aeruginosa* have at least two surface sensing systems that stimulate c-di-GMP production?

The Wsp system is well-known to stimulate production of c-di-GMP in response to growth on a surface through the diguanylate cyclase (DGC) WspR (225) and, more recently, the Pil-Chp system was also implicated in surface-induced stimulation of c-di-GMP production, through the DGC SadC (142). We observed that single mutants of WspR and SadC each have defects in biofilm formation at early timepoints in a crystal violet attachment assay, and a double mutant of both cyclases has an additive defect, suggesting that both of these surface sensing systems play important roles in early biofilm formation. The Wsp system has been shown to influence production of biofilm matrix components, including stimulating production of the Pel and Psl polysaccharides, as well as the adhesin CdrA. While SadC has been shown to influence Pel polysaccharide production (although not transcriptionally) (196), most of the work on the Pil-Chp system to date has been to describe how this system activates Type IV pili production and suppresses flagellar-mediated swarming motility in the lab strain PA14. One hypothesis as to why *P. aeruginosa* has at least two surface sensing systems is that each system could specialize in regulating different aspects of biofilm formation.

Type IV pili are important for initial surface attachment as well as surface exploration (leading to microcolony formation) during early biofilm formation (24). Deletion of PilY1, a protein required for activating SadC in response to surface growth, leads to a defect in type IV pili biogenesis and a delay in the transition from reversible (polar) to irreversible (lateral) surface attachment (142). While a SadC mutant displayed a defect in Pel-dependent congo red binding in PA14, deletion of SadC did not alter transcription of the Pel operon (196). In contrast, a mutant that results in a hyperactive Wsp system (deletion of WspF) results in elevated transcription and production of Pel, Psl, and CdrA (184, 194). One possibility is that the Pil-Chp system specializes in regulation of motility phenotypes during surface sensing, whereas the Wsp system primarily specializes in regulating biofilm matrix production. In PAO1, we found that a WspR mutant has a much more severe defect than SadC in derepression of FleQ from the promoter of CdrA. Perhaps WspR produces more c-di-GMP than SadC during surface sensing, allowing it to specialize in modulation of FleQ activity, which has a lower

affinity for c-di-GMP binding than FimX (55), a c-di-GMP binding protein that plays a role in Type IV pili regulation (203). One challenge in interpreting the relative roles of Wsp and Pil-Chp in surface sensing is that these systems have largely been studied in separate lab strains that we observed to differ in the magnitude of their c-di-GMP production in response to surface growth. By characterizing the dynamics of c-di-GMP production by Wsp and Pil-Chp mutants in both PAO1 and PA14, we hope to be able to shed light on the relative contributions of each system to early biofilm formation.

Are the subcellular localizations of the Pil-Chp and Wsp surface sensing systems a key feature of their activity?

One striking way in which the Wsp system differs from chemotaxis signal transduction complexes is that whereas the chemotaxis chemoreceptors form dense arrays at the cell poles, the Wsp system forms smaller clusters that localize laterally (225). Interestingly, mutations in the WspA, the Wsp system sensor homologous to methyl-accepting chemotaxis proteins (MCPs), that lead to polar localization of the Wsp system abrogated its c-di-GMP signaling activity (190). Thus, the lateral localization of the Wsp system appears to be a key feature of its function. The type IV pili of *P. aeruginosa* are localized to the cell poles (226). In response to growth on a surface, PilY1 localizes to the type IV pili alignment complex, and this localization is required for PilY1 to activate SadC to produce c-di-GMP. Therefore, because type IV pili-mediated mechanosensing of surfaces is thought to be the mechanism by which Pil-Chp senses a surface (142), a key feature of the Pil-Chp system is likely its polar localization. The differential localization of the Wsp and Pil-Chp systems may allow these systems to play distinct, temporal roles in the transition from reversible to irreversible attacgment (Figure 1). In PA14, a SadC mutant is defective for transitioning from polar to lateral surface attachment (196). Perhaps the polar localization of the Pil-Chp system is important for sensing type IV-pili mediated initial polar surface attachment (reversible attachment), activating SadC to produce c-di-GMP, and leading downstream to the transition to lateral attachment to a surface (irreversible attachment). If SadC produces lower levels of c-di-GMP than WspR, then these low levels of c-di-GMP may function to first activate Pel production post-translationally through binding PelD (K_D = 1.9 μM; (205)), which aids in the transition

from reversible to irreversible attachment. Lateral attachment could be indicative that an environment is suitable for adopting a biofilm mode of growth, thus the laterally-localized Wsp system could be activated to begin the energetically costly process of biofilm matrix production through production of higher levels of c-di-GMP that result in derepression of FleQ-regulated promoters.

While this sequence of activation of Pil-Chp first, then Wsp seems to fit with the subcellular localization of each system and agrees with a previously proposed model in which Pil-Chp functions upstream of Wsp (142), we some evidence that suggests that the Wsp system is activated more rapidly than Pil-Chp. In Chapter III, we provided evidence that Pel transcription was highly elevated after only 30 minutes of surface attachment. Pel transcription has previously been shown to be independent of SadC (196) and our reporter data suggest that activation of the Wsp system has the largest impact on FleQ regulated promoters, such as Pel. Furthermore, the Wsp system is constitutively expressed (Dr. Caroline Harwood, unpublished), whereas activation of SadC in response to surface sensing by Pil-Chp occurs only after surface-induced transcription of PilY1 and localization of PilY1 to the outer membrane. Our work represents the most comprehensive comparison of the relative activities of the Wsp and Pil-Chp systems during surface sensing to date, but more work is needed to fully characterize the function and relative temporal activation of each system during surface sensing.

Figures

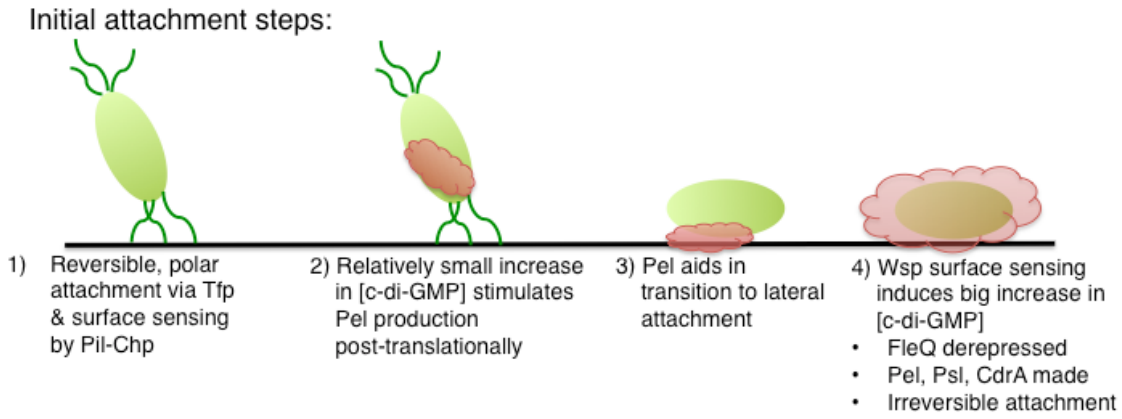

Figure 1. A model depicting how the differential subcellular localizations of the Pil-Chp and Wsp systems could lead to temporal regulation of their activation, leading to distinct contributions to the transition of *P. aeruginosa* from reversible to irreversible attachment. *P. aeruginosa* typically attaches polarly to a surface via Type IV pili (Tfp; dark green lines) during initial attachment, and this polar attachment is a hallmark of the "reversible" attachment phase (1). At this time, the Pil-Chp system could be activated to produce a modest increase in cellular levels of c-di-GMP, which binds the PelD protein and stimulates Pel (red) production post-translationally (2). Pel produced due to activation of the Pil-Chp system could play a role in the transition from polar to lateral attachment, an indication that the cell has become irreversibly attached to the surface (3). Laterally-attached cells sense the surface through the Wsp system to stimulate a comparatively larger increase in cellular c-di-GMP levels through WspR (4). This leads to activation of the FleQ-repressed promoters for Pel, Psl, and CdrA extracellular matrix components and a "commitment" of the cell to the biofilm mode of growth.

REFERENCES

1. Costerton JW, Stewart PS, Greenberg EP. 1999. Bacterial biofilms: a common cause of persistent infections. Science 284:1318–1322.

2. Davey ME, O'toole GA. 2000. Microbial Biofilms: from Ecology to Molecular Genetics. Microbiol Mol Biol Rev 64:847–867.

3. Macalady JL, Jones DS, Lyon EH. 2007. Extremely acidic, pendulous cave wall biofilms from the Frasassi cave system, Italy. Environ Microbiol 9:1402–1414.

4. Schmidt M, Priemé A, Stougaard P. 2006. Bacterial diversity in permanently cold and alkaline ikaite columns from Greenland. Extremophiles 10:551–562.

5. Boomer SM, Noll KL, Geesey GG, Dutton BE. 2009. Formation of Multilayered Photosynthetic Biofilms in an Alkaline Thermal Spring in Yellowstone National Park, Wyoming. Appl Environ Microbiol 75:2464–2475.

6. Westall F, Campbell KA, Bréhéret JG, Foucher F, Gautret P, Hubert A, Sorieul S, Grassineau N, Guido DM. 2015. Archean (3.33 Ga) microbe-sediment systems were diverse and flourished in a hydrothermal context. Geology 43:615–618.

7. LALONDE SV, KONHAUSER KO, REYSENBACH A-L, FERRIS FG. 2005. The experimental silicification of Aquificales and their role in hot spring sinter formation. Geobiology 3:41–52.

8. Costerton JW, Lewandowski Z, Caldwell DE, Korber DR, Lappin-Scott HM. 1995. Microbial biofilms. Annu Rev Microbiol 49:711–745.

9. Lane N. 2015. The unseen world: reflections on Leeuwenhoek (1677) "Concerning little animals." Philos Trans R Soc B Biol Sci 370:20140344.

10. Louis Pasteur. 1922. Memoire sur la fermentation acetique., p. 133–58. *In* Ann Scient de l' Ecole Normale Superieure. Masson et Cie, Paris, France.

11. Römling U, Kjelleberg S, Normark S, Nyman L, Uhlin BE, Åkerlund B. 2014. Microbial biofilm formation: a need to act. J Intern Med 276:98–110.

12. Henrici AT. 1933. Studies of Freshwater Bacteria: I. A Direct Microscopic Technique. J Bacteriol 25:277–287.

13. Zobell CE, Allen EC. 1935. The Significance of Marine Bacteria in the Fouling of Submerged Surfaces. J Bacteriol 29:239–251.

14. MARSHALL KC, STOUT R, MITCHELL R. 1971. Mechanism of the Initial Events in the Sorption of Marine Bacteria to Surfaces. Microbiology 68:337–348.

15. HOIBY N. 1974. PSEUDOMONAS-AERUGINOSA INFECTION IN CYSTIC-FIBROSIS - RELATIONSHIP BETWEEN MUCOID STRAINS OF PSEUDOMONAS-AERUGINOSA AND HUMORAL IMMUNE-RESPONSE. Acta Pathol Microbiol Scand Sect B-Microbiol B 82:551–558.

16. Costerton JW, Geesey GG, Cheng KJ. 1978. How bacteria stick. Sci Am 238:86–95.

17. McCoy WF, Bryers JD, Robbins J, Costerton JW. 1981. Observations of fouling biofilm formation. Can J Microbiol 27:910–917.

18. de Vos WM. 2015. Microbial biofilms and the human intestinal microbiome. Npj Biofilms Microbiomes 1:15005.

19. Donlan R. 2001. Biofilms and device-associated infections. Emerg Infect Dis 7:277–81.

20. Ma L, Conover M, Lu H, Parsek MR, Bayles K, Wozniak DJ. 2009. Assembly and development of the Pseudomonas aeruginosa biofilm matrix. PLoS Pathog 5:e1000354.

21. Colvin KM, Gordon VD, Murakami K, Borlee BR, Wozniak DJ, Wong GCL, Parsek MR. 2011. The Pel Polysaccharide Can Serve a Structural and Protective Role in the Biofilm Matrix of Pseudomonas aeruginosa. PLoS Pathog 7:e1001264.

22. Irie Y, Borlee BR, O'Connor JR, Hill PJ, Harwood CS, Wozniak DJ, Parsek MR. 2012. Self-produced exopolysaccharide is a signal that stimulates biofilm formation in Pseudomonas aeruginosa. Proc Natl Acad Sci 109:20632–20636.

23. Billings N, Ramirez Millan M, Caldara M, Rusconi R, Tarasova Y, Stocker R, Ribbeck K. 2013. The Extracellular Matrix Component Psl Provides Fast-Acting Antibiotic Defense in Pseudomonas aeruginosa Biofilms. PLoS Pathog 9:e1003526.

24. Zhao K, Tseng BS, Beckerman B, Jin F, Gibiansky ML, Harrison JJ, Luijten E, Parsek MR, Wong GCL. 2013. Psl trails guide exploration and microcolony formation in Pseudomonas aeruginosa biofilms. Nature 497:388–391.

25. Armbruster CR, Wolter DJ, Mishra M, Hayden HS, Radey MC, Merrihew G, MacCoss MJ, Burns J, Wozniak DJ, Parsek MR, Hoffman LR. 2016. Staphylococcus aureus Protein A Mediates Interspecies Interactions at the Cell Surface of Pseudomonas aeruginosa. mBio 7.

26. Wei Q, Ma LZ. 2013. Biofilm Matrix and Its Regulation in Pseudomonas aeruginosa. Int J Mol Sci 14:20983–21005.

27. Hall-Stoodley L, Costerton JW, Stoodley P. 2004. Bacterial biofilms: from the Natural environment to infectious diseases. Nat Rev Micro 2:95–108.

28. Hentzer M, Eberl L, Givskov M. 2005. Transcriptome analysis of Pseudomonas aeruginosa biofilm development: anaerobic respiration and iron limitation. Biofilms 2:37–61.

29. Waite RD, Papakonstantinopoulou A, Littler E, Curtis MA. 2005. Transcriptome Analysis of Pseudomonas aeruginosa Growth: Comparison of Gene Expression in Planktonic Cultures and Developing and Mature Biofilms. J Bacteriol 187:6571–6576.

30. O'Toole GA, Kolter R. 1998. Flagellar and twitching motility are necessary for Pseudomonas aeruginosa biofilm development. Mol Microbiol 30:295–304.

31. Vallet I, Olson JW, Lory S, Lazdunski A, Filloux A. 2001. The chaperone/usher pathways of Pseudomonas aeruginosa: identification of fimbrial gene clusters (cup) and their involvement in biofilm formation. Proc Natl Acad Sci U S A 98:6911–6916.

32. Klausen M, Heydorn A, Ragas P, Lambertsen L, Aaes-Jorgensen A, Molin S, Tolker-Nielsen T. 2003. Biofilm formation by Pseudomonas aeruginosa wild type, flagella and type IV pili mutants. Mol Microbiol 48:1511–1524.

33. Brill-Karniely Y, Jin F, Wong GCL, Frenkel D, Dobnikar J. 2017. Emergence of complex behavior in pili-based motility in early stages of P. aeruginosa surface adaptation. Sci Rep 7:45467.

34. Jin F, Conrad JC, Gibiansky ML, Wong GCL. 2011. Bacteria use type-IV pili to slingshot on surfaces. Proc Natl Acad Sci U S A 108:12617–12622.

35. Colvin KM, Irie Y, Tart CS, Urbano R, Whitney JC, Ryder C, Howell PL, Wozniak DJ, Parsek MR. 2012. The Pel and Psl polysaccharides provide Pseudomonas aeruginosa structural redundancy within the biofilm matrix. Environ Microbiol 14:1913–1928.

36. Franklin MJ, Nivens DE, Weadge JT, Howell PL. 2011. Biosynthesis of the Pseudomonas aeruginosa Extracellular Polysaccharides, Alginate, Pel, and Psl. Front Microbiol 2.

37. Jackson KD, Starkey M, Kremer S, Parsek MR, Wozniak DJ. 2004. Identification of psl, a locus encoding a potential exopolysaccharide that is essential for Pseudomonas aeruginosa PAO1 biofilm formation. J Bacteriol 186:4466–4475.

38. McPhee JB, Bains M, Winsor G, Lewenza S, Kwasnicka A, Brazas MD, Brinkman FSL, Hancock REW. 2006. Contribution of the PhoP-PhoQ and PmrA-PmrB Two-Component Regulatory Systems to Mg2+-Induced Gene Regulation in Pseudomonas aeruginosa. J Bacteriol 188:3995–4006.

39. Guragain M, King MM, Williamson KS, Pérez-Osorio AC, Akiyama T, Khanam S, Patrauchan MA, Franklin MJ. 2016. The Pseudomonas aeruginosa PAO1 Two-Component Regulator CarSR Regulates Calcium Homeostasis and Calcium-Induced Virulence Factor Production through Its Regulatory Targets CarO and CarP. J Bacteriol 198:951–963.

40. Dean CR, Poole K. 1993. Expression of the ferric enterobactin receptor (PfeA) of Pseudomonas aeruginosa: involvement of a two-component regulatory system. Mol Microbiol 8:1095–1103.

41. Kreamer NNK, Wilks JC, Marlow JJ, Coleman ML, Newman DK. 2012. BqsR/BqsS Constitute a Two-Component System That Senses Extracellular Fe(II) in Pseudomonas aeruginosa. J Bacteriol 194:1195–1204.

42. Van Alst NE, Picardo KF, Iglewski BH, Haidaris CG. 2007. Nitrate sensing and metabolism modulate motility, biofilm formation, and virulence in Pseudomonas aeruginosa. Infect Immun 75:3780–3790.

43. Chen AI, Dolben EF, Okegbe C, Harty CE, Golub Y, Thao S, Ha DG, Willger SD, O'Toole GA, Harwood CS, Dietrich LEP, Hogan DA. 2014. Candida albicans Ethanol Stimulates

Pseudomonas aeruginosa WspR-Controlled Biofilm Formation as Part of a Cyclic Relationship Involving Phenazines. PLOS Pathog 10:e1004480.

44. Stover CK, Pham XQ, Erwin AL, Mizoguchi SD, Warrener P, Hickey MJ, Brinkman FSL, Hufnagle WO, Kowalik DJ, Lagrou M, Garber RL, Goltry L, Tolentino E, Westbrock-Wadman S, Yuan Y, Brody LL, Coulter SN, Folger KR, Kas A, Larbig K, Lim R, Smith K, Spencer D, Wong GK-S, Wu Z, Paulsen IT, Reizer J, Saier MH, Hancock REW, Lory S, Olson MV. 2000. Complete genome sequence of Pseudomonas aeruginosa PAO1, an opportunistic pathogen. Nature 406:959–964.

45. He K, Bauer CE. 2014. Chemosensory Signaling Systems That Control Bacterial Survival. Trends Microbiol 22:389–398.

46. Ritchings BW, Almira EC, Lory S, Ramphal R. 1995. Cloning and phenotypic characterization of fleS and fleR, new response regulators of Pseudomonas aeruginosa which regulate motility and adhesion to mucin. Infect Immun 63:4868–4876.

47. Mikkelsen H, Sivaneson M, Filloux A. 2011. Key two-component regulatory systems that control biofilm formation in Pseudomonas aeruginosa. Environ Microbiol 13:1666–1681.

48. Kulesekara H, Lee V, Brencic A, Liberati N, Urbach J, Miyata S, Lee DG, Neely AN, Hyodo M, Hayakawa Y, Ausubel FM, Lory S. 2006. Analysis of Pseudomonas aeruginosa diguanylate cyclases and phosphodiesterases reveals a role for bis-(3′-5′)-cyclic-GMP in virulence. Proc Natl Acad Sci U S A 103:2839–2844.

49. Gooderham WJ, Hancock REW. 2009. Regulation of virulence and antibiotic resistance by two-component regulatory systems in Pseudomonas aeruginosa. FEMS Microbiol Rev 33:279–294.

50. Romling U, Galperin MY, Gomelsky M. 2013. Cyclic di-GMP: the first 25 years of a universal bacterial second messenger. Microbiol Mol Biol Rev MMBR 77:1–52.

51. Barraud N, Schleheck D, Klebensberger J, Webb JS, Hassett DJ, Rice SA, Kjelleberg S. 2009. Nitric oxide signaling in Pseudomonas aeruginosa biofilms mediates phosphodiesterase activity, decreased cyclic di-GMP levels, and enhanced dispersal. J Bacteriol 191:7333–7342.

52. Roy AB, Petrova OE, Sauer K. 2012. The Phosphodiesterase DipA (PA5017) Is Essential for Pseudomonas aeruginosa Biofilm Dispersion. J Bacteriol 194:2904–2915.

53. Rybtke MT, Borlee BR, Murakami K, Irie Y, Hentzer M, Nielsen TE, Givskov M, Parsek MR, Tolker-Nielsen T. 2012. Fluorescence-Based Reporter for Gauging Cyclic Di-GMP Levels in Pseudomonas aeruginosa. Appl Environ Microbiol 78:5060–5069.

54. Valentini M, Filloux A. 2016. Biofilms and Cyclic di-GMP (c-di-GMP) Signaling: Lessons from Pseudomonas aeruginosa and Other Bacteria. J Biol Chem 291:12547–12555.

55. Pultz IS, Christen M, Don Kulasekara H, Kennard A, Kulasekara B, Miller SI. 2012. The response threshold of Salmonella PilZ domain proteins is determined by their binding affinities for c-di-GMP. Mol Microbiol 86:1424–1440.

56. Hengge R. 2009. Principles of c-di-GMP signalling in bacteria. Nat Rev Micro 7:263–273.

57. Merritt JH, Ha D-G, Cowles KN, Lu W, Morales DK, Rabinowitz J, Gitai Z, O'Toole GA. 2010. Specific Control of Pseudomonas aeruginosa Surface-Associated Behaviors by Two c-di-GMP Diguanylate Cyclases. mBio 1.

58. Massie JP, Reynolds EL, Koestler BJ, Cong J-P, Agostoni M, Waters CM. 2012. Quantification of high-specificity cyclic diguanylate signaling. Proc Natl Acad Sci 109:12746–12751.

59. Shapiro JA. 1998. Thinking about bacterial populations as multicellular organisms. Annu Rev Microbiol 52:81–104.

60. Balcázar JL, Subirats J, Borrego CM. 2015. The role of biofilms as environmental reservoirs of antibiotic resistance. Front Microbiol 6:1216.

61. Flemming H-C, Wingender J, Szewzyk U, Steinberg P, Rice SA, Kjelleberg S. 2016. Biofilms: an emergent form of bacterial life. Nat Rev Micro 14:563–575.

62. Nadell CD, Drescher K, Foster KR. 2016. Spatial structure, cooperation and competition in biofilms. Nat Rev Micro 14:589–600.

63. van Gestel J, Vlamakis H, Kolter R. 2015. Division of Labor in Biofilms: the Ecology of Cell Differentiation. Microbiol Spectr 3:MB-0002-2014.

64. Haagensen JAJ, Klausen M, Ernst RK, Miller SI, Folkesson A, Tolker-Nielsen T, Molin S. 2007. Differentiation and Distribution of Colistin- and Sodium Dodecyl Sulfate-Tolerant Cells in Pseudomonas aeruginosa Biofilms. J Bacteriol 189:28–37.

65. Wessel AK, Arshad TA, Fitzpatrick M, Connell JL, Bonnecaze RT, Shear JB, Whiteley M. 2014. Oxygen Limitation within a Bacterial Aggregate. mBio 5.

66. Schreiber F, Littmann S, Lavik G, Escrig S, Meibom A, Kuypers MMM, Ackermann M. 2016. Phenotypic heterogeneity driven by nutrient limitation promotes growth in fluctuating environments. Nat Microbiol 1:16055.

67. Vroom JM, De Grauw KJ, Gerritsen HC, Bradshaw DJ, Marsh PD, Watson GK, Birmingham JJ, Allison C. 1999. Depth Penetration and Detection of pH Gradients in Biofilms by Two-Photon Excitation Microscopy. Appl Environ Microbiol 65:3502–3511.

68. Stewart PS, Franklin MJ. 2008. Physiological heterogeneity in biofilms. Nat Rev Microbiol 6:199–210.

69. Williamson KS, Richards LA, Perez-Osorio AC, Pitts B, McInnerney K, Stewart PS, Franklin MJ. 2012. Heterogeneity in Pseudomonas aeruginosa Biofilms Includes Expression of Ribosome Hibernation Factors in the Antibiotic-Tolerant Subpopulation and Hypoxia-Induced Stress Response in the Metabolically Active Population. J Bacteriol 194:2062–2073.

70. Bjarnsholt T, Jensen PO, Fiandaca MJ, Pedersen J, Hansen CR, Andersen CB, Pressler T, Givskov M, Hoiby N. 2009. Pseudomonas aeruginosa biofilms in the respiratory tract of cystic fibrosis patients. Pediatr Pulmonol 44:547–558.

71. Singh PK, Schaefer AL, Parsek MR, Moninger TO, Welsh MJ, Greenberg EP. 2000. Quorum-sensing signals indicate that cystic fibrosis lungs are infected with bacterial biofilms. Nature 407:762–764.

72. Lewis K. 2007. Persister cells, dormancy and infectious disease. Nat Rev Microbiol 5:48–56.

73. Dubnau D, Losick R. 2006. Bistability in bacteria. Mol Microbiol 61:564–572.

74. Elowitz MB, Levine AJ, Siggia ED, Swain PS. 2002. Stochastic Gene Expression in a Single Cell. Science 297:1183.

75. Casadesús J, Low D. 2006. Epigenetic Gene Regulation in the Bacterial World. Microbiol Mol Biol Rev 70:830–856.

76. Christen M, Kulasekara HD, Christen B, Kulasekara BR, Hoffman LR, Miller SI. 2010. Asymmetrical Distribution of the Second Messenger c-di-GMP upon Bacterial Cell Division. Science 328:1295–1297.

77. Bruger EL, Waters CM. 2016. Bacterial Quorum Sensing Stabilizes Cooperation by Optimizing Growth Strategies. Appl Environ Microbiol 82:6498–6506.

78. Hibbing ME, Fuqua C, Parsek MR, Peterson SB. 2010. Bacterial competition: surviving and thriving in the microbial jungle. Nat Rev Micro 8:15–25.

79. LeRoux M, Peterson SB, Mougous JD. 2015. Bacterial danger sensing. J Mol Biol 427:3744–3753.

80. Korgaonkar AK, Whiteley M. 2011. Pseudomonas aeruginosa Enhances Production of an Antimicrobial in Response to N-Acetylglucosamine and Peptidoglycan. J Bacteriol 193:909–917.

81. Pierson LS, Pierson EA. 2010. Metabolism and function of phenazines in bacteria: impacts on the behavior of bacteria in the environment and biotechnological processes. Appl Microbiol Biotechnol 86:1659–1670.

82. LeRoux M, Kirkpatrick RL, Montauti EI, Tran BQ, Peterson SB, Harding BN, Whitney JC, Russell AB, Traxler B, Goo YA, Goodlett DR, Wiggins PA, Mougous JD. 2015. Kin cell lysis is a danger signal that activates antibacterial pathways of Pseudomonas aeruginosa. eLife 4:e05701.

83. McFarland KA, Dolben EL, LeRoux M, Kambara TK, Ramsey KM, Kirkpatrick RL, Mougous JD, Hogan DA, Dove SL. 2015. A self-lysis pathway that enhances the virulence of a pathogenic bacterium. Proc Natl Acad Sci U S A 112:8433–8438.

84. Hood RD, Singh P, Hsu F, Güvener T, Carl MA, Trinidad RRS, Silverman JM, Ohlson BB, Hicks KG, Plemel RL, Li M, Schwarz S, Wang WY, Merz AJ, Goodlett DR, Mougous JD.

2010. A Type VI Secretion System of Pseudomonas aeruginosa Targets a Toxin to Bacteria. Cell Host Microbe 7:25–37.

85. Bongiorni MG, Tascini C, Tagliaferri E, Di Cori A, Soldati E, Leonildi A, Zucchelli G, Ciullo I, Menichetti F. 2012. Microbiology of cardiac implantable electronic device infections. Europace.

86. Yamane K, Hirose H, Mather PJ, Silvestry SC. 2011. Mycotic Pseudoaneurysm of the Ascending Aorta After Heart Transplantation: Case Report. Transplant Proc 43:2055–2058.

87. Sousa C, Botelho C, Rodrigues D, Azeredo J, Oliveira R. 2012. Infective endocarditis in intravenous drug abusers: an update. Eur J Clin Microbiol Infect Dis 31:2905–2910.

88. Hauser AR, Jain M, Bar-Meir M, McColley SA. 2011. Clinical Significance of Microbial Infection and Adaptation in Cystic Fibrosis. Clin Microbiol Rev 24:29–70.

89. Gavin PJ, Suseno MT, Cook FV, Peterson LR, Thomson RB Jr. Left-sided endocarditis caused by Pseudomonas aeruginosa: successful treatment with meropenem and tobramycin. Diagn Microbiol Infect Dis 47:427–430.

90. Bicanic T., Eykyn S. 2002. Hospital-acquired, Native Valve Endocarditis Caused by Pseudomonas aeruginosa. J Infect 44:137–139.

91. Kaplan JB. 2010. Biofilm Dispersal: Mechanisms, Clinical Implications, and Potential Therapeutic Uses. J Dent Res 89:205–218.

92. Flemming H-C, Wingender J. 2010. The biofilm matrix. Nat Rev Micro 8:623–633.

93. Absalon C, Ymele-Leki P, Watnick PI. 2012. The Bacterial Biofilm Matrix as a Platform for Protein Delivery. mBio 3:e00127-12.

94. Cystic Fibrosis Foundation. 2012. Patient registry: annual data report 2006. Cystic Fibrosis Foundation, Bethesda, MD.

95. Wolter DJ, Emerson JC, McNamara S, Buccat AM, Qin X, Cochrane E, Houston LS, Rogers GB, Marsh P, Prehar K, Pope CE, Blackledge M, Déziel E, Bruce KD, Ramsey BW, Gibson RL, Burns JL, Hoffman LR. 2013. Staphylococcus aureus Small-Colony Variants Are Independently Associated With Worse Lung Disease in Children With Cystic Fibrosis. Clin Infect Dis 57:384–391.

96. Sagel SD, Sontag MK, Accurso FJ. 2009. Relationship between antimicrobial proteins and airway inflammation and infection in cystic fibrosis. Pediatr Pulmonol 44:402–409.

97. Hudson VL, Wielinski CL, Regelmann WE. 1993. Prognostic implications of initial oropharyngeal bacterial flora in patients with cystic fibrosis diagnosed before the age of two years. J Pediatr 122:854–860.

98. Stewart PS, William Costerton J. Antibiotic resistance of bacteria in biofilms. The Lancet 358:135–138.

99. Thurlow LR, Hanke ML, Fritz T, Angle A, Aldrich A, Williams SH, Engebretsen IL, Bayles KW, Horswill AR, Kielian T. 2011. Staphylococcus aureus Biofilms Prevent Macrophage Phagocytosis and Attenuate Inflammation In Vivo. J Immunol 186:6585–6596.

100. Hoffman LR, Déziel E, D'Argenio DA, Lépine F, Emerson J, McNamara S, Gibson RL, Ramsey BW, Miller SI. 2006. Selection for Staphylococcus aureus small-colony variants due to growth in the presence of Pseudomonas aeruginosa. Proc Natl Acad Sci 103:19890–19895.

101. Mashburn LM, Jett AM, Akins DR, Whiteley M. 2005. Staphylococcus aureus Serves as an Iron Source for Pseudomonas aeruginosa during In Vivo Coculture. J Bacteriol 187:554–566.

102. Pastar I, Nusbaum AG, Gil J, Patel SB, Chen J, Valdes J, Stojadinovic O, Plano LR, Tomic-Canic M, Davis SC. 2013. Interactions of Methicillin Resistant Staphylococcus aureus USA300 and Pseudomonas aeruginosa in Polymicrobial Wound Infection. PLoS ONE 8:e56846.

103. Filkins LM, Graber JA, Olson DG, Dolben EL, Lynd LR, Bhuju S, O'Toole GA. 2015. Coculture of Staphylococcus aureus with Pseudomonas aeruginosa Drives S. aureus towards Fermentative Metabolism and Reduced Viability in a Cystic Fibrosis Model. J Bacteriol 197:2252–2264.

104. Pernet E, Guillemot L, Burgel P-R, Martin C, Lambeau G, Sermet-Gaudelus I, Sands D, Leduc D, Morand PC, Jeammet L, Chignard M, Wu Y, Touqui L. 2014. Pseudomonas aeruginosa eradicates Staphylococcus aureus by manipulating the host immunity. Nat Commun 5.

105. Foster TJ. 2005. Immune evasion by staphylococci. Nat Rev Micro 3:948–958.

106. Iordanescu S, Surdeanu M. 1976. Two restriction and modification systems in Staphylococcus aureus NCTC8325. J Gen Microbiol 96:277–281.

107. Zybailov B, Mosley AL, Sardiu ME, Coleman MK, Florens L, Washburn MP. 2006. Statistical analysis of membrane proteome expression changes in Saccharomyces cerevisiae. J Proteome Res 5:2339–2347.

108. Ton-That H, Liu G, Mazmanian SK, Faull KF, Schneewind O. 1999. Purification and characterization of sortase, the transpeptidase that cleaves surface proteins of Staphylococcus aureus at the LPXTG motif. Proc Natl Acad Sci 96:12424–12429.

109. Becker S, Frankel MB, Schneewind O, Missiakas D. 2014. Release of protein A from the cell wall of Staphylococcus aureus. Proc Natl Acad Sci U S A 111:1574–1579.

110. Peterson PK, Verhoef J, Sabath LD, Quie PG. 1977. Effect of protein A on staphylococcal opsonization. Infect Immun 15:760–764.

111. Forsgren A, Sjoquist J. 1966. "Protein A" from S. aureus. I. Pseudo-immune reaction with human gamma-globulin. J Immunol Baltim Md 1950 97:822–827.

112. Lyczak JB, Cannon CL, Pier GB. 2000. Establishment of Pseudomonas aeruginosa infection: lessons from a versatile opportunist. Microbes Infect Inst Pasteur 2:1051–1060.

113. Folkesson A, Jelsbak L, Yang L, Johansen HK, Ciofu O, Hoiby N, Molin S. 2012. Adaptation of Pseudomonas aeruginosa to the cystic fibrosis airway: an evolutionary perspective. Nat Rev Micro 10:841–851.

114. Kosorok MR, Jalaluddin M, Farrell PM, Shen G, Colby CE, Laxova A, Rock MJ, Splaingard M. 1998. Comprehensive analysis of risk factors for acquisition of Pseudomonas aeruginosa in young children with cystic fibrosis. Pediatr Pulmonol 26:81–88.

115. Rosenfeld M, Emerson J, McNamara S, Thompson V, Ramsey BW, Morgan W, Gibson RL. 2012. Risk factors for age at initial Pseudomonas acquisition in the cystic fibrosis epic observational cohort. J Cyst Fibros Off J Eur Cyst Fibros Soc 11:446–453.

116. Windmüller N, Witten A, Block D, Bunk B, Spröer C, Kahl BC, Mellmann A. 2015. Transcriptional adaptations during long-term persistence of Staphylococcus aureus in the airways of a cystic fibrosis patient. Int J Med Microbiol 305:38–46.

117. Huse HK, Kwon T, Zlosnik JEA, Speert DP, Marcotte EM, Whiteley M. 2013. Pseudomonas aeruginosa Enhances Production of a Non-Alginate Exopolysaccharide during Long-Term Colonization of the Cystic Fibrosis Lung. PLoS ONE 8:e82621.

118. McElroy KE, Hui JGK, Woo JKK, Luk AWS, Webb JS, Kjelleberg S, Rice SA, Thomas T. 2014. Strain-specific parallel evolution drives short-term diversification during Pseudomonas aeruginosa biofilm formation. Proc Natl Acad Sci 111:E1419–E1427.

119. Marvig RL, Sommer LM, Molin S, Johansen HK. 2015. Convergent evolution and adaptation of Pseudomonas aeruginosa within patients with cystic fibrosis. Nat Genet 47.

120. Starkey M, Hickman JH, Ma L, Zhang N, De Long S, Hinz A, Palacios S, Manoil C, Kirisits MJ, Starner TD, Wozniak DJ, Harwood CS, Parsek MR. 2009. Pseudomonas aeruginosa rugose small-colony variants have adaptations that likely promote persistence in the cystic fibrosis lung. J Bacteriol 191:3492–3503.

121. Uhlén M, Guss B, Nilsson B, Götz F, Lindberg M. 1984. Expression of the gene encoding protein A in Staphylococcus aureus and coagulase-negative staphylococci. J Bacteriol 159:713–719.

122. DeLeon S, Clinton A, Fowler H, Everett J, Horswill AR, Rumbaugh KP. 2014. Synergistic Interactions of Pseudomonas aeruginosa and Staphylococcus aureus in an In Vitro Wound Model. Infect Immun.

123. Hartleib JK Nicola Dickinson, Richard B Chhatwal, Gursharan S Sixma, Jan J Hartford, Orla M Foster, Timothy J Peters, Georg Kehrel, Beate E Herrmann, Mathias. 2000. Protein A is the von Willebrand factor binding protein onStaphylococcus aureus. Blood 96:2149–2156.

124. Gomez MI, O'Seaghdha M, Magargee M, Foster TJ, Prince AS. 2006. Staphylococcus aureus protein A activates TNFR1 signaling through conserved IgG binding domains. J Biol Chem 281:20190–20196.

125. Ribot EM, Fair MA, Gautom R, Cameron DN, Hunter SB, Swaminathan B, Barrett TJ. 2006. Standardization of pulsed-field gel electrophoresis protocols for the subtyping of Escherichia coli O157:H7, Salmonella, and Shigella for PulseNet. Foodborne Pathog Dis 3.

126. Hayden HS, Lim R, Brittnacher MJ, Sims EH, Ramage ER, Fong C, Wu Z, Crist E, Chang J, Zhou Y, Radey M, Rohmer L, Haugen E, Gillett W, Wuthiekanun V, Peacock SJ, Kaul R, Miller SI, Manoil C, Jacobs MA. 2012. Evolution of Burkholderia pseudomallei in Recurrent Melioidosis. PLoS ONE 7:e36507.

127. Simpson JT, Wong K, Jackman SD, Schein JE, Jones SJM, Birol İ. 2009. ABySS: A parallel assembler for short read sequence data. Genome Res 19:1117–1123.

128. Brittnacher MJ, Fong C, Hayden HS, Jacobs MA, Radey M, Rohmer L. 2011. PGAT: a multistrain analysis resource for microbial genomes. Bioinformatics 27:2429–2430.

129. Hyatt D, Chen G-L, LoCascio P, Land M, Larimer F, Hauser L. 2010. Prodigal: prokaryotic gene recognition and translation initiation site identification. BMC Bioinformatics 11:119.

130. Marchler-Bauer A, Lu S, Anderson JB, Chitsaz F, Derbyshire MK, DeWeese-Scott C, Fong JH, Geer LY, Geer RC, Gonzales NR, Gwadz M, Hurwitz DI, Jackson JD, Ke Z, Lanczycki CJ, Lu F, Marchler GH, Mullokandov M, Omelchenko MV, Robertson CL, Song JS, Thanki N, Yamashita RA, Zhang D, Zhang N, Zheng C, Bryant SH. 2010. CDD: a Conserved Domain Database for the functional annotation of proteins. Nucleic Acids Res 39:D225–D229.

131. Hsieh EJ, Hoopmann MR, MacLean B, MacCoss MJ. 2009. Comparison of Database Search Strategies for High Precursor Mass Accuracy MS/MS Data. J Proteome Res 9:1138–1143.

132. Eng JK, McCormack AL, Yates III JR. 1994. An approach to correlate tandem mass spectral data of peptides with amino acid sequences in a protein database. J Am Soc Mass Spectrom 5:976–989.

133. Kall L, Canterbury JD, Weston J, Noble WS, MacCoss MJ. 2007. Semi-supervised learning for peptide identification from shotgun proteomics datasets. Nat Meth 4:923–925.

134. Zhang B, Chambers MC, Tabb DL. 2007. Proteomic Parsimony through Bipartite Graph Analysis Improves Accuracy and Transparency. J Proteome Res 6:3549–3557.

135. Novick RP. 1991. [27] Genetic systems in Staphylococci, p. 587–636. *In* Jeffrey H. Miller (ed.), Methods in Enzymology. Academic Press.

136. Rohmer L, Jacobs MA, Brittnacher MJ, Fong C, Hayden HS, Hocquet D, Weiss EJ, Radey M, Germani Y, Talukder KA, Hager AJ, Kemner JM, Sims-Day EH, Matamouros S, Hager KR, Miller SI. 2014. Genomic analysis of the emergence of 20th century epidemic dysentery. BMC Genomics 15:355.

137. Mishra M, Byrd MS, Sergeant S, Azad AK, Parsek MR, McPhail L, Schlesinger LS, Wozniak DJ. 2012. Pseudomonas aeruginosa Psl polysaccharide reduces neutrophil phagocytosis and the oxidative response by limiting complement-mediated opsonization. Cell Microbiol 14:95–106.

138. McDonough KA, Rodriguez A. 2011. The myriad roles of cyclic AMP in microbial pathogens, from signal to sword. Nat Rev Microbiol 10:27–38.

139. Hauryliuk V, Atkinson GC, Murakami KS, Tenson T, Gerdes K. 2015. Recent functional insights into the role of (p)ppGpp in bacterial physiology. Nat Rev Microbiol 13:298–309.

140. Gorke B, Stulke J. 2008. Carbon catabolite repression in bacteria: many ways to make the most out of nutrients. Nat Rev Micro 6:613–624.

141. Fong JCN, Yildiz FH. 2008. Interplay between cyclic AMP-cyclic AMP receptor protein and cyclic di-GMP signaling in Vibrio cholerae biofilm formation. J Bacteriol 190:6646–6659.

142. Luo Y, Zhao K, Baker AE, Kuchma SL, Coggan KA, Wolfgang MC, Wong GCL, O'Toole GA. 2015. A Hierarchical Cascade of Second Messengers Regulates Pseudomonas aeruginosa Surface Behaviors. mBio 6.

143. Lory S, Wolfgang M, Lee V, Smith R. 2004. The multi-talented bacterial adenylate cyclases. Int J Med Microbiol IJMM 293:479–482.

144. Witte G, Hartung S, Büttner K, Hopfner K-P. 2008. Structural Biochemistry of a Bacterial Checkpoint Protein Reveals Diadenylate Cyclase Activity Regulated by DNA Recombination Intermediates. Mol Cell 30:167–178.

145. Huynh TN, Woodward JJ. 2016. Too much of a good thing: regulated depletion of c-di-AMP in the bacterial cytoplasm. Curr Opin Microbiol 30:22–29.

146. Bowman L, Zeden MS, Schuster CF, Kaever V, Grundling A. 2016. New Insights into the Cyclic Di-adenosine Monophosphate (c-di-AMP) Degradation Pathway and the Requirement of the Cyclic Dinucleotide for Acid Stress Resistance in Staphylococcus aureus. J Biol Chem 291:26970–26986.

147. Commichau FM, Dickmanns A, Gundlach J, Ficner R, Stülke J. 2015. A jack of all trades: the multiple roles of the unique essential second messenger cyclic di-AMP. Mol Microbiol 97:189–204.

148. Corrigan RM, Abbott JC, Burhenne H, Kaever V, Grundling A. 2011. c-di-AMP is a new second messenger in Staphylococcus aureus with a role in controlling cell size and envelope stress. PLoS Pathog 7:e1002217.

149. Corrigan RM, Campeotto I, Jeganathan T, Roelofs KG, Lee VT, Gründling A. 2013. Systematic identification of conserved bacterial c-di-AMP receptor proteins. Proc Natl Acad Sci 110:9084–9089.

150. Schuster CF, Bellows LE, Tosi T, Campeotto I, Corrigan RM, Freemont P, Gründling A. 2016. The second messenger c-di-AMP inhibits the osmolyte uptake system OpuC in Staphylococcus aureus. Sci Signal 9:ra81.

151. Dengler V, McCallum N, Kiefer P, Christen P, Patrignani A, Vorholt JA, Berger-Bachi B, Senn MM. 2013. Mutation in the C-di-AMP cyclase dacA affects fitness and resistance of methicillin resistant Staphylococcus aureus. PloS One 8:e73512.

152. Gries CM, Bruger EL, Moormeier DE, Scherr TD, Waters CM, Kielian T. 2016. Cyclic di-AMP Released from Staphylococcus aureus Biofilm Induces a Macrophage Type I Interferon Response. Infect Immun 84:3564–3574.

153. McFarland AP, Luo S, Ahmed-Qadri F, Zuck M, Thayer EF, Goo YA, Hybiske K, Tong L, Woodward JJ. 2017. Sensing of Bacterial Cyclic Dinucleotides by the Oxidoreductase RECON Promotes NF-κB Activation and Shapes a Proinflammatory Antibacterial State. Immunity 46:433–445.

154. Woodward JJ, Iavarone AT, Portnoy DA. 2010. c-di-AMP Secreted by Intracellular Listeria monocytogenes Activates a Host Type I Interferon Response. Science 328:1703.

155. Wurtzel O, Yoder-Himes DR, Han K, Dandekar AA, Edelheit S, Greenberg EP, Sorek R, Lory S. 2012. The Single-Nucleotide Resolution Transcriptome of Pseudomonas aeruginosa Grown in Body Temperature. PLOS Pathog 8:e1002945.

156. Smirnov A, Förstner KU, Holmqvist E, Otto A, Günster R, Becher D, Reinhardt R, Vogel J. 2016. Grad-seq guides the discovery of ProQ as a major small RNA-binding protein. Proc Natl Acad Sci U S A 113:11591–11596.

157. Pérez-Martínez I, Haas D. 2011. Azithromycin Inhibits Expression of the GacA-Dependent Small RNAs RsmY and RsmZ in Pseudomonas aeruginosa. Antimicrob Agents Chemother 55:3399–3405.

158. Sheidy DT, Zielke RA. 2013. Analysis and Expansion of the Role of the Escherichia coli Protein ProQ. PLOS ONE 8:e79656.

159. Smith MN, Crane RA, Keates RAB, Wood JM. 2004. Overexpression, purification, and characterization of ProQ, a posttranslational regulator for osmoregulatory transporter ProP of Escherichia coli. Biochemistry (Mosc) 43:12979–12989.

160. G. Chaulk S, Smith−Frieday MN, Arthur DC, Culham DE, Edwards RA, Soo P, Frost LS, Keates RAB, Glover JNM, Wood JM. 2011. ProQ Is an RNA Chaperone that Controls ProP Levels in Escherichia coli. Biochemistry (Mosc) 50:3095–3106.

161. Milner JL, Grothe S, Wood JM. 1988. Proline porter II is activated by a hyperosmotic shift in both whole cells and membrane vesicles of Escherichia coli K12. J Biol Chem 263:14900–14905.

162. MacMillan SV, Alexander DA, Culham DE, Kunte HJ, Marshall EV, Rochon D, Wood JM. 1999. The ion coupling and organic substrate specificities of osmoregulatory transporter ProP in Escherichia coli. Biochim Biophys Acta BBA - Biomembr 1420:30–44.

163. Wood JM. 1999. Osmosensing by bacteria: signals and membrane-based sensors. Microbiol Mol Biol Rev MMBR 63:230–262.

164. Jiang M, Sullivan SM, Walker AK, Strahler JR, Andrews PC, Maddock JR. 2007. Identification of novel Escherichia coli ribosome-associated proteins using isobaric tags and multidimensional protein identification techniques. J Bacteriol 189:3434–3444.

165. Attaiech L, Boughammoura A, Brochier-Armanet C, Allatif O, Peillard-Fiorente F, Edwards RA, Omar AR, MacMillan AM, Glover M, Charpentier X. 2016. Silencing of natural transformation by an RNA chaperone and a multitarget small RNA. Proc Natl Acad Sci 113:8813–8818.

166. Thomason MK, Storz G. 2010. Bacterial antisense RNAs: How many are there and what are they doing? Annu Rev Genet 44:167–188.

167. Ventre I, Goodman AL, Vallet-Gely I, Vasseur P, Soscia C, Molin S, Bleves S, Lazdunski A, Lory S, Filloux A. 2006. Multiple sensors control reciprocal expression of Pseudomonas aeruginosa regulatory RNA and virulence genes. Proc Natl Acad Sci U S A 103:171–176.

168. Brencic A, McFarland KA, McManus HR, Castang S, Mogno I, Dove SL, Lory S. 2009. The GacS/GacA signal transduction system of Pseudomonas aeruginosa acts exclusively through its control over the transcription of the RsmY and RsmZ regulatory small RNAs. Mol Microbiol 73:434–445.

169. Irie Y, Starkey M, Edwards AN, Wozniak DJ, Romeo T, Parsek MR. 2010. Pseudomonas aeruginosa biofilm matrix polysaccharide Psl is regulated transcriptionally by RpoS and post-transcriptionally by RsmA. Mol Microbiol 78:158–172.

170. Sonnleitner E, Bläsi U. 2014. Regulation of Hfq by the RNA CrcZ in Pseudomonas aeruginosa Carbon Catabolite Repression. PLOS Genet 10:e1004440.

171. Attaiech L, Glover JNM, Charpentier X. RNA Chaperones Step Out of Hfq's Shadow. Trends Microbiol 25:247–249.

172. Kai T, Tateda K, Kimura S, Ishii Y, Ito H, Yoshida H, Kimura T, Yamaguchi K. 2009. A low concentration of azithromycin inhibits the mRNA expression of N-acyl homoserine lactone synthesis enzymes, upstream of lasI or rhlI, in Pseudomonas aeruginosa. Pulm Pharmacol Ther 22:483–486.

173. Olejniczak M, Storz G. 2017. ProQ/FinO-domain proteins: Another ubiquitous family of RNA matchmakers? Mol Microbiol.

174. Hmelo LR, Borlee BR, Almblad H, Love ME, Randall TE, Tseng BS, Lin C, Irie Y, Storek KM, Yang JJ, Siehnel RJ, Howell PL, Singh PK, Tolker-Nielsen T, Parsek MR, Schweizer HP, Harrison JJ. 2015. Precision-engineering the Pseudomonas aeruginosa genome with two-step allelic exchange. Nat Protoc 10:1820–1841.

175. Choi K-H, Schweizer HP. 2006. mini-Tn7 insertion in bacteria with single attTn7 sites: example Pseudomonas aeruginosa. Nat Protoc 1:153–161.

176. Silverman JM, Agnello DM, Zheng H, Andrews BT, Li M, Catalano CE, Gonen T, Mougous JD. 2013. Haemolysin coregulated protein is an exported receptor and chaperone of type VI secretion substrates. Mol Cell 51:584–593.

177. Huynh TN, Luo S, Pensinger D, Sauer J-D, Tong L, Woodward JJ. 2015. An HD-domain phosphodiesterase mediates cooperative hydrolysis of c-di-AMP to affect bacterial growth and virulence. Proc Natl Acad Sci U S A 112:E747–E756.

178. Sureka K, Choi PH, Precit M, Delince M, Pensinger DA, Huynh TN, Jurado AR, Goo YA, Sadilek M, Iavarone AT, Sauer J-D, Tong L, Woodward JJ. 2014. The cyclic dinucleotide c-di-AMP is an allosteric regulator of metabolic enzyme function. Cell 158:1389–1401.

179. Yabuuchi E, Oyama A. 1971. Achromobacter xylosoxidans n. sp. from human ear discharge. Jpn J Microbiol 15:477–481.

180. Nelson KE, Weinel C, Paulsen IT, Dodson RJ, Hilbert H, Martins dos Santos VAP, Fouts DE, Gill SR, Pop M, Holmes M, Brinkac L, Beanan M, DeBoy RT, Daugherty S, Kolonay J, Madupu R, Nelson W, White O, Peterson J, Khouri H, Hance I, Chris Lee P, Holtzapple E, Scanlan D, Tran K, Moazzez A, Utterback T, Rizzo M, Lee K, Kosack D, Moestl D, Wedler H, Lauber J, Stjepandic D, Hoheisel J, Straetz M, Heim S, Kiewitz C, Eisen JA, Timmis KN, Dusterhoft A, Tummler B, Fraser CM. 2002. Complete genome sequence and comparative analysis of the metabolically versatile Pseudomonas putida KT2440. Environ Microbiol 4:799–808.

181. Holmqvist E, Wright PR, Li L, Bischler T, Barquist L, Reinhardt R, Backofen R, Vogel J. 2016. Global RNA recognition patterns of post-transcriptional regulators Hfq and CsrA revealed by UV crosslinking in vivo. EMBO J 35:991–1011.

182. Huangyutitham V, Güvener ZT, Harwood CS. 2013. Subcellular Clustering of the Phosphorylated WspR Response Regulator Protein Stimulates Its Diguanylate Cyclase Activity. mBio 4.

183. Hickman JW, Harwood CS. 2008. Identification of FleQ from Pseudomonas aeruginosa as a c-di-GMP-responsive transcription factor. Mol Microbiol 69:376–389.

184. Borlee BR, Goldman AD, Murakami K, Samudrala R, Wozniak DJ, Parsek MR. 2010. Pseudomonas aeruginosa uses a cyclic-di-GMP-regulated adhesin to reinforce the biofilm extracellular matrix. Mol Microbiol 75:827–842.

185. Baraquet C, Harwood CS. 2015. FleQ DNA Binding Consensus Sequence Revealed by Studies of FleQ-Dependent Regulation of Biofilm Gene Expression in Pseudomonas aeruginosa. J Bacteriol 198:178–186.

186. Baraquet C, Murakami K, Parsek MR, Harwood CS. 2012. The FleQ protein from Pseudomonas aeruginosa functions as both a repressor and an activator to control gene expression from the pel operon promoter in response to c-di-GMP. Nucleic Acids Res 40:7207–7218.

187. Whitchurch CB, Leech AJ, Young MD, Kennedy D, Sargent JL, Bertrand JJ, Semmler ABT, Mellick AS, Martin PR, Alm RA, Hobbs M, Beatson SA, Huang B, Nguyen L, Commolli JC, Engel JN, Darzins A, Mattick JS. 2004. Characterization of a complex chemosensory signal transduction system which controls twitching motility in Pseudomonas aeruginosa. Mol Microbiol 52:873–893.

188. Fulcher NB, Holliday PM, Klem E, Cann MJ, Wolfgang MC. 2010. The Pseudomonas aeruginosa Chp chemosensory system regulates intracellular cAMP levels by modulating adenylate cyclase activity. Mol Microbiol 76:889–904.

189. Persat A, Inclan YF, Engel JN, Stone HA, Gitai Z. 2015. Type IV pili mechanochemically regulate virulence factors in Pseudomonas aeruginosa. Proc Natl Acad Sci 112:7563–7568.

190. O'Connor JR, Kuwada NJ, Huangyutitham V, Wiggins PA, Harwood CS. 2012. Surface sensing and lateral subcellular localization of WspA, the receptor in a chemosensory-like system leading to c-di-GMP production. Mol Microbiol 86:720–729.

191. Kuchma SL, Ballok AE, Merritt JH, Hammond JH, Lu W, Rabinowitz JD, O'Toole GA. 2010. Cyclic-di-GMP-Mediated Repression of Swarming Motility by Pseudomonas aeruginosa: the pilY1 Gene and Its Impact on Surface-Associated Behaviors. J Bacteriol 192:2950–2964.

192. Almblad H, Harrison JJ, Rybtke M, Groizeleau J, Givskov M, Parsek MR, Tolker-Nielsen T. 2015. The Cyclic AMP-Vfr Signaling Pathway in Pseudomonas aeruginosa Is Inhibited by Cyclic Di-GMP. J Bacteriol 197:2190–2200.

193. Almblad H, Harrison JJ, Rybtke M, Groizeleau J, Givskov M, Parsek MR, Tolker-Nielsen T. 2015. Erratum for Almblad et al., The Cyclic AMP-Vfr Signaling Pathway in Pseudomonas aeruginosa Is Inhibited by Cyclic Di-GMP. J Bacteriol 197:2731–2731.

194. Hickman JW, Tifrea DF, Harwood CS. 2005. A chemosensory system that regulates biofilm formation through modulation of cyclic diguanylate levels. Proc Natl Acad Sci U S A 102:14422–14427.

195. Kuchma SL, Brothers KM, Merritt JH, Liberati NT, Ausubel FM, O'Toole GA. 2007. BifA, a cyclic-Di-GMP phosphodiesterase, inversely regulates biofilm formation and swarming motility by Pseudomonas aeruginosa PA14. J Bacteriol 189:8165–8178.

196. Merritt JH, Brothers KM, Kuchma SL, O'Toole GA. 2007. SadC Reciprocally Influences Biofilm Formation and Swarming Motility via Modulation of Exopolysaccharide Production and Flagellar Function. J Bacteriol 189:8154–8164.

197. Kulasekara BR, Kamischke C, Kulasekara HD, Christen M, Wiggins PA, Miller SI. 2013. c-di-GMP heterogeneity is generated by the chemotaxis machinery to regulate flagellar motility. eLife 2:e01402.

198. Güvener ZT, Harwood CS. 2007. Subcellular location characteristics of the Pseudomonas aeruginosa GGDEF protein, WspR, indicate that it produces cyclic-di-GMP in response to growth on surfaces. Mol Microbiol 66:1459–1473.

199. Jennings LK, Storek KM, Ledvina HE, Coulon C, Marmont LS, Sadovskaya I, Secor PR, Tseng BS, Scian M, Filloux A, Wozniak DJ, Howell PL, Parsek MR. 2015. Pel is a cationic exopolysaccharide that cross-links extracellular DNA in the Pseudomonas aeruginosa biofilm matrix. Proc Natl Acad Sci U S A 112:11353–11358.

200. Skerker JM, Berg HC. 2001. Direct observation of extension and retraction of type IV pili. Proc Natl Acad Sci U S A 98:6901–6904.

201. Semmler AB, Whitchurch CB, Mattick JS. 1999. A re-examination of twitching motility in Pseudomonas aeruginosa. Microbiol Read Engl 145 (Pt 10):2863–2873.

202. Wolfe AJ, Visick KL. 2008. Get the Message Out: Cyclic-Di-GMP Regulates Multiple Levels of Flagellum-Based Motility. J Bacteriol 190:463–475.

203. Jain R, Behrens A-J, Kaever V, Kazmierczak BI. 2012. Type IV Pilus Assembly in Pseudomonas aeruginosa over a Broad Range of Cyclic di-GMP Concentrations. J Bacteriol 194:4285–4294.

204. Baker P, Hill PJ, Snarr BD, Alnabelseya N, Pestrak MJ, Lee MJ, Jennings LK, Tam J, Melnyk RA, Parsek MR, Sheppard DC, Wozniak DJ, Howell PL. 2016. Exopolysaccharide biosynthetic glycoside hydrolases can be utilized to disrupt and prevent Pseudomonas aeruginosa biofilms. Sci Adv 2.

205. Whitney JC, Colvin KM, Marmont LS, Robinson H, Parsek MR, Howell PL. 2012. Structure of the cytoplasmic region of PelD, a degenerate diguanylate cyclase receptor that regulates exopolysaccharide production in Pseudomonas aeruginosa. J Biol Chem 287:23582–23593.

206. Chan K-G, Priya K, Chang C-Y, Abdul Rahman AY, Tee KK, Yin W-F. 2016. Transcriptome analysis of Pseudomonas aeruginosa PAO1 grown at both body and elevated temperatures. PeerJ 4:e2223.

207. O'Toole GA, Kolter R. 1998. Initiation of biofilm formation in Pseudomonas fluorescens WCS365 proceeds via multiple, convergent signalling pathways: a genetic analysis. Mol Microbiol 28:449–461.

208. VOGEL HJ, BONNER DM. 1956. Acetylornithinase of Escherichia coli: partial purification and some properties. J Biol Chem 218:97–106.

209. Krell T, Lacal J, Busch A, Silva-Jimenez H, Guazzaroni M-E, Ramos JL. 2010. Bacterial sensor kinases: diversity in the recognition of environmental signals. Annu Rev Microbiol 64:539–559.

210. Brogden KA, Guthmiller JM, Taylor CE. 2005. Human polymicrobial infections. The Lancet 365:253–255.

211. Thammavongsa V, Kim HK, Missiakas D, Schneewind O. 2015. Staphylococcal manipulation of host immune responses. Nat Rev Micro 13:529–543.

212. O'Seaghdha M, van Schooten CJ, Kerrigan SW, Emsley J, Silverman GJ, Cox D, Lenting PJ, Foster TJ. 2006. Staphylococcus aureus protein A binding to von Willebrand factor A1 domain is mediated by conserved IgG binding regions. FEBS J 273:4831–4841.

213. Claes J, Vanassche T, Peetermans M, Liesenborghs L, Vandenbriele C, Vanhoorelbeke K, Missiakas D, Schneewind O, Hoylaerts MF, Heying R, Verhamme P. 2014. Adhesion of Staphylococcus aureus to the vessel wall under flow is mediated by von Willebrand factor-binding protein. Blood 124:1669–1676.

214. Percival SL, Suleman L, Vuotto C, Donelli G. 2015. Healthcare-associated infections, medical devices and biofilms: risk, tolerance and control. J Med Microbiol 64:323–334.

215. Fang G, Keys TF, Gentry LO, Harris AA, Rivera N, Getz K, Fuchs PC, Gustafson M, Wong ES, Goetz A, Wagener MM, Yu VL. 1993. Prosthetic Valve Endocarditis Resulting from Nosocomial Bacteremia: A Prospective, Multicenter Study. Ann Intern Med 119:560–567.

216. Bao P, Kodra A, Tomic-Canic M, Golinko MS, Ehrlich HP, Brem H. 2009. The Role of Vascular Endothelial Growth Factor in Wound Healing. J Surg Res 153:347–358.

217. Wang C, Baker BM, Chen CS, Schwartz MA. 2013. Endothelial cell sensing of flow direction. Arterioscler Thromb Vasc Biol 33:10.1161/ATVBAHA.113.301826.

218. Moldoveanu B, Otmishi P, Jani P, Walker J, Sarmiento X, Guardiola J, Saad M, Yu J. 2009. Inflammatory mechanisms in the lung. J Inflamm Res 2:1–11.

219. Powers ME, Wardenburg JB. 2014. Igniting the Fire: Staphylococcus aureus Virulence Factors in the Pathogenesis of Sepsis. PLOS Pathog 10:e1003871.

220. Toyofuku M, Roschitzki B, Riedel K, Eberl L. 2012. Identification of Proteins Associated with the Pseudomonas aeruginosa Biofilm Extracellular Matrix. J Proteome Res 11:4906–4915.

221. Boucher JC, Schurr MJ, Yu H, Rowen DW, Deretic V. 1997. Pseudomonas aeruginosa in cystic fibrosis: role of mucC in the regulation of alginate production and stress sensitivity. Microbiology 143:3473–3480.

222. Byrd MS, Sadovskaya I, Vinogradov E, Lu H, Sprinkle AB, Richardson SH, Ma L, Ralston B, Parsek MR, Anderson EM, Lam JS, Wozniak DJ. 2009. Genetic and biochemical analyses of the Pseudomonas aeruginosa Psl exopolysaccharide reveal overlapping roles for polysaccharide synthesis enzymes in Psl and LPS production. Mol Microbiol 73:622–638.

223. Starkey M, Hickman JH, Ma L, Zhang N, De Long S, Hinz A, Palacios S, Manoil C, Kirisits MJ, Starner TD, Wozniak DJ, Harwood CS, Parsek MR. 2009. Pseudomonas aeruginosa Rugose Small-Colony Variants Have Adaptations That Likely Promote Persistence in the Cystic Fibrosis Lung. J Bacteriol 191:3492–3503.

224. Colvin KM, Irie Y, Tart CS, Urbano R, Whitney JC, Ryder C, Howell PL, Wozniak DJ, Parsek MR. 2012. The Pel and Psl polysaccharides provide Pseudomonas aeruginosa structural redundancy within the biofilm matrix. Environ Microbiol 14:10.1111/j.1462-2920.2011.02657.x.

225. Guvener ZT, Harwood CS. 2007. Subcellular location characteristics of the Pseudomonas aeruginosa GGDEF protein, WspR, indicate that it produces cyclic-di-GMP in response to growth on surfaces. Mol Microbiol 66:1459–1473.

226. Fuerst JA, Hayward AC. 1969. Surface appendages similar to fimbriae (pili) on pseudomonas species. J Gen Microbiol 58:227–237.

"Messieurs, c'est les microbes qui auront le dernier mot."

- Louis Pasteur